! DRAFT !

Asko Ellman & Matti Linjama

Modeling and Simulating Fluid Power Systems

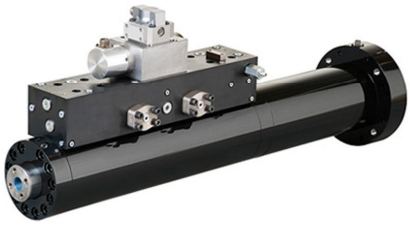

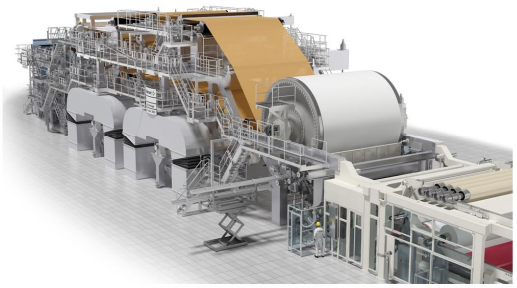

LOGO?

Latin symbols

A	area	[m^2]
A_{cyl}	cross-sectional area of cylinder (piston)	[m^2]
A_{fc}	cross-sectional area of flow channel	[m^2]
$A_{fc,vc}$	cross-sectional area of vena contracta	[m^2]
$A_{pop,e}$	end surface area of poppet	[m^2]
$A_{vs,e}$	end surface area of spool	[m^2]
b_v	viscose friction coefficient	[N]
c_p	specific heat	[J/kgK]
Ca	cavitation number	[-]
Ca_{cr}	critical cavitation number	[-]
C_c	contraction coefficient	[-]
C_d	discharge coefficient	[-]
$C_{d,u}$	ultimate discharge coefficient	[-]
C_p	pressure coefficient	[-]
C_q	flow coefficient	[-]
$C_{q,cav}$	flow coefficient, cavitating flow	[-]
$C_{q,turb}$	flow coefficient, approximate value	[-]
C_v	velocity coefficient	[-]
d	diameter	[m]
d_{fc}	diameter of flow channel	[m]
d_{vp}	diameter of valve port	[m]
D_H	hydraulic diameter	[m]
D_{pop}	diameter of poppet	[m]
D_{vb}	diameter of valve bore	[m]
D_{vs}	diameter of valve spool	[m]
f	frequency	[Hz]
Fm	flow number	[-]
F	force	[N]
F_B	viscose friction force	[N]
F_{ctrl}	control force	[N]
F_{cyl}	cylinder net force	[N]
F_C	Coulomb friction force	[N]
F_f	flow force	[N]
$F_{f,dyn}$	dynamic flow force	[N]
$F_{f,mn}$	relation of flow and pressure forces	[-]
$F_{f,r}$	resultant flow force	[N]
F_p	pressure force	[N]
F_{pre}	? force	[N]
F_R	spring force	[N]
F_S	static friction force	[N]
F_μ	friction force	[N]
g	acceleration of gravity	[m/s^2]
h_g	gap height	[m]
$\mathbf{H}$	vector function	[-]
I	momentum	[kgm/s]
I	current	[A]
k	polytropic gas constant	[-]
k_A	area coefficient	[m]

k_R	spring constant	[N/m]
$k_{R,cs}$	spring constant of cylinder seal	[N/m]
$k_{R,h}$	hydraulic spring constant	[N/m]
k_v	valve flow coefficient, leakage coefficient	[?]
K_{air}	bulk modulus of air	[Pa]
K_e	effective bulk modulus	[Pa]
K_f	bulk modulus of fluid	[Pa]
K_{hose}	bulk modulus of hose	[Pa]
K_I	valve gain (control current → spool transition)	[-]
K_{sgn}	coefficient of hyperbolic tangent function	[-]
K_S	system gain	[-]
l_{fr}	length of frictional area in throttle	[m]
l_g	gap length	[m]
l_{thr}	length of throttle	[m]
l_{vb}	valve bore distance	[m]
l_{vc}	length of vena contracta	[m]
m	mass	[kg]
m_{air}	mass of air	[kg]
m_f	mass of fluid	[kg]
m_{f+air}	mass of fluid-air mixture	[kg]
m_{pop}	mass of poppet	[kg]
$\mathbf{M}$	inertia matrix	[-]
p	pressure	[Pa] [bar]
p_{at}	atmospheric pressure	[Pa] [bar]
p_{cyl}	cylinder pressure	[Pa] [bar]
p_L	load pressure	[Pa] [bar]
p_m	motor pressure	[Pa] [bar]
p_{op}	pressure at operating point	[Pa] [bar]
p_{ref}	reference pressure	[Pa] [bar]
p_{tm}	torque motor pressure	[Pa] [bar]
p_{valve}	valve inlet pressure	[Pa] [bar]
p_{vc}	pressure at vena contracta	[Pa] [bar]
Δp	pressure difference	[Pa] [bar]
Δp_{op}	pressure difference at operating point	[Pa] [bar]
Δp_s	pressure loss	[Pa] [bar]
$\Delta p_{A\rightarrow B}$	pressure difference over port A to port B	[Pa] [bar]
$\Delta p_{A\rightarrow T}$	pressure difference over port A to port T	[Pa] [bar]
$\Delta p_{B\rightarrow T}$	pressure difference over port B to port T	[Pa] [bar]
$\Delta p_{P\rightarrow A}$	pressure difference over port P to port A	[Pa] [bar]
$\Delta p_{P\rightarrow B}$	pressure difference over port P to port B	[Pa] [bar]
$\Delta p_{P\rightarrow T}$	pressure difference over port P to port B	[Pa] [bar]
q_V	flow rate	[m^3/s] [l/min]
$q_{V,cyl}$	cylinder flow rate	[m^3/s] [l/min]
$q_{V,L}$	load flow rate	[m^3/s] [l/min]
$q_{V,m}$	motor flow rate	[m^3/s] [l/min]
$q_{V,turb}$	flow rate, turbulent flow	[m^3/s] [l/min]
$q_{V,A\rightarrow B}$	flow rate from port A to port B	[m^3/s]
$q_{V,A\rightarrow T}$	flow rate from port A to port T	[m^3/s]
$q_{V,B\rightarrow T}$	flow rate from port B to port T	[m^3/s]
$q_{V,P\rightarrow A}$	flow rate from port P to port A	[m^3/s]

$q_{V,P\rightarrow B}$	flow rate from port P to port B	[m^3/s]
$q_{V,P\rightarrow T}$	flow rate from port P to port B	[m^3/s]
$\mathbf{Q}$	vector of generalized forces	[-]
r_{pop}	radius of poppet	[m]
R	gas constant	[J/kgK]
Re	Reynold's number	[-]
Re_{cr}	critical Reynold's number	[-]
Re_{tr}	Reynold's number in transition point	[-]
S_c	solubility constant	[-]
T_m	torque of motor	[Nm]
T_μ	friction torque, torque loss	[Nm]
t	time	[s]
u_{valve}	control quantity of valve	[-]
U_{fc}	circumference of cross-section of flow channel	[m]
v	velocity, flow velocity	[m/s]
v_{cyl}	cylinder (piston) velocity	[m/s]
v_{vc}	flow velocity at vena contracta	[m/s]
V	volume	[m^3]
V_{air}	volume of air	[m^3]
V_{cyl}	volume of cylinder	[m^3]
V_{ctrl}	control volume	[m^3]
V_f	volume of fluid	[m^3]
V_{hose}	volume of hose	[m^3]
V_{tm}	swept volume of torque motor	[m^3]
V_m	swept volume of motor	[m^3]
x	transition, valve opening	[m]
x_{cyl}	cylinder (piston) transition	[m]
x_{vs}	valve spool transition, valve opening	[m]
X	general coefficient, used in simplifying of equations	[-]
y	layer thickness	[m]
Y	general coefficient, used in simplifying of equations	[-]
z	elevation	[m]
z_{cs}	bend of the cylinder seal	[m]
$\mathbf{z}$	vector of mechanical states	[-]

$K_{\alpha D}$	laminar flow coefficient	[-]	liittyy kuvaan 29, muttei esiinny siinä.

Greek symbols

α	thermal expansion coefficient of volume	[1/K]
α_{con}	cone angle	[°] [rad]
α_f	flow angle	[°] [rad]
α_{ori}	orifice angle	[°] [rad]
α_{pop}	chamfer angle of poppet	[°] [rad]
α_{soc}	chamfer angle of socket	[°] [rad]
α_x	opening angle of circle segment	[°] [rad]
Γ	eigenvalue	[-]
Δ	difference	[-]
ε	eccentrity	[-]
η	dynamic viscosity	[Pa×s]
η_{hm}	hydromechanical efficiency	[-]
η_v	volumetric efficiency	[-]
η_t	total efficiency	[-]
ρ	density	[kg/m^3]
ρ_{air}	density of air	[kg/m^3]
ρ_f	density of fluid	[kg/m^3]
ν	kinematic viscosity	[m^2/s] [cSt]
ζ	loss factor	[N/m^2]
ζ_d	damping coefficient	[?]
$\zeta_{d,cs}$	damping constant of cylinder seal	[Ns/m]
θ	temperature	[°C] [K]
$\Delta\theta$	temperature difference	[°C] [K]
λ	Darcy-Weisbach friction factor	[-]
Λ	relative portion	[-]
$\Lambda_{air,undiss}$	relative portion of undissolved air in fluid-air mixture	[-]
τ	shear stress	[N/m^2]
τ_t	time constant	[?]
φ	rotation angle	[°] [rad]
φ_m	rotation angle of motor	[°] [rad]
φ_{tm}	rotation angle of torque motor	[°] [rad]
$\psi_{valve,op}$	valve dynamics	[-]
ω_n	natural angular velocity	[-]
α_A	maximum value of discharge coefficient, kai?	[°], kuva 29.
α_D	maximum value of discharge coefficient	[-], kuva 29.
α_{Dmax}	maximum value of discharge coefficient	[-], liittyy kuvaan 29, muttei esiinny siinä.
Ψ	function	[-], kaavat 154 ja 155.

Subindexes

0	initial state
1,2,3,etc.	different points in a system, running index
abs	absolute
air	air
am	ambient
at	atmospheric
aux	auxiliary
cav	cavitation
ch	characteristic
closed	closed
con	cone
cr	critical
ctrl	control
cyl	cylinder
d	drain, leakage
diss	dissolved
dyn	dynamic
e	effective, end
ex	external
f	fluid, flow
f+air	fluid-air mixture
fc	flow channel
g	gap
L	load
m	motor
max	maximum
meas	measured
mech	mechanical
min	minimum
op	operating point
open	open
pop	poppet
rd	reduced
ref	reference
rel	relative
s	loss
sat	saturation
soc	socket
st	static
t	time
t	total
theor	theoretical
thr	throttle
tm	torque motor
tr	transition point
turb	turbulenttinen
valve	valve
vc	vena contracta

vb	valve bore
vs	valve spool

Sinisellä merkittyjä alaindeksejä ei toistaiseksi ole prujussa, ovat tässä vaan sen varalta, että…

Superscripts

max	maximum
min	minimum

1 Virtual testing

1.1 General

The word **Simulation** refers to imitating the operation of a real system with a model that is usually based on a mathematical description of the system. If the model covers the real system with an adequate accuracy, it can be called the **Virtual prototype** of the system that enables virtual testing of the system in operational conditions that correspond real life both in normal work cycles and also in severe loading and control conditions. In best case this can be done even without building a physical prototype of the apparatus.

Time domain simulation analyses the response of a system to a step, ramp or impulse type **stimulus**. **Frequency domain simulation** in turn analyses the system response to sinewise alternating stimulus. Frequency response is an informative way to study the dynamic characteristics of a system, however, it can be presented only to a **linear** or **linearized system** in a one single **operating point**. The results of time domain simulation resemble measurements done with a real apparatus or a system, but several of those are needed in order to be able to draw conclusions over the real operation of the system.

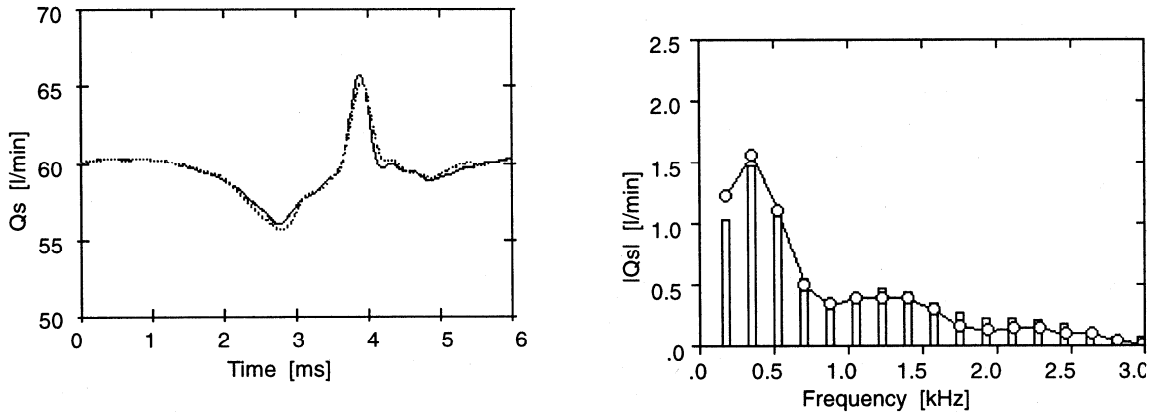

Figure 1 Time and frequency response. [Kuvaa muutettava seuraavasti: Frequency → f, Time → t, Qs → q_V]

However, the information obtained by simulation is very dependent on the detail level of the simulation model. In order to be able to imitate the behavior of a system the model has, firstly, to contain all the **essential physical phenomena affecting to the behavior**, and secondly, the **parameters of these phenomena** have to be known. When these conditions are met, it is possible to obtain quantitative results and the numerical values of simulation results correspond to the measurement results well. On the other hand, with a simpler model it is possible to obtain qualitative results, whose numerical values do not accurately correspond to the measured values, but the effect of changes in parameter values and also the operation logic of simulated apparatus can be deduced from the simulation results.

Simulation does not give the system's optimal dimensioning as a result, in stead, this has to be deduced from simulated system responses using "trial and error"-method by comparing the effect of constructive parameters on the characteristics of the system. Systems typically have numerous parameters which in turn have several alternative value levels. As a result of this, the parameter space can easily grow too large, so the first task is to **reduce the parameter space**, i.a., by **static dimensioning**. To visualize the importance of this, let's take a system that has, e.g., ten different

components each of which having ten possible nominal sizes and calculate the time needed to find the optimal dimensioning solution with the help of computer simulation when calculating a single response takes one second:

$10\,! = 3628800 \times 1\ \text{s} = 42\ \text{days}\,!$

The purpose of static dimensioning is to select values for most of the system parameters and simulation is used to find optimal values for the remaining parameters.

Finding optimal dimensioning is also made difficult by the fact that defining a single quantity that represents the optimality of dimensioning is usually difficult and requires expertise. Thus simulation model does not reduce the need of expertise, but it mainly offers a tool to a specialist designer.

1.2 The needs

Shortening the time of product development. Time-to-market has become ever more important part of the profitability and competitiveness of a new product. Shortening of the product development time requires beefing up the design methods and minimizing the number of prototype stages.

Mastering of the product development process. Managing the product development process of a complicated product is made easier if a virtual prototype exists that conforms the development stage of the product.

Rising the automation and performance level. Enhancing the performance usually complicates the design of a machine or an apparatus. In the design of a well controllable, effective and lightweight machine system several opposing or even contradictory requirements have to be reconciled.

Enhancing the quality of design. The customers buying end products specify the properties and/or characteristics of the product ever more precisely. Reaching the central target values of the quality measures of the end product and minimizing their variation is thus ever more important. Managing the warranty costs is essential specially in large manufacturing series.

Integrating or embedding microelectronics in end products. Several hydraulically operated machines use digital control system that enables reaching better productivity and ergonomy. Digital control systems enable realizing many functions that would not be possible with analog technology. On the other hand, designing and testing of a multiform control system have become more difficult.

Support for marketing. The customers want to be confirmed about the functionality and the properties of the product already when they make the decision of procurement. The documents and software created during the design process of the product can be used to support the marketing.

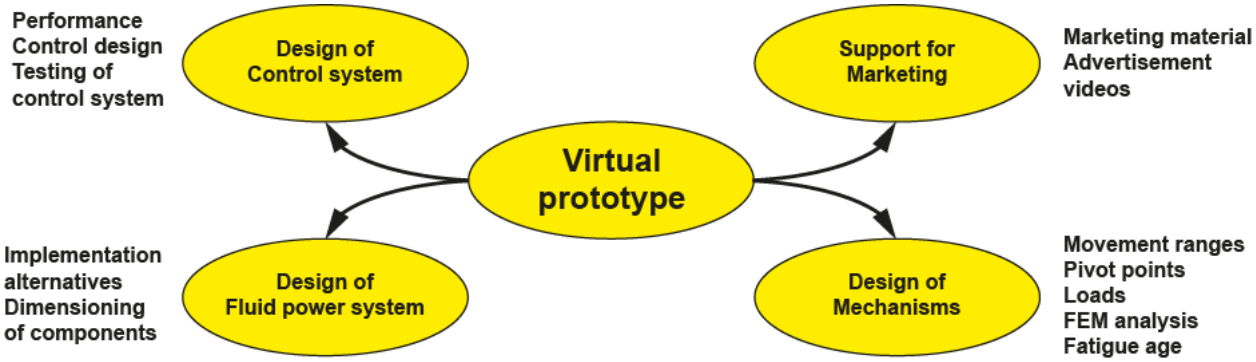

Figure 2. Use of virtual prototype.

The possibilities of computer-assisted product design are shown in Fig. 3.

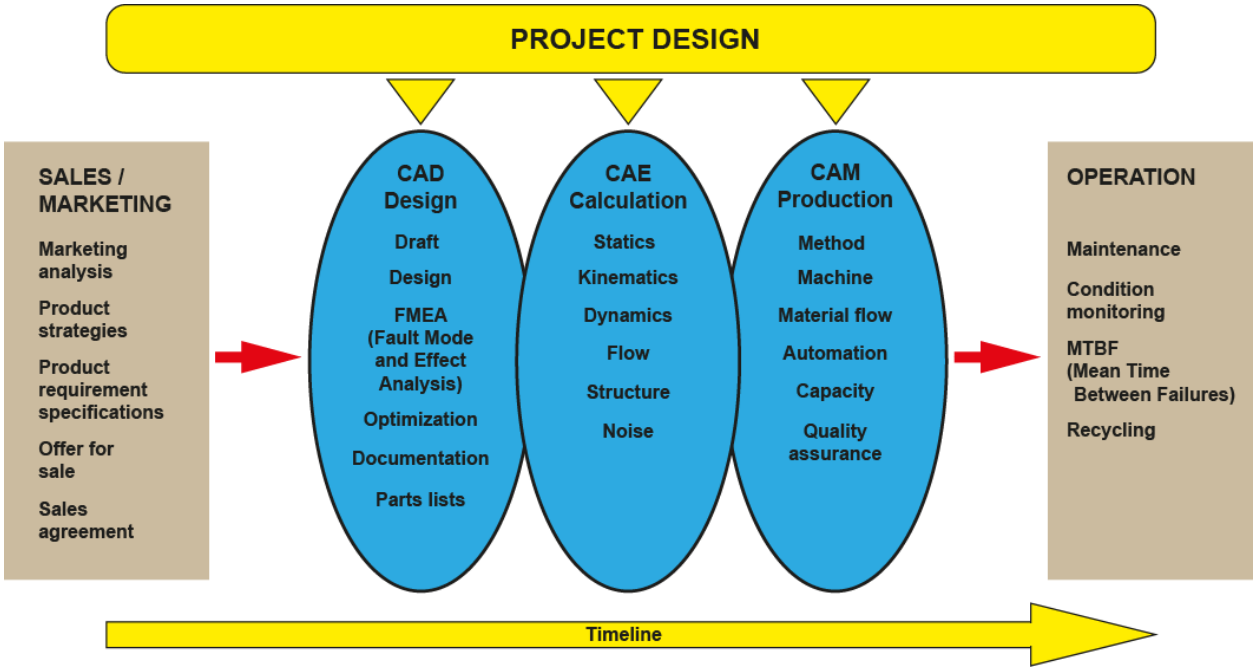

Figure 3. Computer-assisted product design.

1.3 Pros and cons

Compared to making measurements the simulation has following pros and cons:

+ testing the physical system can be expensive or even dangerous.
+ simulation can either substitute several prototype stages or replace them completely. This results into savings in product development time and also in design, material and manufacturing costs.
+ possibility to test various measurement, component and control algorithm alternatives in order to reach efficient and accurate operation of the machine.
+ dynamic properties of machines will be well understood and they can be argumented to the customers. Problems arising out of changed process factors can be understood and solved quickly.

+ research and product development engineers are able to test exceptional product ideas which speeds up utilizing new innovations.
+ experimental measurement of some quantities can be difficult, inaccurate or impossible.
+ experimental research takes typically a long time.
+ measurement errors are possible to occur.
+ replicating same measurement conditions several times can be difficult.
- prototype usually exists and its properties can be measured.
- making measurements of the most important quantities (pressure, displacement) is easy.
- implementation of a simulation model requires significant amount of work and expertise. At least one person in a company has to be familiarized with simulations.
- requires changes also in company culture. (DOES THIS APPLY NOWADAYS?)
- misinterpreted results can lead to wrong decisions.

1.4 Implementation

Simulation is usually implemented with computers using special simulation programs. These programs are available to almost all operating systems and platforms, but the largest selection is offered to PC environment and UNIX workstations. Working with simulation programs is usually **interactive** and the results are obtained and can be analyzed almost instantly. In **batch processing** the results are calculated for a longer period of time and are analyzed only afterwards.

It is possible to couple a simulator (i.e. simulation model) together with a part of a real system. This is done, e.g., when a real controller is wished to be tuned up in a simulated environment. This type of execution is called **hardware-in-the-loop** simulation. Also a human can be connected to the system to control the simulated apparatus. This kind of execution is called **man-in-the-loop** simulation which is used, e.g., in training simulators or when operator's preferences are wished to be clarified. When simulator is coupled with a visual animation of operating environment the result is called **virtual reality**.

Simulation project can be divided into following phases
· Defining the task
· Formulation of the model
· Finding out the parameter values of the model
· Simulations
· Interpretation of the results

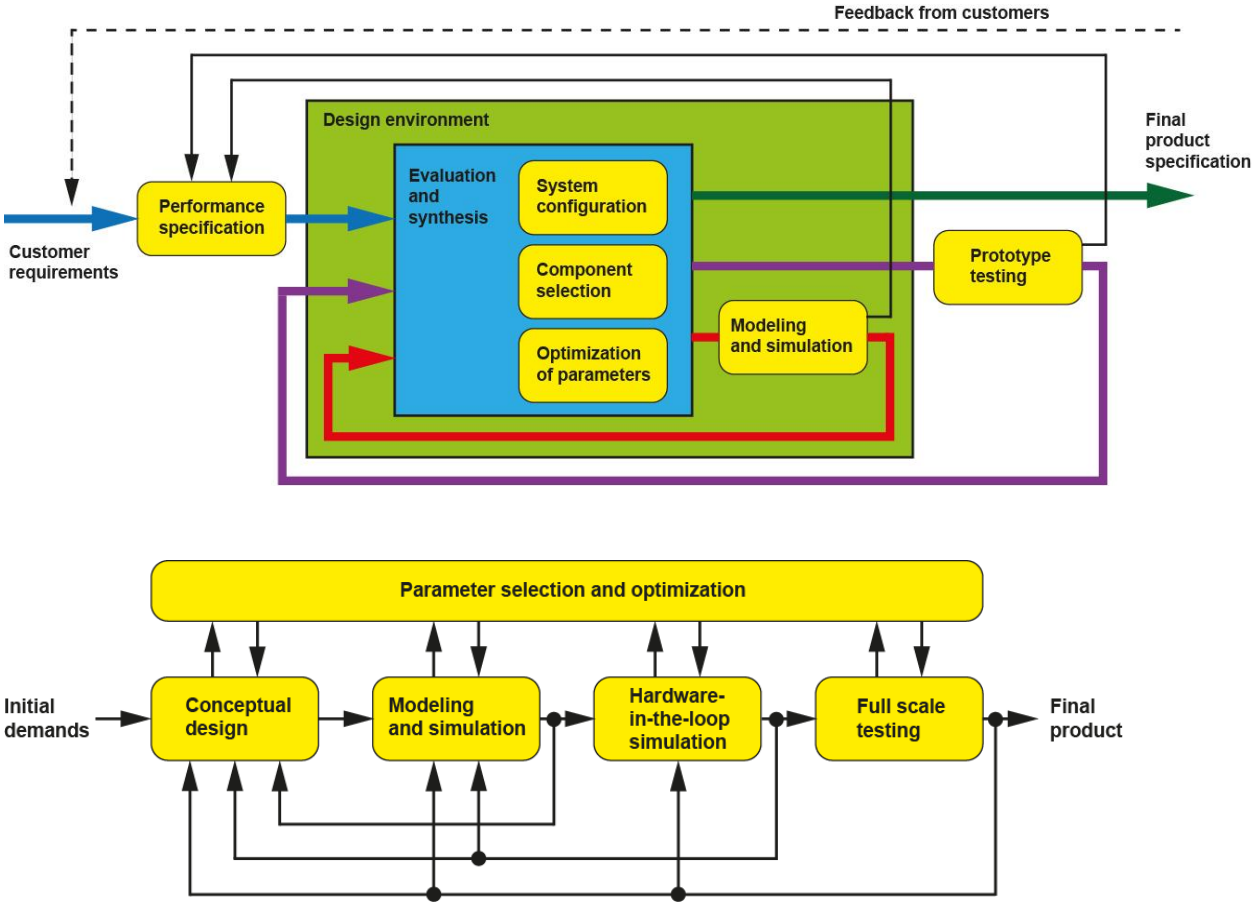

Figure 4. Operations model of simulation-assisted design.

Simulation project can fail for, e.g., following reasons

- The objective is vague
- Lack of expertise and human resources
- Model is too simple
- Tools are incorrect
- Documentation is insufficient
- Results are unillustrative or are otherwise misinterpreted

1.5 Special problems / challenges

- Nonlinearities: turbulent flow mechanism, finite displacements of valves and actuators, closing of flow channels, friction, clearances and saturation.
- Mathematical rigidity of the simulation model, i.e., the differencies between system's various time constants are several tenfolds in magnitude. The largest time constant of the system determines the minimum length of time window and on the other hand the smallest time constant determines the maximum value of calculation step. As a result, the numerical solving of the model can be laborious.
- Availability of parameter values. Manufacturers of hydraulic components are usually short-spoken of the parameter data of their products. In addition, some of the system parameters, especially the dynamics related, are not precisely known.
- Dynamic properties of hydraulic system are in interconnection with the dynamics of the total machine. In order to obtain the loading that falls on hydraulic system it is usually necessary to

model also the mechanisms and work process of the total machine. The resulting total model can be large and laborious to solve.

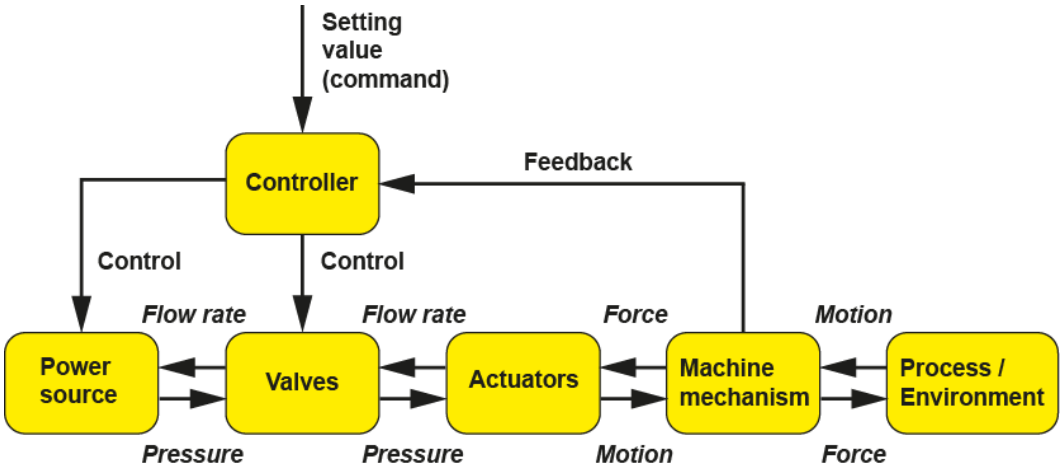

Figure 5. Interactions in hydraulically operated machine mechanism.

1.6 Feasibility of the model

Feasibility of the model is affected by:

- qualitative accuracy
- operational range
- identification ability
- parameter sensitivity
- stability
- computing speed

1.7 Golden rules of simulation

- always imitate the real world
- recognize what and when to idealize
- divide the problem to a set of controllable subsystems – model them one at a time
- model little by little and test – model little by little and test…
- make sure that you understand all the results and phenomena before you continue
- model what has to be modeled not what is easiest to model
- model only what has to be modeled not everything that you are able to model

1.8 Sectors of virtual testing

Virtual testing requires familiarity of applications, software, theory and parameter knowledge.

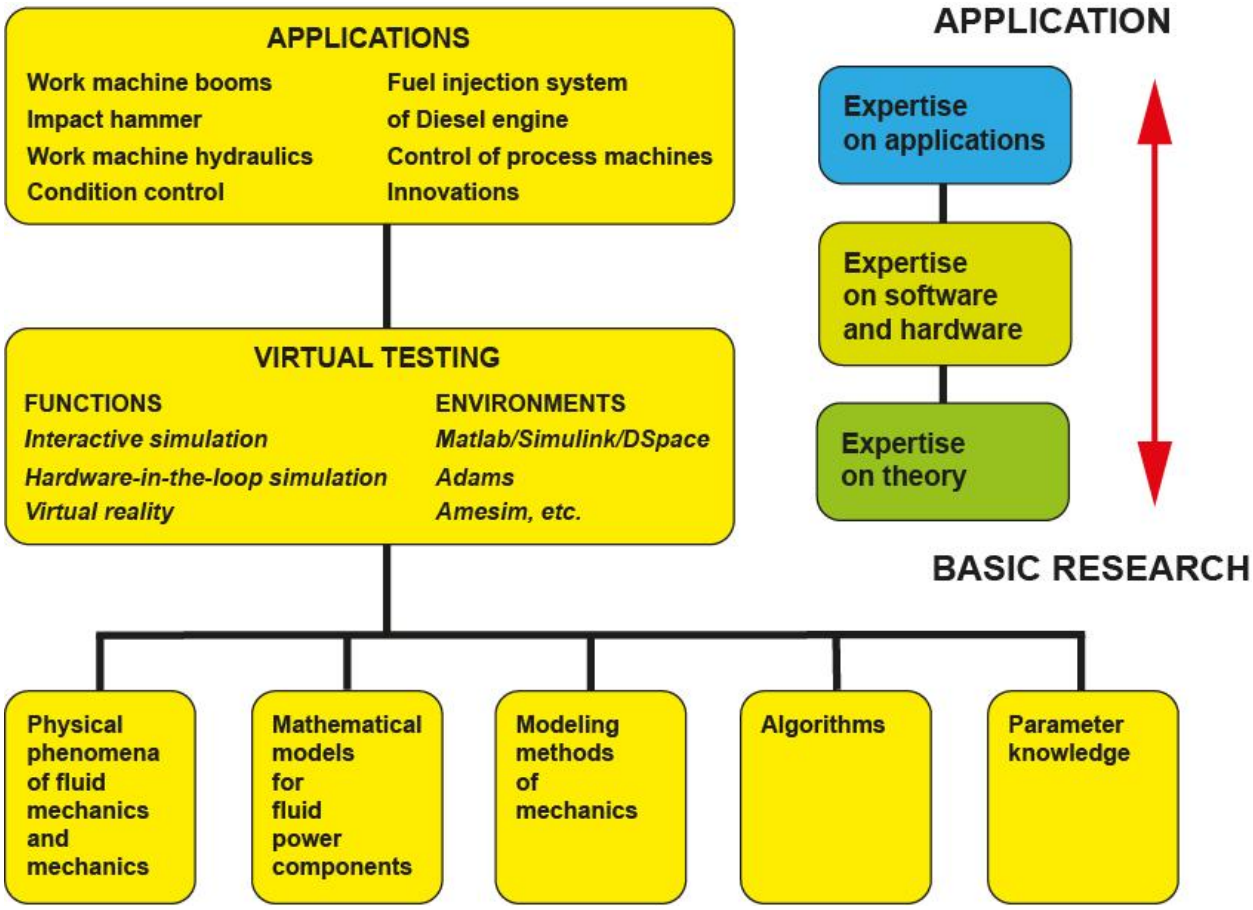

Figure 6. Sectors of virtual testing.

Simulation response is affected by
- model
- parameters
- integration algorithm

Question 1: Explain the concepts of qualitative and quantitative analysis.

Question 2. What factors affect to the validity of simulation results?

Question 3. Explain the characteristics of hydraulics systems in relation to modeling and simulation.

Question 4. What are the three main benefits of virtual testing?

Question 5. What are the three main frailties of virtual testing?

2 Modeling of fluid

2.1 Approximation of state equation of fluid

State equation of ideal gas

$$r = \frac{p}{Rq} \tag{2.1}$$

Density of fluid is a function of pressure and temperature. Let's define a state equation for fluid in relation to density that depends upon pressure and temperature. The state equation is impossible to deduce exactly from physical laws, but since the changes in density as a function of pressure and temperature are small, the first term of Taylor series can be used to approximate the state equation

$$r_f = r_{f,0} + \left(\frac{\partial r_f}{\partial p}\right)_0 (p - p_0) + \left(\frac{\partial r_f}{\partial q}\right)_0 (q - q_0) \tag{2.2}$$

where
r_f = fluid density
p = pressure
θ = temperature
$r_{f,0}$ = fluid density in initial state
p_0 = pressure in initial state
θ_0 = temperature in initial state

The most used form for linearized equation is:

$$r_f = r_{f,0}\left[1 + \frac{1}{K_f}(p - p_0) - a\,(q - q_0)\right] \tag{2.3}$$

where

$$K_f = r_{f,0}\left(\frac{\partial p}{\partial r_f}\right)_0 \text{ and } a = -\frac{1}{r_{f,0}}\left(\frac{\partial r_f}{\partial q}\right)_0$$

The quantity K_f is called the isothermic compression modulus or shortly and simply the bulk modulus, and it defines the change in pressure divided by the change in density in constant temperature. The quantity a is thermal expansion coefficient of volume and it defines the change in volume resulting from the change in temperature in constant pressure.

Hereafter an approximation will be used from where the thermal expansion coefficient α is omitted. The change in density will be calculated only as a function of pressure and by taking into account the air in fluid.

2.2 Air in the fluid

Air is present in the hydraulic system in two different ways.

1. Separated air, where air appears in form of single bubbles. In a running hydraulic system the amount of separated air is 0.1–5 % (vol.)
2. Dissolved air, where air is disperged into the molecular structure of fluid and is invisible. The amount of dissolved air in saturated fluid is represented by Henry's law

$$\frac{V_{\text{air,diss}}}{V_{\text{f}}} = S_{\text{c}} \frac{p}{p_{\text{at}}} \qquad (2.4)$$

where

$V_{\text{air,diss}}$ = volume of dissolved air in STP (standard temperature and pressure, 1 bar ja 273 K)
V_{f} = volume of fluid
S_{c} = solubility constant
p = prevailing fluid pressure
p_{at} = atmospheric pressure (1 bar)

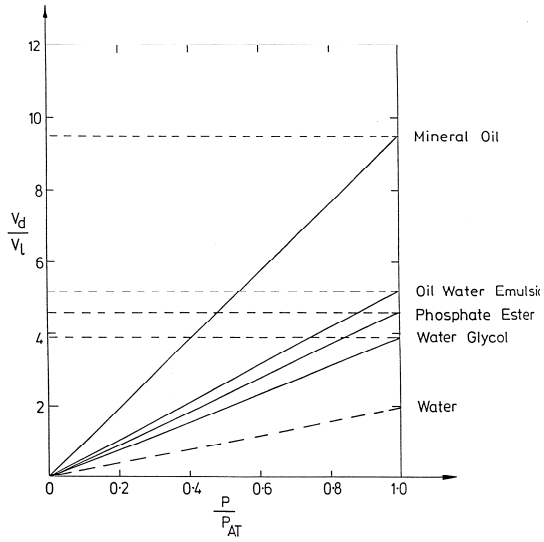

Figure 7. Amount of dissolved air in different hydraulic fluids. [Kuvaan muutettava $V_{\text{d}} \rightarrow V_{\text{air,diss}}$, $V_{\text{L}} \rightarrow V_{\text{f}}$, $\text{P} \rightarrow p$, $\text{P}_{\text{AT}} \rightarrow p_{\text{at}}$]

The momentary amount of dissolved air in fluid can either be greater or smaller than the amount given by Henry's law in which case fluid is either supersaturated or unsaturated. The elapsed time needed to reach the equilibrium state depends on the admixture of the fluid and the interface area between the fluid and air. The air separates from fluid quickly, but dissolves slowly. The dissolved air in fluid does not affect the properties of the fluid unlike the free air. Since the dissolved air in fluid always aspires to reach state of equilibrium the dissolved air is potential free air. When the pressure drops the dissolved air tries to separate from the fluid and to form free air in form of bubbles (compare, e.g., opening of soft drink bottle).

2.3 Density

Density of fluid is determined as mass per volume unit.

$$\rho_f = \frac{m_f}{V_f} \qquad (2.5)$$

where
m_f = mass of fluid

When pressure rises also the density rises and when temperature rises the density decreases. If the air concentration of fluid is low the density of fluid varies only little with pressure. On high concentrations the density depends heavily on pressure and on low values of pressure the density collapses (cavitation of fluid).

Fluid-air mixture is two-phase. Only the separated air has an effect on the properties of the fluid.

Fluid parameters
$\rho_{f,0}$ = density of fluid in initial state (p_0, θ_0)
$\rho_{air,0}$ = density of air in initial state (p_0, θ_0)
K_f = bulk modulus of fluid
k = polytropic gas constant
$\Lambda_{air,undiss}$ = relative portion of undissolved air in fluid-air mixture in initial state (p_0, θ_0)
p_0 = pressure in initial state

Variables
m_f = mass of fluid
m_{air} = mass of air
m_{f+air} = mass of fluid-air mixture
V_{air} = volume of air
V_f = volume of fluid
V_t = total volume (= $V_{air} + V_f = V_{f+air}$)
ρ_f = density of fluid
ρ_{f+air} = density of fluid-air mixture
p = pressure in fluid-air mixture

Define the air concentration, i.a., relative portion of free air of fluid-air mixture in initial state

$$\Lambda_{air,undiss} = \frac{V_{air,0}}{V_{f,0} + V_{air,0}} \qquad (2.6)$$

where subindex 0 refers to initial state.

Consider a unit volume in initial state where pressure and temperature have values (p_0, θ_0).

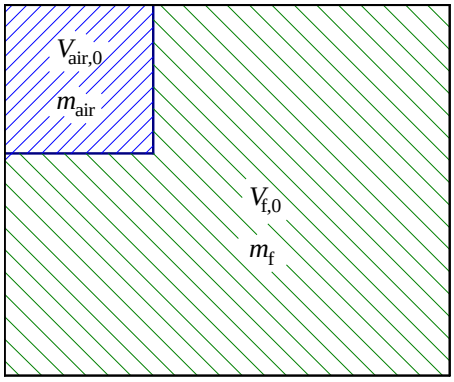

Figure X1. Unit volume consisting of separate fluid and air volumes in initial state.

In initial state the volume of air is

$$V_{air,0} = \mathrm{L}_{air,undiss} \tag{2.7}$$

Mass of air is constant, only the volume changes as a function of pressure

$$m_{air} = \mathrm{L}_{air,undiss}\, \rho_{air,0} \tag{2.8}$$

Volume of air is

$$p_0 V_{air,0}^{k} = p V_{air}^{k} \tag{2.9}$$

$$V_{air} = \left(\frac{p_0}{p}\right)^{\frac{1}{k}} \mathrm{L}_{air,undiss} \tag{2.10}$$

Volume of fluid in initial state

$$V_{f,0} = 1 - \mathrm{L}_{air,undiss} \tag{2.11}$$

Mass of fluid

$$m_f = \rho_{f,0} V_{f,0} \tag{2.12}$$

Volume of fluid is

$$V_f = \frac{V_{f,0}}{1 + \frac{1}{K_f}(p - p_0)} = \frac{1 - \mathrm{L}_{air,undiss}}{1 + \frac{1}{K_f}(p - p_0)} \tag{2.13}$$

Density of fluid-air mixture is

$$\rho_{f+air} = \frac{m_{air} + m_f}{V_{air} + V_f} \tag{2.14}$$

$$\rho_{f+air} = \frac{\Lambda_{air,undiss}\,\rho_{air} + \rho_{f,0}(1 - \Lambda_{air,undiss})}{\left(\frac{p_0}{p}\right)^{\frac{1}{\kappa}}\Lambda_{air,undiss} + \frac{1 - \Lambda_{air,undiss}}{1 + \frac{1}{K_f}(p - p_0)}} \tag{2.15}$$

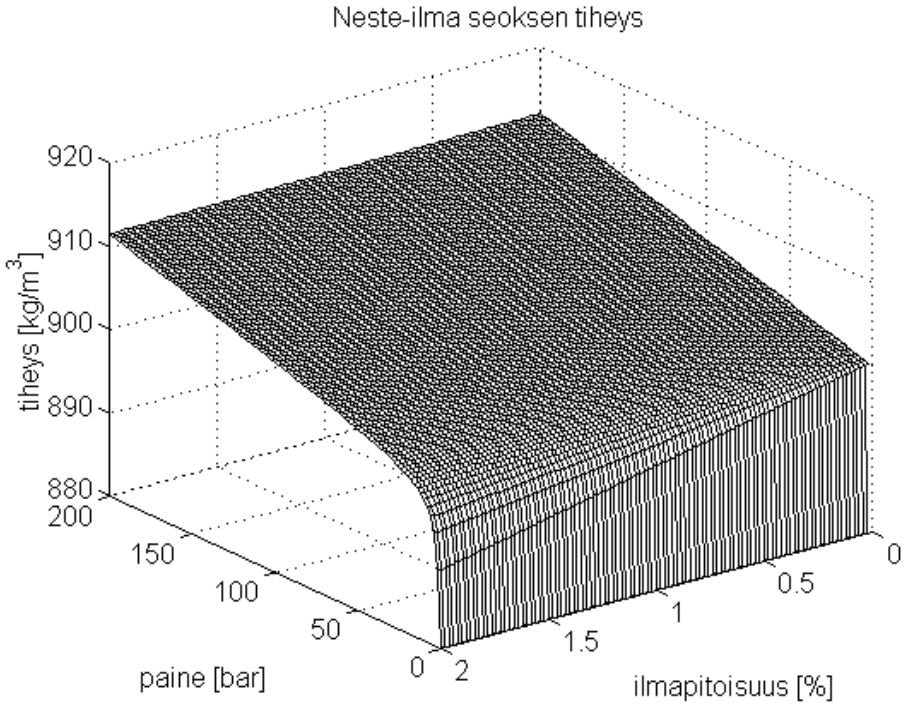

Figure 8. An example of fluid density as a function of pressure and concentration of separated air. [Kuvan tekstit käännettävä englanniksi. Kuvaan muutettava tiheys → ρ_f, paine → p, ilmapitoisuus → $\Lambda_{air,undiss}$×100]

2.4 Compressibility

Compressibility expresses the dependence of fluid volume on pressure and is typically described with bulk modulus K_f.

$$K_f = -V_{f,0}\frac{dp}{dV_f} = -\frac{m_{f,0}}{\rho_{f,0}}\frac{\partial p}{\partial \rho_f}\frac{\partial \rho_f}{\partial V} = -\frac{m_{f,0}}{\rho_{f,0}}\frac{\partial p}{\partial \rho_f}\frac{-m_{f,0}}{V_0^2} = \rho_{f,0}\frac{1}{\frac{\partial \rho_f}{\partial p}} \tag{2.16}$$

The bulk modulus of oils used in hydraulic systems is in range 150–1400 MPa. Value of bulk modulus depends on temperature, pressure and air concentration of fluid. Bulk modulus rises with pressure, but the effect is minor and when operating under pressures of 30 MPa the effect can be considered neglible. The effect of temperature is more significant and with rising temperature the value of bulk modulus decreases. The effect of free air is the most significant and with rising

concentration of free air the bulk modulus decreases rapidly and can reach values of only 150 MPa.

The value of effective bulk modulus $K_{e,f+air}$ of fluid-air mixture can be solved by substituting the density of this mixture into the definition of bulk modulus according to the approximation of state equation. The density of fluid-air mixture is solved by substituting $p = p_0$.

$$\rho_{f+air,0} = \varepsilon_{air,undiss}\,\rho_{air} + \rho_{f,0}\,(1 - \varepsilon_{air,undiss}) \tag{2.17}$$

$$K_e = \rho_{f+air,0}\,\frac{1}{\frac{\partial \rho_{f+air}}{\partial p}} \tag{2.18}$$

$$K_{e,f+air} = -\frac{\left(\frac{p_0}{p}\right)^{\frac{1}{k}}\varepsilon_{air,undiss} + \frac{1-\varepsilon_{air,undiss}}{\left(1+\frac{p-p_0}{K_f}\right)^2}}{-\frac{\left(\frac{p_0}{p}\right)^{\frac{1}{k}}\varepsilon_{air,undiss}}{k\,p} - \frac{1-\varepsilon_{air,undiss}}{\left(1+\frac{p-p_0}{K_f}\right)^2 K_f}} \tag{2.19}$$

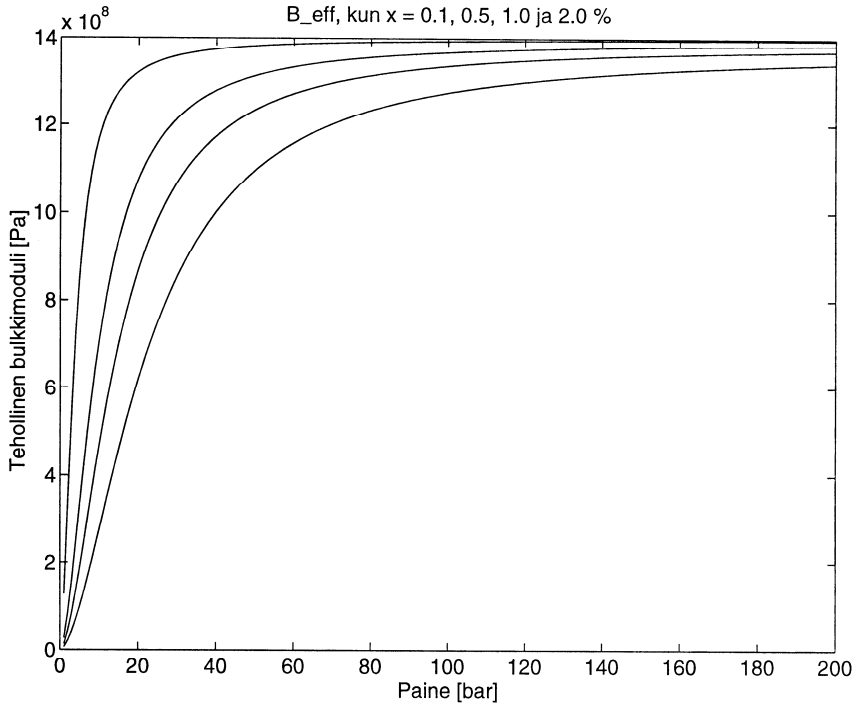

Figure 9. Effective bulk modulus of fluid-air mixture as a function of pressure. [Kuvan tekstit käännettävä englanniksi. Kuvaan muutettava B_eff → K_e, Paine → p, Tehollinen bulkkimoduli → K_e]

2.5 Continuity equation

The equation for pressure generation in control volume V_{ctrl} is derived by using the continuity equation based on mass conservation in which the density and bulk modulus are assumed to be constants. The control volume is a certain geometric volume whose magnitude in initial state is $V_{\mathrm{ctrl},0}$. The mass of fluid in this volume is the difference between incoming and outgoing mass flow.

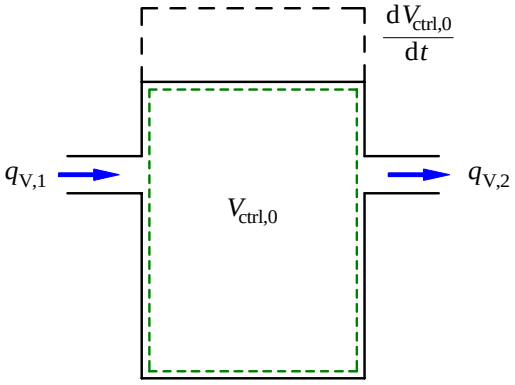

Figure 10. Control volume.

$$\sum \frac{\mathrm{d}m_{\mathrm{f},1}}{\mathrm{d}t} - \sum \frac{\mathrm{d}m_{\mathrm{f},2}}{\mathrm{d}t} = \frac{\mathrm{d}m_{\mathrm{f}}}{\mathrm{d}t} = \frac{\mathrm{d}\left(\rho_{\mathrm{f}} V_{\mathrm{f},0}\right)}{\mathrm{d}t} \tag{2.20}$$

On the other hand the mass flow can be determined with flow rate

$$\frac{\mathrm{d}m_{\mathrm{f}}}{\mathrm{d}t} = \rho_{\mathrm{f}} q_{\mathrm{V}} \tag{2.21}$$

Since the density of incoming and outgoing fluid is the same, it yields to

$$\sum \rho_{\mathrm{f},1} q_{\mathrm{V},1} - \sum \rho_{\mathrm{f},2} q_{\mathrm{V},2} = \rho_{\mathrm{f}} \frac{\mathrm{d}V_{\mathrm{ctrl},0}}{\mathrm{d}t} + V_{\mathrm{ctrl}} \frac{\mathrm{d}\rho_{\mathrm{f}}}{\mathrm{d}t} \tag{2.22}$$

When determining (as in Kirchhoff's law) the incoming flow as positive and the outgoing flow as negative, the flows can be summed. Using the determination of density conforming the approximation of state equation and by substituting and differentiating the continuity equation gets a form of

$$\rho_{\mathrm{f}} = \rho_{\mathrm{f},0} + \frac{\rho_{\mathrm{f}}}{K_{\mathrm{f}}} p \tag{2.23}$$

$$\left(\rho_{\mathrm{f},0} + \frac{\rho_{\mathrm{f},0}}{K_{\mathrm{f}}} p\right) \sum q_{\mathrm{V}} = \rho_{\mathrm{f},0} \frac{\partial V_{\mathrm{ctrl}}}{\partial t} + V_{\mathrm{ctrl},0} \frac{\partial \rho_{\mathrm{f}}}{\partial t}$$

$$\rho_{\mathrm{f},0}\left[\left(1 + \frac{1}{K_{\mathrm{f}}} p\right) \sum q_{\mathrm{V}} - \frac{\partial V_{\mathrm{ctrl}}}{\partial t}\right] = V_{\mathrm{ctrl},0} \frac{\partial \rho_{\mathrm{f}}}{\partial p} \frac{\partial p}{\partial t}$$

$$\rho_{f,0}\left(1+\frac{1}{K_f}p\right)\sum q_V-\frac{\partial V_{ctrl}}{\partial t}=V_{ctrl,0}\,\rho_{f,0}\frac{1}{K_e(p)}\frac{\partial p}{\partial t}$$

$$\left(1+\frac{1}{K_f}p\right)\sum q_V-\frac{\partial V_{ctrl}}{\partial t}=\frac{V_{ctrl,0}}{K_e(p)}\frac{\partial p}{\partial t}$$

$$\frac{dp}{dt}=\frac{K_e(p)}{V_{ctrl,0}}\left[\left(1+\frac{1}{K_f}p\right)\sum q_V-\frac{\partial V_{ctrl}}{\partial t}\right] \qquad (2.24)$$

Equation (*2.24*) can be simplified

1. By assuming $p << K_f$ in which case the error in calculated density is approx. 2 % at pressure level of 200 bar.
2. By assuming K_e to be constant. The resulting error in calculated density is acceptable at pressure levels over 100 bar, but at lower pressure levels this assumption results into significant errors especially if the air concentration of fluid is high.

Using these assumptions results into the equation of pressure generation that is widely used in hydraulics but which does not fully comply the law of mass conservation.

$$\frac{dp}{dt}=\frac{K_e}{V_{ctrl,0}}\left[\sum q_V-\frac{\partial V_{ctrl}}{\partial t}\right] \qquad (2.25)$$

2.6 Viscosity

Viscosity describes the internal friction of the fluid. It has been experimentally noted that the flow velocity on a surface of an object placed in flow is zero. This holds for both internal and external flow. When fluid particles move in relation to each other the molecular forces induce shear stress

$$\tau=\eta\frac{dv}{dy} \qquad (2.26)$$

where dv is the velocity difference between two fluid layers, dy is the distance between those layers and η is the **absolute i.e. dynamic viscosity**. The **kinematic viscosity** which is usually used in theoretic examinations is determined

$$\nu=\frac{\eta}{\rho_f} \qquad (2.27)$$

Kinematic viscosity is announced usually in units of cSt (centistoke), 1 cSt = 10^{-6} m^2/s.

Unlike water, the viscosity of hydraulic oils is highly dependent on temperature. The viscosity decreases with rising temperature and the fluid flows easier. Also the pressure has an effect on the viscosity which rises with rising pressure, but in normal pressure ranges (under 40 MPa) the rise is insignificant. Besides these, also the free air in fluid has a minor viscosity rising effect.

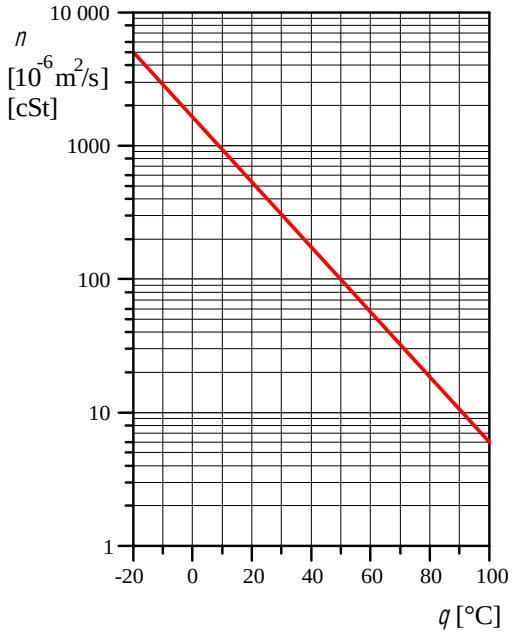

Figure 11. An example of viscosity of hydraulic oil as a function of temperature.

θ_1 = 233 K (= -40 ºC) → ν = 1200 cSt
θ_2 = 273 K (= 0 ºC) → ν = 78 cSt
θ_3 = 313 K (= 40 ºC) → ν = 26 cSt
θ_4 = 373 K (= 100 ºC) → ν = 10 cSt

HUOM: YLLÄOLEVAT LUKUARVOT EIVÄT LIITY KUVAAN 11

The temperature dependence of viscosity can be expressed according to ASTM D 341-43:

$$n_3 = e^{\Phi} - 0.7 \qquad (2.28)$$

where

$$\Phi = e^{Y}$$

$$Y = Y_1 - \frac{Y_1 - Y_2}{X_1 - X_2}(X_1 - X_3)$$

$$X_1 = \log(q_1) \quad Y_1 = \log(\log(n_1 + 0.7))$$
$$X_2 = \log(q_2) \quad Y_2 = \log(\log(n_2 + 0.7))$$
$$X_3 = q_3$$

θ_1 = temperature at first determination point [K]
n_1 = viscosity at temperature θ_1 [cSt]
θ_2 = temperature at second determination point [K]
n_2 = viscosity at temperature θ_2 [cSt]
θ_3 = temperature at operating point [K]

Question 1: Explain the effect of temperature and pressure on viscosity.

Question 2: Explain the meaning of Henry's law.

Question 3: How does the temperature, pressure and free air affect to the value of bulk modulus?

Question 4: Calculate the effective bulk modulus $K_{e,1}$ with accurate equation (*2.24*) and $K_{e,2}$ with approximative equation (*2.18*) when p_0 = 1 bar, K_f = 1500 MPa, $K_{air} = 1.4 \times p$, $V_{air,0}$ = 0.002 m^3 , V_t = 0.1 m^3 , k = 1.4, all values in standard temperature and pressure (STP) and
p = 50 bar ($K_{e,1}$ = 1156 MPa , $K_{e,2}$ = 1208 MPa)
p = 150 bar ($K_{e,1}$ = 1411 MPa , $K_{e,2}$ = 1471 MPa)

3 Flow in valves

3.1 Bernoulli equation

Consider a stationary flow of non-compressible and frictionless fluid in a piping system with varying elevations and flow channel forms. The statement of the conservation of energy that combines the local pressure energy, potential energy and kinetic energy in each point of the system is called the Bernoulli equation

$$p + \rho g z + \frac{\rho v^2}{2} = \text{constant} \qquad (3.1)$$

When Bernoulli equation is applied to two points of a system and also the friction induced losses between those points are taken into account the resulting equation is:

$$p_1 + \rho g z_1 + \frac{\rho v_1^2}{2} = p_2 + \rho g z_2 + \frac{\rho v_2^2}{2} + \Delta p_s \qquad (3.2)$$

where Δp_s is the loss term.

3.2 Flow types and flow related phenomena

A throttle in hydraulic system resists fluid flow and thus it can be used to control volume flow. The throttle geometries used in hydraulic valves can have several forms.

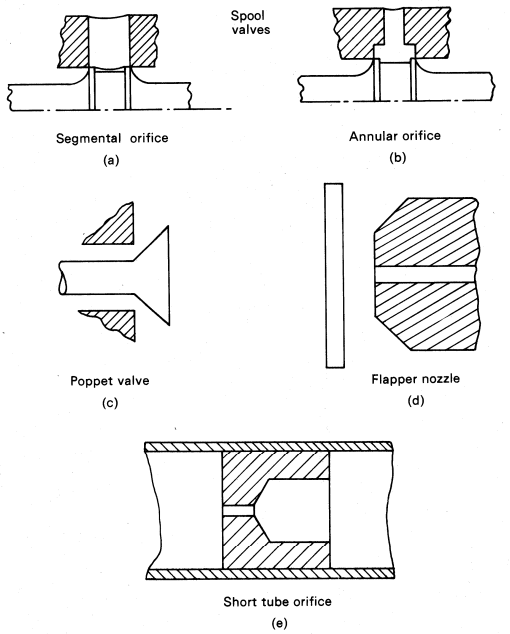

Figure 12. Throttle geometries used in hydraulic valves [10].

Flow can be either laminar or turbulent by nature. In laminar (aka layered or streamlined) flow all fluid particles follow a certain path called streamline and move parallel in relation to each other. When the flow velocity increases the flow becomes turbulent, in which the fluid particles move chaotically but on average to a certain flow direction.

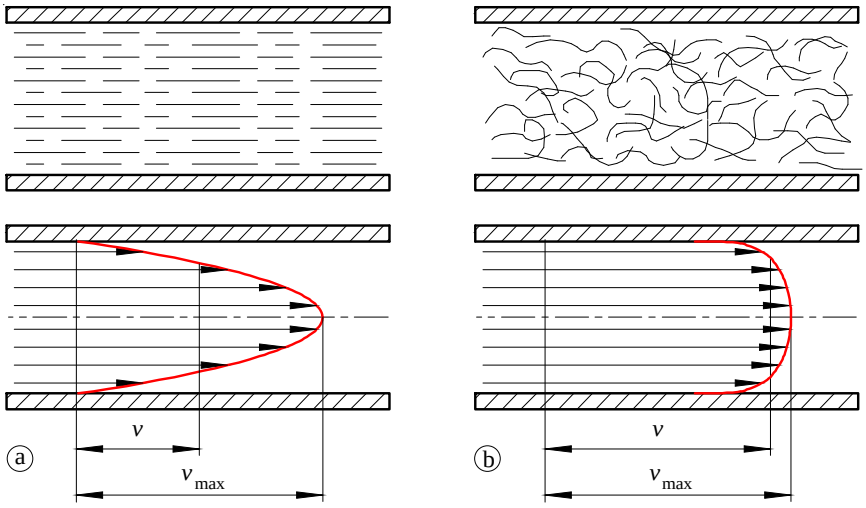

Figure 13. Laminar (a) and turbulent (b) flow [7].

The flow type can be solved computationally with the help of unitless Reynold's number (*Re*), which represents the ratio of inertial forces to viscous forces in fluid. This computational number is compared with an experimentally determined critical Reynold's number (Re_{cr}), which expresses the point when change for laminar flow to turbulent occurs. Flow is laminar when $Re < Re_{cr}$, and turbulent when $Re > Re_{cr}$. The value of critical Reynold's number varies with the properties of flow channel, Table 1 presents values for some typical channel cases.

Table 1. Values for critical Reynold's number. [7]

Flow channel	$\boldsymbol{Re_{cr}}$
Round, smooth surfaced tubes	2000–2300
Central smooth surfaced gaps	1100–1200
Noncentral smooth surfaced gaps	1000–1050
Central grooved gaps	700
Noncentral grooved gaps	400
Control grooves of spool valves	250–275
Flap and conical seat valves	25–100

Reynold's number is defined as [7]

$$Re = \frac{v D_H}{n} \tag{3.3}$$

where D_H is hydraulic diameter [7]:

$$D_H = \frac{4 A_{fc}}{U_{fc}} \tag{3.4}$$

where A_{fc} is the area and U_{fc} is the circumference of the cross-section of flow channel.

Flow does not change instantly from laminar to turbulent, but through a transition region, where the both flow types appear combined.

3.2.1 Flow in nozzles

Consider an abrubt narrowing of the circumference of a flow channel (i.e. throttle). The Bernoulli equation for this can be written as [7].

$$p_1 + \rho_f g z_1 + \frac{\rho_f v_1^2}{2} = p_2 + \rho_f g z_2 + \frac{\rho_f v_2^2}{2} \qquad (3.5)$$

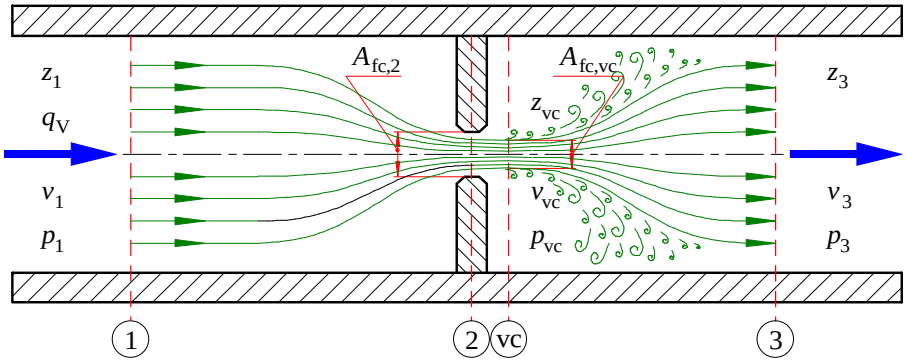

Figure 14. Laminar (left) and turbulent (right) flow in a throttle. Kuvaan liittyvään tekstiin voisi laittaa maininnan virtauksen käyttäytymisestä kuristuksessa ja kuvauksen eri tarkastelupisteiden ”olemuksesta”.

The area of circumference of the throttle is assumed to be substantially smaller compared to the corresponding area of the pipe and thus according to the continuity equation $v_2 \gg v_1$. The observation points 1 and 2 (on central axis of the pipe) are on the same elevation and thus $z_1 = z_2$. With these assumptions the equation is simplified to [7]

$$p_1 - p_2 = \frac{\rho_f v_2^2}{2} \qquad (3.6)$$

which points out that in the throttle the pressure energy turns partially to kinetic energy. By substituting the continuity equation to the above and solving the volume flow it results into [7]

$$q_{V,2} = A_{fc,2}\sqrt{\frac{2\Delta p}{\rho_f}} \qquad (3.7)$$

where $q_{V,2}$ is the flow passing through the throttle with pressure difference Δp.

Besides pressure difference, density and flow area, the flow passing through the throttle is also affected by the properties of the flow port, like shape and the sharpness of the edges. These properties are taken into account with discharge coefficient C_d. The equation can now be written un general form [7]:

$$q_V = C_d A_{fc}\sqrt{\frac{2\Delta p}{\rho_f}} \qquad (3.8)$$

3.2.2 Flow in narrow gaps

In hydraulics narrow (typically circular) gaps are used for bearing and sealing purposes. Flow characteristics of narrow gaps are interesting when studying, e.g., the leakage flows in spool valves or lubricating properties of bearings. The flow through a narrow circular gap is typically calculated with traditional laminar flow equation [2], which covers the both cases of central and noncentral gaps. [Tämän tekstin tueksi tarvitaan kuva yhtälön kuvaamasta tilanteesta]

$$q_V = \frac{\left(1 + 1.5\left(\frac{\varepsilon}{h_g}\right)^2\right)\pi D_{vs} h_g^3}{12\,\rho_f\,\nu\,l_g}\Delta p \qquad (3.9)$$

However, the gaps in hydraulic components are usually relatively short for which cases the above equation gives too high values of volume flow. Ellman et al. [2] has formulated a model that enables more precise calculation of volume flow. The pressure losses in narrow gaps are comprised of the losses in circular gap and the end (inflow and outflow) losses. The pressure loss in circular gap can be calculated with equation (*3.6*) and the end losses with equation

$$\Delta p = \zeta\,\rho_f\,\frac{v^2}{2} \qquad (3.10)$$

Value of loss factor ζ for inflow to a sharp edged gap is 0.5 and for outflow 1.0 [13]. These two can be combined to a one loss factor ζ = 1.5. By combining the equations (*3.9*) and (*3.10*) Ellman et al. suggest the following model to calculate the laminar flow through a circular gap [2]:

$$q_V = \frac{Y_2}{2}\left(\sqrt{\left(\frac{Y_2}{Y_1}\right)^2 + 4\Delta p} - \frac{Y_2}{Y_1}\right) \qquad (3.11)$$

where

$$Y_1 = \frac{\left(1 + 1.5\left(\frac{\varepsilon}{h_g}\right)^2\right)\pi D_{vs} h_g^3}{12\,r_f\,\nu\,l_g} \quad ; \quad Y_2 = \frac{1}{\sqrt{\zeta}}\,p\,D_{vs}\,h_g\sqrt{\frac{2}{r_f}}$$

With high viscosity-temperature dependent fluids the temperature of the fluid has a strong effect on the magnitude of flow passing through the gap. Besides the temperature of inflowing fluid (θ_1) also the temperature rise in the gap must be taken into account. This temperature rise and the temperature of outflowing fluid (θ_2) can be calculated using the power loss occurring in the gap (equation (*3.10*)).

$$\Delta p\,q_V = \Delta q\,\dot{m}\,c_p \quad ; \quad q_2 = \frac{\Delta p}{r_f\,c_p} + q_1 \qquad (3.12)$$

3.3 Equation for turbulent flow in throttles

Consider the sharp edged throttle in Fig. 14 (see also Fig. 18). With high values of Reynold's number the fluid flowing through the throttle forms a jet flow whose narrowest point (vc) is called *vena contracta*. On the downstream side of this point the turbulence causes the spreading and mixing of the jet flow.

When considering the energy in the cross-sections of upstream point (1) and in vena contracta (vc) the Bernoulli equation yields to a form [12]:

$$p_1 + \frac{\rho_f}{2} v_1^2 = p_{vc} + \frac{\rho_f}{2} v_{vc}^2 + \Delta p_s \qquad (3.13)$$

where Δp_s is friction loss between cross-section points 1 and vc, ρ_f is density of fluid and v is flow velocity. The continuity of flow yields to a equation [12]:

$$A_{fc,1}\, v_1 = A_{fc,2}\, v_2 = A_{fc,vc}\, v_{vc} \qquad (3.14)$$

where A_{fc} is the cross-sectional flow area.

Cross-sectional area $A_{fc,vc}$ is relative to the area of the opening of throttle and can be calculated by multiplying the area of throttle ($A_{fc,2}$) with **contraction coefficient C_c** [12]:

$$A_{fc,vc} = C_c\, A_{fc,2} \qquad (3.15)$$

Combining the equations (*3.13*), (*3.14*) and (*3.15*) yields to [11];

$$v_{vc} = \frac{1}{\sqrt{1 - \left(C_c \frac{A_{fc,2}}{A_{fc,1}}\right)^2}} \sqrt{\frac{2}{\rho_f}(p_1 - p_{vc}) - \Delta p_s} \qquad (3.16)$$

Next let's define the **velocity coefficient C_v** [12]

$$C_v = \sqrt{1 - \frac{\Delta p_s}{\Delta p}} \qquad (3.17)$$

where $\Delta p = p_1 - p_{vc}$.

Using the definition of velocity coefficient the equation (*3.16*) yields to [12]:

$$v_{vc} = \frac{C_v}{\sqrt{1 - \left(C_c \frac{A_{fc,2}}{A_{fc,1}}\right)^2}} \sqrt{\frac{2\Delta p}{\rho_f}} \qquad (3.18)$$

Since flow rate $q_V = A_{fc,vc}\, v_{vc} = A_{fc,2}\, v_2$, the equation (*3.18*) can be written in form of [12]:

$$q_V = \frac{C_v\, C_c\, A_{fc,2}}{\sqrt{1 - \left(C_c \frac{A_{fc,2}}{A_{fc,1}} \right)^2}} \sqrt{\frac{2\,\Delta p}{\rho_f}} \qquad (3.19)$$

Next let's define the **discharge coefficient C_d** [12]

$$C_d = C_c\, C_v \qquad (3.20)$$

With this the equation (*3.19*) gets a form of [12]:

$$q_V = \frac{C_d\, A_{fc,2}}{\sqrt{1 - \left(C_c \frac{A_{fc,2}}{A_{fc,1}} \right)^2}} \sqrt{\frac{2\,\Delta p}{\rho_f}} \qquad (3.21)$$

If the cross-sectional area on the upstream side is large (as it usually is in hydraulic systems) the significance of the velocity of incoming flow is minor and the equation for volume flow can be presented as [12]:

$$q_V = C_d\, A_{fc,2} \sqrt{\frac{2\,\Delta p}{\rho_f}} \qquad (3.22)$$

In typical hydraulic components the measurement of the value of discharge coefficient C_d according to its definition is practically impossible. According to equation (*3.22*) the coefficient was determined semi-empirically as follows [12]:

$$C_d = \frac{q_V}{A_{fc,2} \sqrt{\frac{2\,\Delta p}{\rho_f}}} \qquad (3.23)$$

where Δp is the pressure difference between the upstream point of flow (1) and vena contracta (vc). In real valves it is almost without exception impossible to measure the pressure in vena contracta and thus it is common to determine the discharge coefficient using the pressure difference between an upstream point and a point that is located to a suitable distance downstream from the throttle. However, the coefficient measured this way is not discharge coefficient even though it is often incorrectly referred as such. This type of measurement results to a coefficient called **flow coefficient C_q** which is determined by equation [12]:

$$C_q = \frac{q_V}{A_{fc,2} \sqrt{\frac{2(p_1 - p_3)}{\rho_f}}} \qquad (3.24)$$

where p_3 is the pressure of a arbitrarily selected downstream point.

In hydraulics the product C_qA is typically known, since it can be defined by measuring the pressure difference over the throttle and the volume flow passing through the throttle. C_qA is usually announced in component data sheets.

3.3.1 Modified model of throttle

The derivate of traditional turbulent throttle equation results into value of infinity when the pressure difference over the throttle decreases down to zero. This is numerically problematic since in this case the integration algorithms typically used in simulation software either stop calculation completely or continue it with very small steps which results into long computing times. Ellman and Piché have proposed an empirical model that can be used to avoid this problem [2]. The model is comprised of laminar and turbulent parts whose transition region is smooth and the model does not have a singular derivate. Thus it is applicable to very accurate and trouble-free simulation.

Numerical problem arises always when the pressure difference over the throttle reduces down to zero. The problem is caused by the singular derivate of pressure in conventional equation for turbutent throttle (*3.21*).

The dependence of volume flow passing through a throttle as a function of the pressure difference over the throttle and the Reynold's number prevailing in transition point is presented in Fig. 15. The numerical problemacy of calculation that occurs with low values of pressure difference and Reynold's number is noticeable in the figure.

Since simulation in hydraulic systems typically concentrates on turbulent flow related phenomena the throttle model does not have to be exactly accurate in the region of laminar flow. On the contrary it is rather desirable that the model is based on a low number of available physical parameters because the parameter data required in accurate modeling is rarely available. The model to be presented next is based on these conclusions.

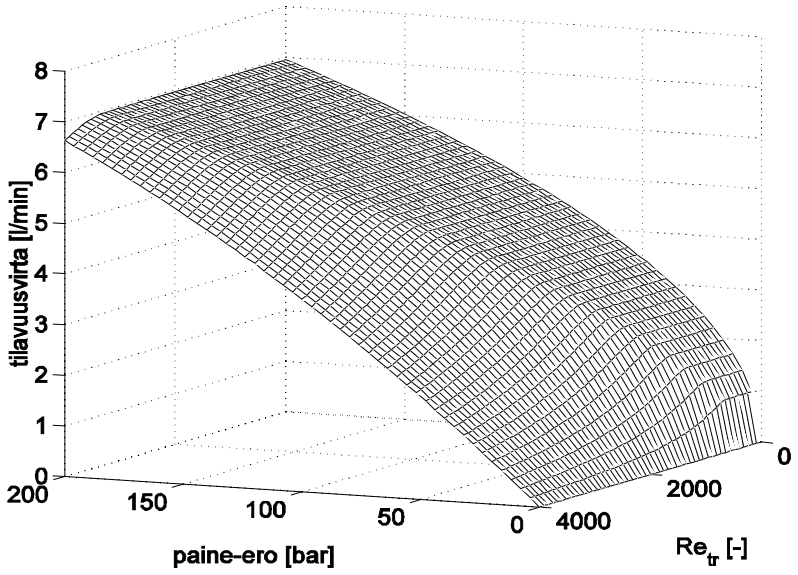

Figure 15. Volume flow in a throttle as a function of D*p* ja Re_{tr}. [Kuvan tekstit käännettävä englanniksi. Kuvaa muutettava seuraavasti: tilavuusvirta → q_V, paine-ero → Δp].

The volume flow through the throttle can be determined with two parameters, flow coefficient C_q and Reynold's number *Re*. Of these the first is defined in equation (3.24) and the latter in equation (*3.3*).

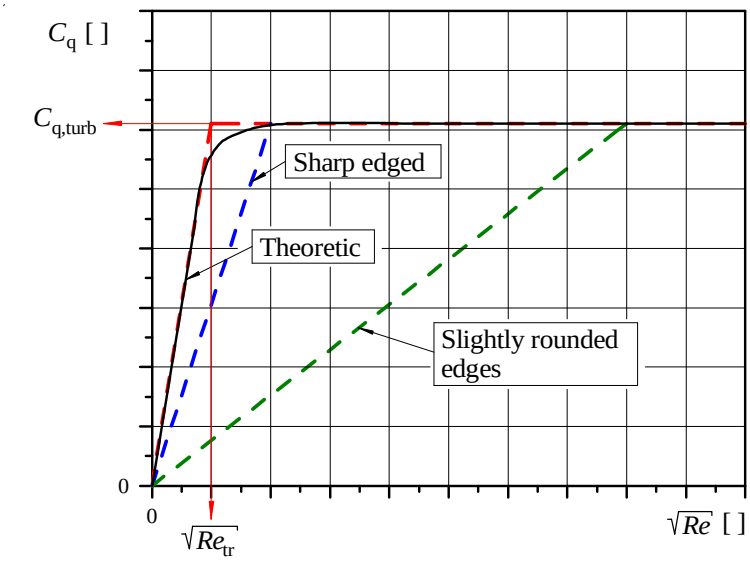

Figure 16. Flow coefficient as a function of Reynold's number with different types of throttle edges.

Fig. 16 presents the typical C_q - $\sqrt{Re}$ dependence. When the pressure difference is greater than the transition pressure difference Δp_{tr} the flow coefficient is approximated with a constant $C_{q,turb}$. This corresponds to high Reynold's numbers and the equation of volume flow yields a familiar form [1]:

$$q_V(\Delta p) = q_{V,turb}(\Delta p) := C_{q,turb}\, A_{fc} \sqrt{\frac{2\,\Delta p}{\rho_f}} \quad ; (\Delta p > \Delta p_{tr}) \tag{3.25}$$

Derivate of the volume flow function is assumed to have a value conforming to the slope of the dashed line in Fig. 16 when Δp = 0 [2]:

$$q_V^*(0) = \frac{2\,C_{q,turb}^{\ 2}\, A_{fc}\, D_{H,fc}}{\rho_f\, \nu\, Re_{tr}} \tag{3.26}$$

where Re_{tr} is the Reynold's number in transition point. Model uses a polynome to smooth out the transition between laminar and turbulent flow conditions. The polynome in equation (*3.27*) satisfies the continuity of q_V and q_V^* in transition point and also the requirement $q_V(0)$ = 0 [2].

$$q_V(\Delta p) = \frac{3\,A_{fc}\,\nu\,Re_{tr}}{4\,D_{H,fc}} \left(\frac{\Delta p}{\Delta p_{tr}}\right) \left(3 - \frac{\Delta p}{\Delta p_{tr}}\right); (0 \le \Delta p \le \Delta p_{tr}) \tag{3.27}$$

The flow turns from laminar to turbulent in point [2]:

$$\Delta p_{\mathrm{tr}} = \frac{9\,Re_{\mathrm{tr}}^{\,2}\,\rho_{\mathrm{f}}\,\nu^{2}}{8\,C_{\mathrm{q,turb}}^{\,2}\,D_{\mathrm{H,fc}}^{\,2}} \qquad (3.28)$$

This corresponds to Reynold's number $1.5 \times Re_{\mathrm{tr}}$. Thus the model replaces the infinite derivate of throttle equation with a finite derivate in point of $\Delta p = 0$. This enables the converging of integrating algorithms with all values of pressure difference.

3.3.2 Cavitation

The term cavitation refers to a process that includes nucleation of vapour- and/or gas-filled bubbles in fluid, the growth of the bubbles and finally their collapse. These bubbles are formed in fluid whose pressure for a reason or another reduces to a level that is lower than the vapour pressure of the fluid in the prevailing fluid temperature. When these bubbles are again subjected to a higher pressure they collapse rapidly which can cause very high pressures.

[Sisältönsä puolesta edellisen kappaleen tulisi kuulua: Cavitation is a process where vapour- and/or gas-filled bubbles are formed in fluid as a result of the fluid pressure reducing to level that is lower than the vapour pressure of the fluid in the prevailing fluid temperature. When these bubbles are subjected to a higher pressure they collapse very rapidly which can cause very high but short lived local pressures (i.e. pressure shocks).]

When the fluid pressure reduces sufficiently the air dissolved in fluid starts to separate through a process in which the dissolved air diffuses through a wall of nucleing and growing bubble thus forming free air. If the fluid pressure reduces down to the vapour pressure of the fluid in the prevailing temperature the bubble starts also to fill with vapour. In the following, this air and vapour-filled bubble is called the cavitation bubble. When the growing bubble is subjected to a rising pressure it's growth stops first and when the pressure rises enough the bubble starts to shrink. Eventually the bubble vanishes as a result of vapour condensation and air dissolving back into fluid. If the bubble is mostly vapour-filled and is subjected to a rapid pressure rise the vanishing happens "explosively" which phenomena is usually called the collapsing or implosion of the bubble. If the gas concentration of the bubble is high the vanishing process is slower and less dramatic.

Consider the sharp edged throttle presented in Fig. 17. The graph indicates the change in static pressure with different values of downstream pressures p_3 of throttle when the volume flow through the throttle is kept constant. Static pressure reaches its minimum value at the point where the cross-sectional area of flow is at narrowest and the flow velocity is at highest (*vena contracta*). In the following, the pressure upstream of the throttle is called the supply pressure p_1 and the pressure downstream of the throttle is called the back pressure p_3.

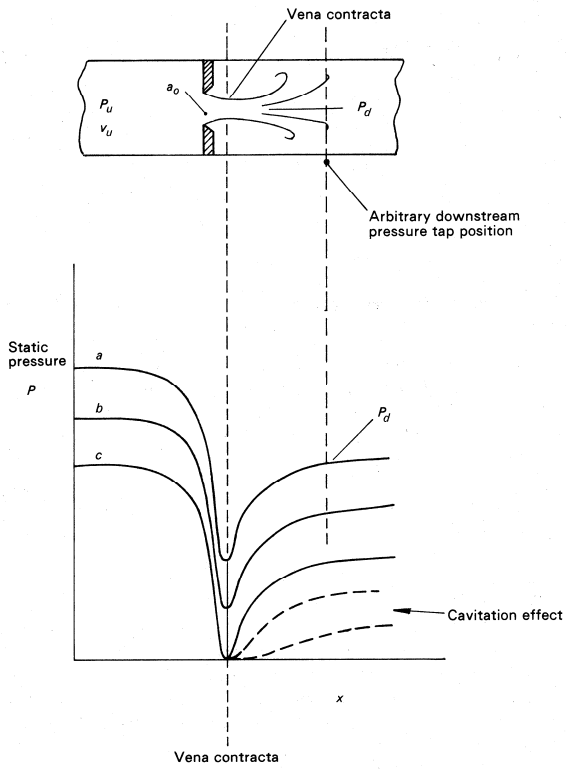

Figure 17. Behaviour of static pressure in a throttle [12]. [Kuvaa muutettava seuraavasti: $P_u \rightarrow p_1$, $P_d \rightarrow p_3$, $P \rightarrow p$, $v_u \rightarrow v_1$, $a_0 \rightarrow A_{fc,2}$].

At sufficiently high values of back pressure (continuous lines a, b and c in Fig. 17) the pressure difference between supply and back pressures remains constant at all of the pressure levels. When the back pressure gets a sufficiently low value the fluid pressure at the narrowest point of flow reaches the level of vapour pressure of the fluid and the flow starts to cavitate (line c). If the back pressure is reduced further the cavitation area extends ever longer downstream of the throttle (dashed lines). The faster is the pressure rise downstream of the throttle the violently the cavitation bubbles collapse ("implosion").

When the pressure difference over the throttle gets a sufficiently high value the flow starts to cavitate. This begins if the front edge of throttle is sufficiently sharp and the flow comes loose of the throttle wall. In this case the vapour filled volume and the point of *vena contracta* is formed inside the throttle, Fig. 18. If the back pressure is reduced the cavitation phenomena intensifies and the vapour filled volume/area in the throttle extends ever further. [Tässä kohtaa tämän jutun juonta täyttyy vähän korjailla, jotta lukijalle käy selväksi, että aluksi käsiteltiin kavitointia nesteessä (vapaat kavitaatiokuplat) ja tässä sitten kavitaatiokuplan muodostumista kuristuksen sisään, ei vapaiksi kupliksi nesteeseen.]

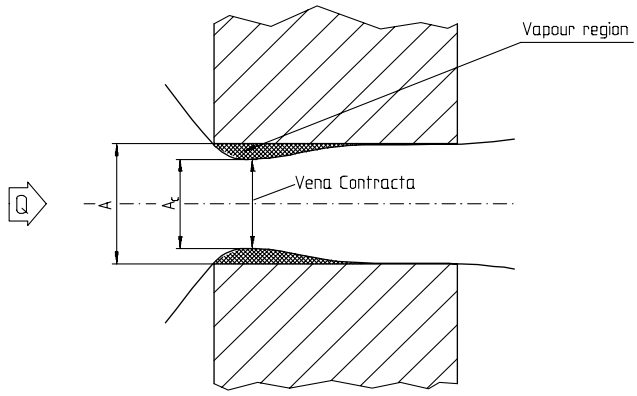

Figure 18. Flow comes loose at the front end of the throttle and fluid flows through an aperture (*vena contracta*) whose cross-sectional area is smaller than the diameter of the throttle suggests [9]. [Kuvaa muutettava seuraavasti: Q → q_V, A → $A_{fc,2}$, A_C → $A_{fc,vc}$].

When cavitation intensifies enough the flow through the throttle does not increase any more although the back pressure is reduced. This phenomena is called the saturation or choking of flow and this happens when the throttle is mainly filled with vapour. The prevailing flow type is hypercritical [vai onko se supercritical] vapour flow. Figure 19 presents the theoretic (i.e. calculated) and the measured (i.e. actual) characteristic curve for a throttle, the presence of cavitation is obvious.

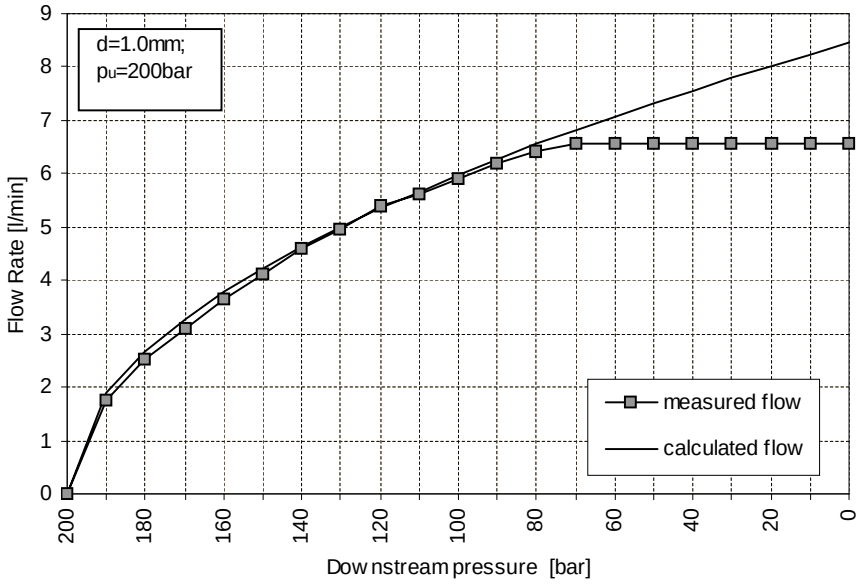

Figure 19. Theoretically and experimentally determined characteristic curves for a throttle as a function of up- and downstream pressure difference [9]. [Kuvaa muutettava seuraavasti: downstream pressure → p_3, flow rate → q_V, p_u → p_1, d → $D_{H,fc}$].

Let's define **cavitation number *Ca***, that expresses the probability or strength of cavitation [12].

$$Ca = \frac{p_3 - p_v}{p_1 - p_3} \qquad (3.29)$$

where p_v is the vapour pressure of the fluid. Cavitation starts when Ca takes the value Ca_{cr} which is called the critical cavitation number. Flow cavitates when $Ca < Ca_{cr}$, and does not when $Ca > Ca_{cr}$. The dependence of critical cavitation number on supply pressure and the diameter of throttle is presented in Fig. 20. Equations for calculating the cavitation number [vai onko flow number tai flow coefficient?] for different valve structures are presented later.

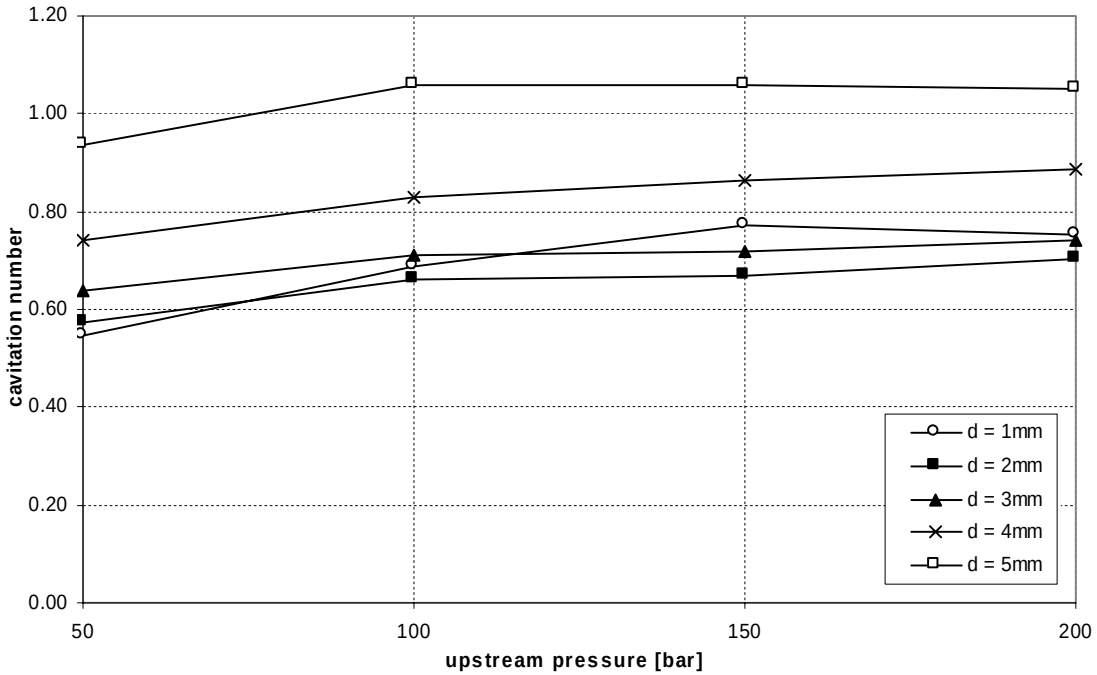

Figure 20. Critical cavitation numbers for a throttle as a function of different supply pressures and throttle diameters [8]. [Kuvaa muutettava seuraavasti: cavitation number → Ca, upstream pressure → p_1, d → $D_{H,fc}$].

Schmidt and Corradini have presented a simple model for calculating the cavitation number [vai onko flow number tai flow coefficient?] both for cavitating and non-cavitating (cavitation free) flow [14]. In this model the cavitation number [vai onko flow number tai flow coefficient?] takes a constant value in case of non-cavitating flow and in case of cavitating flow the cavitation number [vai onko flow number tai flow coefficient?] is calculated with following equations [14]:

$$C_{q,cav} = C_c \sqrt{Ca^*} \tag{3.30}$$

where: $$Ca^* = \frac{p_1 - p_v}{p_1 - p_3} \tag{3.31}$$

As shown above (Fig. 18), when cavitation occurs the vapour-filled volume/area blocks a part of the cross-sectional area of the throttle and fluid flows through a smaller aperture (vena contracta, $A_{fc,vc}$). The contraction coefficient C_c expresses the ratio of cross-sectional areas $A_{fc,vc}$ and $A_{fc,2}$ (cp. equation (*3.15*)).

3.3.3 Throttle dynamics

It is generally assumed that the pressure and volume flow characteristics of hydraulic components comply with the steady state characteristics at all times. This kind of quasistatic approximation is widely used to model the behavior of different components and the effect of viscose friction while performing transient flow calculations. However it is apparent that this assumption leads to an error of some magnitude and thus it is important to evaluate if the error is significant in relation to the result of calculation.

Funk et al. [3] have proposed a model for studying fast phenomena in throttles. It is generally assumed [tässä on edellisen kappaleen kertausta] that the steady state characteristics model the behavior of a throttle equally good both in transient and steady state conditions. However, in hydraulic systems there are circumstances where the very short time lasting transients have a high significance. The model takes also into account the axial dimension of throttle and thus the model can be applied to throttle formed hydraulic components and short pipes/ducts.

According to [3] the differential equation representing the dynamics of throttle can be written as:

$$p_1 - p_3 = \left[\frac{r_f}{\sqrt{\frac{C_c A_{fc,2} \rho}{2}}} + \frac{r_f l_{thr}}{A_{fc,2}}\right]\frac{dq_V}{dt} + \left[\frac{r_f}{2(C_c A_{fc,2})^2} + \frac{r_f / l_{thr}}{2 D_{H,thr} A_{fc,2}^2}\right] q_V^2 \qquad (3.32)$$

Linearizing the equation in the operation point (op) yields to following transfer function:

$$\frac{q_V}{\Delta p} = \frac{\frac{1}{2\sqrt{Y_2 \Delta p_{op}}}}{\frac{Y_1}{2\sqrt{Y_2 \Delta p_{op}}} s + 1} \qquad (3.33)$$

where: $Y_1 = \frac{r_f}{\sqrt{\frac{C_c A_{fc,2} \rho}{2}}} + \frac{r_f l_{thr}}{A_{fc,2}}$ and $Y_2 = \frac{r_f}{2(C_c A_{fc,2})^2} + \frac{r_f / l_{thr}}{2 D_{H,thr} A_{fc,2}^2}$

Thus the time constant is:

$$t_t = \frac{Y_1}{2\sqrt{Y_2 \Delta p_{op}}} \qquad (3.34)$$

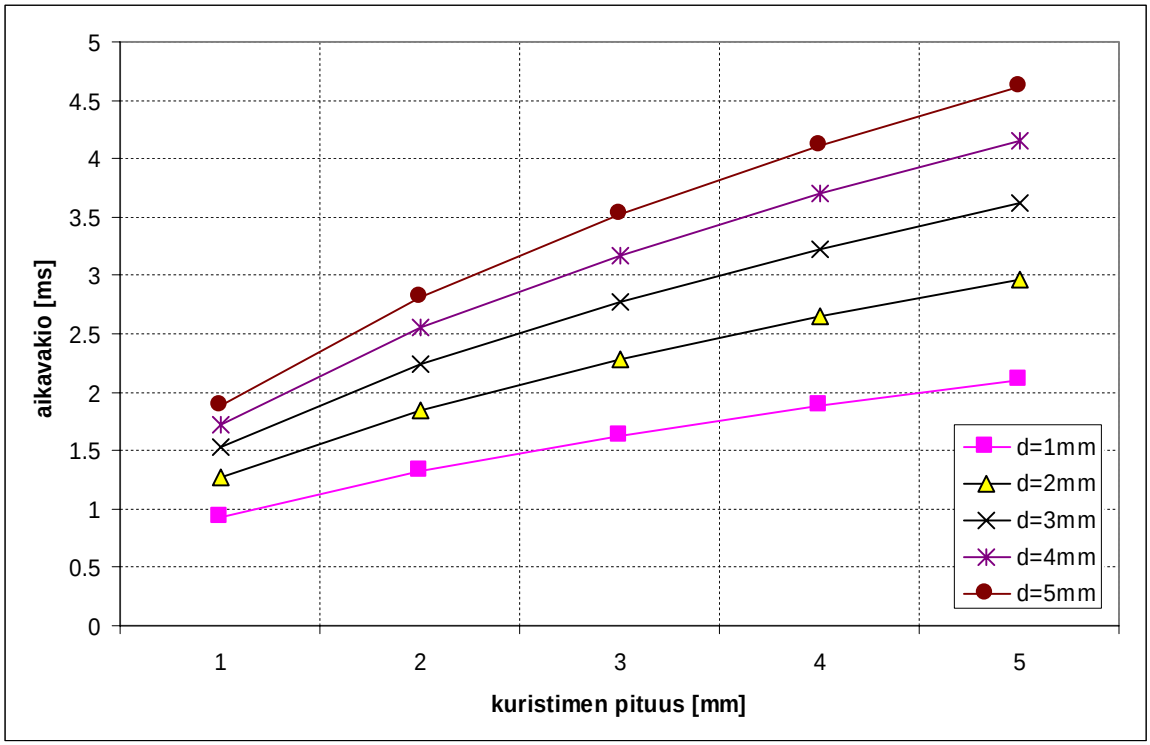

Figure 21. Dependence of time constant on the diameter and length of throttle. [Kuvan tekstit käännettävä englanniksi. Kuvaa muutettava seuraavasti: kuristimen pituus → l_{thr}, aikavakio → τ_t, d → $D_{H,thr}$].

3.4 Flow characteristics of different throttle geometries

This chapter discusses the flow characteristics of some different throttle geometries based on the analyses of von Mises and also on some experimental results. The analyses of von Mises apply for non-viscose fluids, i.e., flows whose Reynold's number is infinite.

3.4.1 Spool valve

Figure 22 (a) presents the flow conditions that von Mises used in one of his measurements. The side wall of the tank has an opening that rises from the bottom of the tank. Figure (b) in turn presents how the results of the measurement are applicable also to the flow through a spool valve. The graph presents the defined contraction coeffiecient C_c and flow angle α_f as a function of the valve opening x_1. With very small openings C_c takes value of 0.673 and when the opening is increased C_c decreases and reaches value of 0.20 when x_1 has value 5.0. Flow angle in turn takes the value of 69° with small openings and roughly 53° when when x_1 has value 5.0.

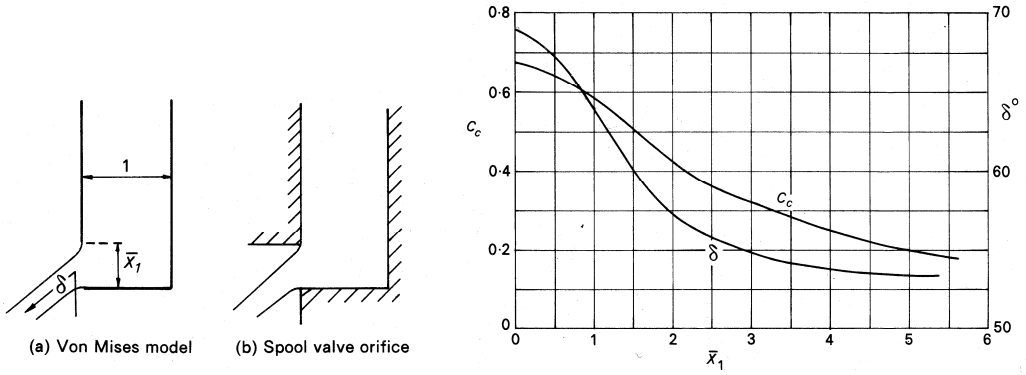

Figure 22. Contraction coefficient and flow angle in an ideal spool valve (side opening) [12]. [Kuvaa muutettava seuraavasti: $\bar{X}_1 \rightarrow x_1$, $\delta \rightarrow \alpha_f$, $C_c \rightarrow C_c$].

Another flow condition used by von Mises is presented in Fig. 23. The graph presents the effect of the opening x_2 to contraction coefficient and flow angle. With very small openings C_c takes value of 0.673 and 1.0 with maximum opening. Flow angle in turn takes the value of 21° with small openings and 0° with maximum opening.

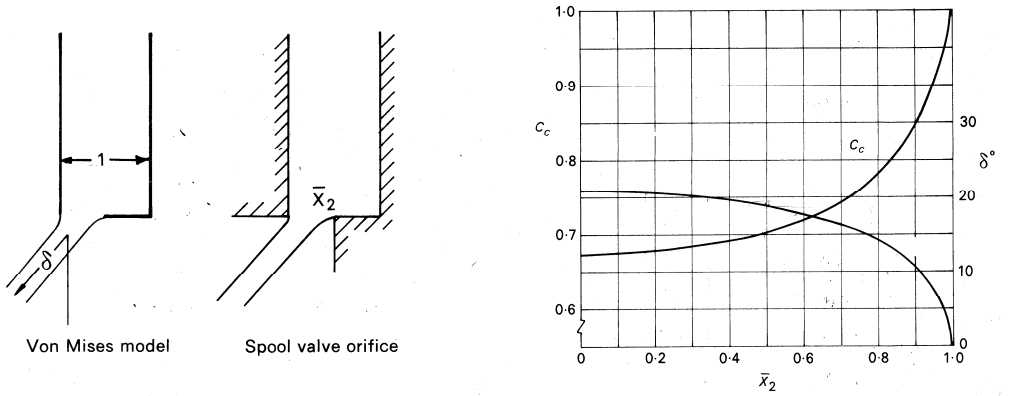

Figure 23. Contraction coefficient and flow angle in an ideal spool valve (bottom opening) [12]. [Kuvaa muutettava seuraavasti: $\bar{X}_2 \rightarrow x_2$, $\delta \rightarrow \alpha_f$, $C_c \rightarrow C_c$].

In spool valves the opening x is usually very small and thus the values of 0.673 for contraction coefficient and 69° for flow angle are applicable.

The above mentioned results are applicable to valves that have no clearance between valve body and spool which is, however, needed to enable the movement of spool inside the body. This clearance has an effect on the characteristics of the valve and the effect becomes significant at very small openings of the valve. The contraction coefficient and flow angle of real valves can be defined by combining the two above presented von Mises cases (Figs. 22 and 23). The increase of clearance increases also the contraction coefficient.

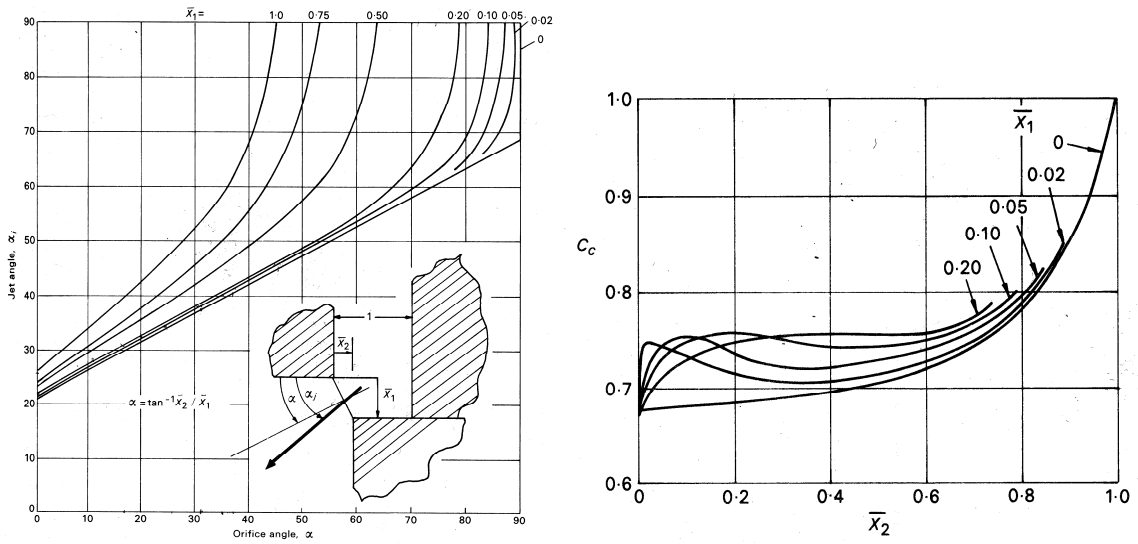

Figure 24. Contraction coeffiecient and flow angle as a function of clearance and opening [12]. [Kuvaa muutettava seuraavasti: $\alpha \rightarrow \alpha_{ori}$, $\alpha_i \rightarrow \alpha_f$, $\bar{X}_1 \rightarrow x_1$, $\bar{X}_2 \rightarrow x_2$, $C_c \rightarrow C_c$].

In some spool valves the cross-section of the throttle takes a form of a circle segment. The discharge coefficient C_d for this type of structure as a function of Reynold's number and with different openings is presented in Fig. 25

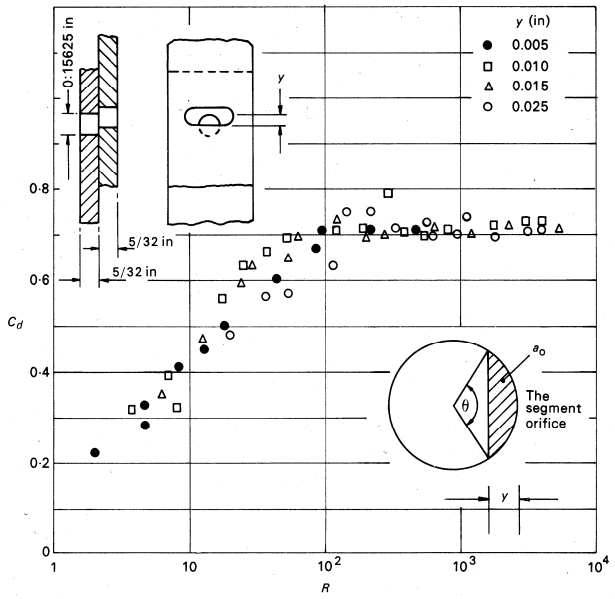

Figure 25. Discharge coefficient C_d as a function of Reynold's number for a circle segment formed throttle [12]. [Kuvaa muutettava seuraavasti: $R \rightarrow Re$, $y \rightarrow x$, $\theta \rightarrow \alpha_x$, $a_o \rightarrow A_{fc,2}$, $C_d \rightarrow C_d$].

Figure 26 presents the dependence of flow coefficient C_q on cavitation number and flow number in two-dimensional spool valve throttle. In this case the flow number is calculated with equation [12]:

$$Fm = \frac{2x}{n}\sqrt{\frac{2(p_1 - p_3)}{r_f}} \qquad (3.35)$$

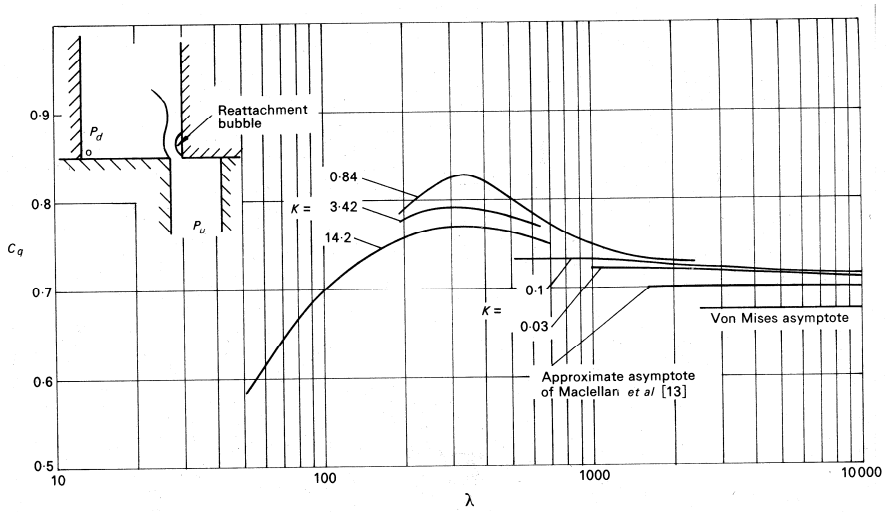

Figure 26. Flow coefficient C_q in two-dimensional spool valve throttle as a function of cavitation number *Ca* and flow number *Fm* [12]. [Kuvaa muutettava seuraavasti: $\lambda \rightarrow Fm$, $K \rightarrow Ca$, $P_u \rightarrow p_1$, $P_d \rightarrow p_3$, $C_q \rightarrow C_q$].

The flow coefficient C_q reaches its peak values in the flow number range $50 < Fm < 400$ and settles to a value of 0.71 at high flow number values. This value is higher than the von Mises proposed 0.673 and is due to the curving of the flow.

3.4.2 Seat valve

The results that von Mises obtained when measuring flow discharging from a conical channel can be applied to seat valves as is presented in Fig. 27. It is to be noticed that in this case the flow follows the surface of the poppet, i.e., the flow angle is equivalent to the half of the coning angle of the poppet ($\alpha_{fc,half} = \alpha_{pop} = 0.5 \times \alpha_{con} = \alpha_f$). [Näitä merkintöjä voisi olla alla olevassa kuvassa]

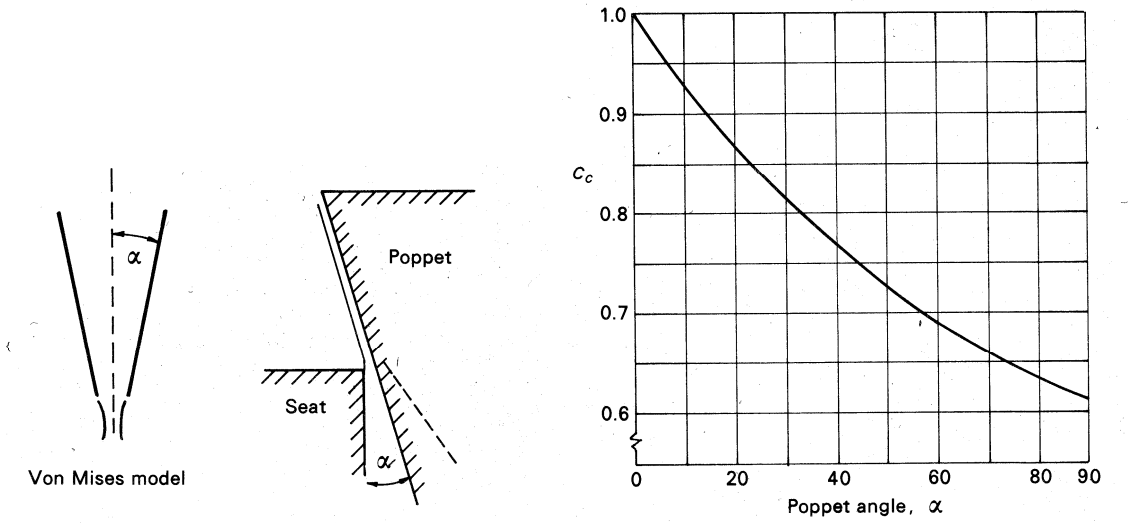

Figure 27. Contraction coefficients for seat valve as a function of poppet angle [12]. [Kuvaa muutettava seuraavasti: $\alpha \rightarrow \alpha_{fc,half}$, $\alpha \rightarrow \alpha_{pop}$, $C_c \rightarrow C_c$].

Figure 28 presents experimentally obtained flow coefficient C_q as a function of flow number *Fm* for a case where the poppet had a coning angle of 45°, the edges of seat were sharp and the fluid was mineral oil.

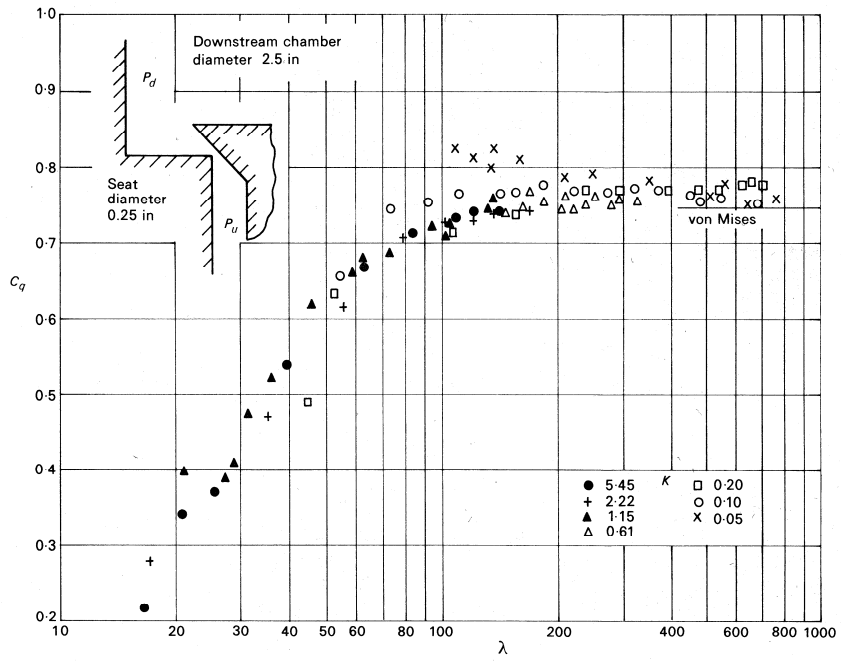

Figure 28. Experimental values of flow coefficient C_q for a 45° coned seat valve [12]. [Kuvaa muutettava seuraavasti: $\lambda \rightarrow Fm$, $K \rightarrow Ca$, $P_u \rightarrow p_1$, $P_d \rightarrow p_3$, $C_q \rightarrow C_q$].

The flow number for a seat valve can be calculated with equation [12]:

$$Fm = \frac{2x\sin(a_{pop})}{n}\sqrt{\frac{2(p_1 - p_3)}{r_f}} \qquad (3.36)$$

The behavior of flow coefficient in Figs. 26 (spool valve) and 28 (poppet valve) have similar trend. With large values of *Fm* the flow coefficient C_q takes a value of 0.77 which is close to von Mises value of 0.746. This is no surprise since the flow follows the surface of the poppet which was also the basis of von Mises' experiment.

Lu [11] has studied the discharge coefficients of various seat valve geometries. Figure 29 presents the results for four valves as a function of Reynold's number.

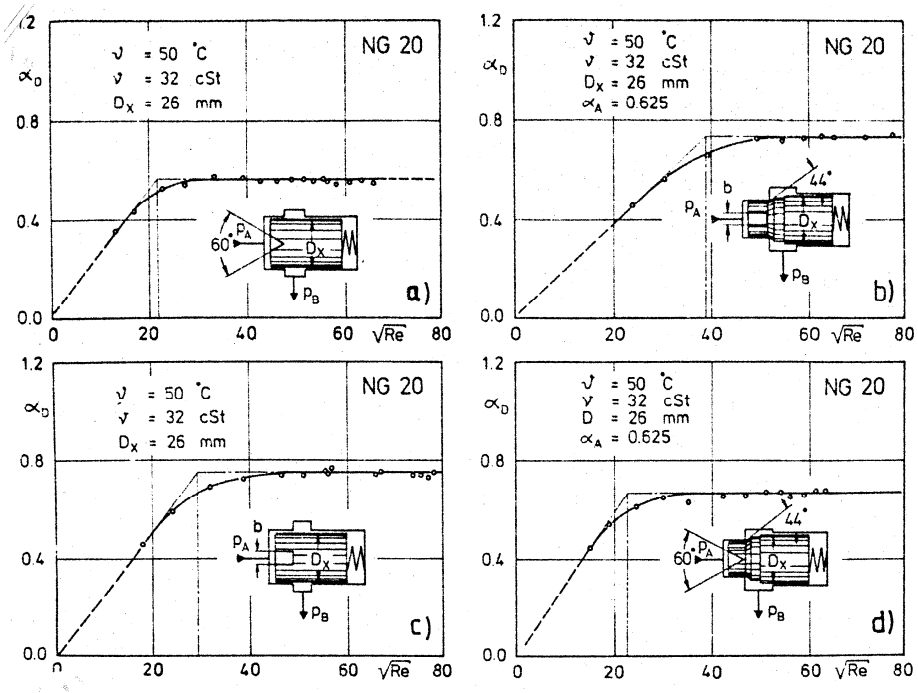

Figure 29. Discharge coefficients for different kind of seat valve geometries [11]. [Kuvaa muutettava seuraavasti: $R \rightarrow Re$, $\upsilon \rightarrow \theta$, $D_x \rightarrow D_{vs}$, $b \rightarrow D_{H,fc}$, $p_A \rightarrow p_1$, $p_B \rightarrow p_3$, $\alpha_A \rightarrow \alpha_1$]

Johnston et al. in turn studied the effect of the shape of the poppet and socket/chuck on the flow coefficient. In their measurements the flow was cavitation free in which case the discharge coefficient for a certain valve geometry and opening is solely a function of Reynold's number. The used range of *Re* was 2500–35000. Figure 30 presents a schematic structure of the studied valve. The flow coefficient C_q remains relatively constant on the studied *Re* range as been noted also in the previous figures. In the following figures the flow coefficients are presented as a function of opening.

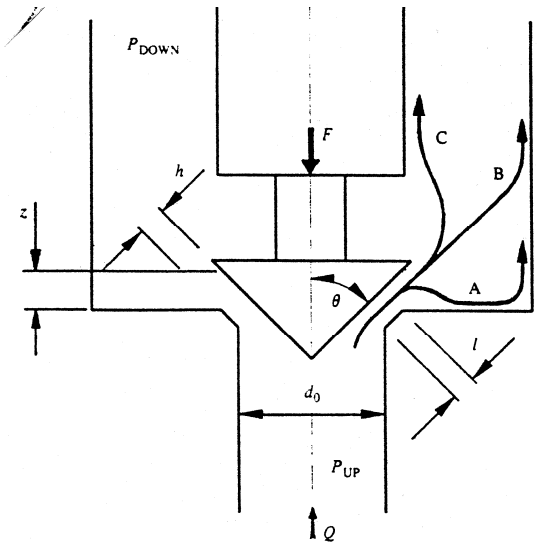

Figure 30. Schematic structure of a poppet valve [6]. [Kuvaa muutettava seuraavasti: $z \rightarrow x$, $h \rightarrow h_g$, $l \rightarrow l_g$, $d_0 \rightarrow d_1$, $\theta \rightarrow \alpha_{pop}$, $Q \rightarrow q_V$, $P_{UP} \rightarrow p_1$, $P_{DOWN} \rightarrow p_3$].

Figure 31 presents the effect of the coning angle of the poppet to the flow coefficient. The markers in the figure indicate the average values of measurements on the total range of volume flow. The theoretical values (i.e. lines) have been calculated using the values predicted by von

Mises and assuming that no recovery of pressure takes place ($p_{vc} = p_3$), and by taking the upstream momentum into account with equation [6]: [Kaava on tarkistettava alkuperäislähteestä, alkuperäisessä $A_{fc,1}$:n tilalla oli A_o ja $A_{fc,thr}$:n tilalla oli a]

$$C_q = C_d \left(1 - \left(\frac{C_d A_{fc,thr}}{A_{fc,1}} \right)^2 \right)^{-0.5} \tag{77}$$

$$C_q = \frac{C_d}{\sqrt{1 - \left(\frac{C_d A_{fc,thr}}{A_{fc,1}} \right)^2}} \tag{3.37}$$

The results show that the change in the opening has only a minor effect on flow coefficient C_q, but with decreasing coning angle the coefficient takes higher values. The reason for this is that when the flow passes through the valve the fluid has to make a smaller change to its flow direction than with higher values of coning angle.

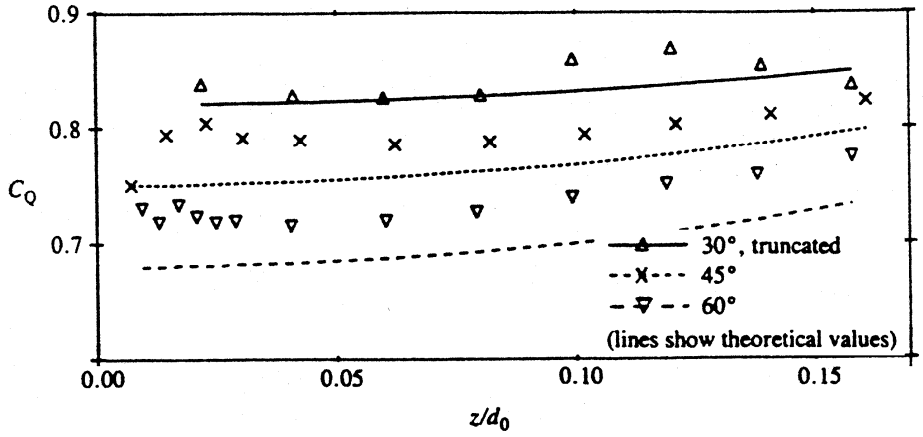

Figure 31. The effect of coning angle of poppet on the flow coefficient [6]. [Kuvaa muutettava seuraavasti: $z \rightarrow x$, $d_0 \rightarrow d_1$, $C_Q \rightarrow C_q$].

When studying conical shaped poppets three different flow cases (A, B and C in Fig. 30) have been observed. Case A where the flow adheres to the surface of the socket is dominant with large coning angles and small openings. Case B is the most common and case C appears usually with small coning angles. Sometimes it is no possible to predict to which direction the flow settles in certain conditions but the flow can stabilize into two directions. In these cases the flow direction has been observed to be history dependent, sudden changes in flow volume or valve opening may result into different flow directions. Figure 32 presents the flow coefficient C_q as a finction of opening in two flow cases. The results show that the flow pattern has no significant effect on the value of the flow coefficient. This is because the flow conditions are similar with the exception of the direction of flow leaving the poppet surface, the contraction coefficient and recovery of pressure remain unchanged.

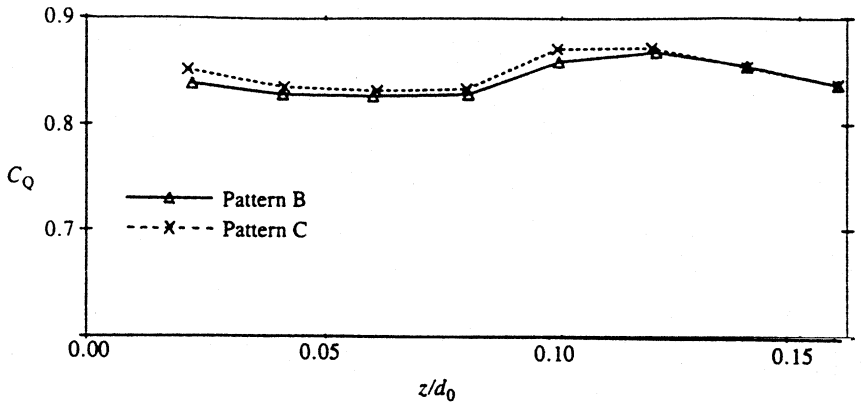

Figure 32. The effect of flow direction on the flow coefficient [6]. [Kuvaa muutettava seuraavasti: $z \rightarrow x$, $d_0 \rightarrow d_1$, $C_Q \rightarrow C_q$].

When studying a valve that has a flow force compensating poppet two different flow patterns were observed. The flow coefficient of this kind of poppet does not, however, differ significantly from the case of "conventional" conical poppet.

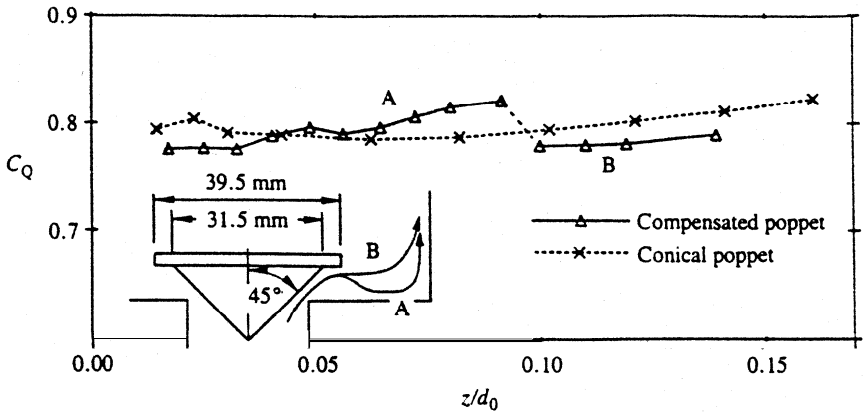

Figure 33. The effect of compensated poppet on flow coefficient [6]. [Kuvaa muutettava seuraavasti: $z \rightarrow x$, $d_0 \rightarrow d_1$, $C_Q \rightarrow C_q$].

Measurements were also made with valves in which the socket was chamfered to an angle corresponding the coning angle of poppet. In this case the contact between poppet and socket is not lineal but annular type surface contact. Figure 34 presents measurement results obtained with a poppet that has coning angle of 45° and with different sizes of chamfer. The flow case in these measurements was B (cp. Fig. 30). It is apparent that with small openings the flow coefficient C_q takes high values and decreases with large openings finally approaching the value determined for sharp edged poppet. This can be explained by the separating and adhering of the flow. At the edge of the chamfer the flow separates from the surfaces and with small openings of the valve it adheres back to the poppet and the socket while still in the region of the chamfer. In this case the recovery of pressure is significant which leads to increase of C_q. With large openings the flow does not adhere back in the chamfer region and therefore no recovery of pressure takes place. The flow coefficient takes its largest value at high sizes of chamfer.

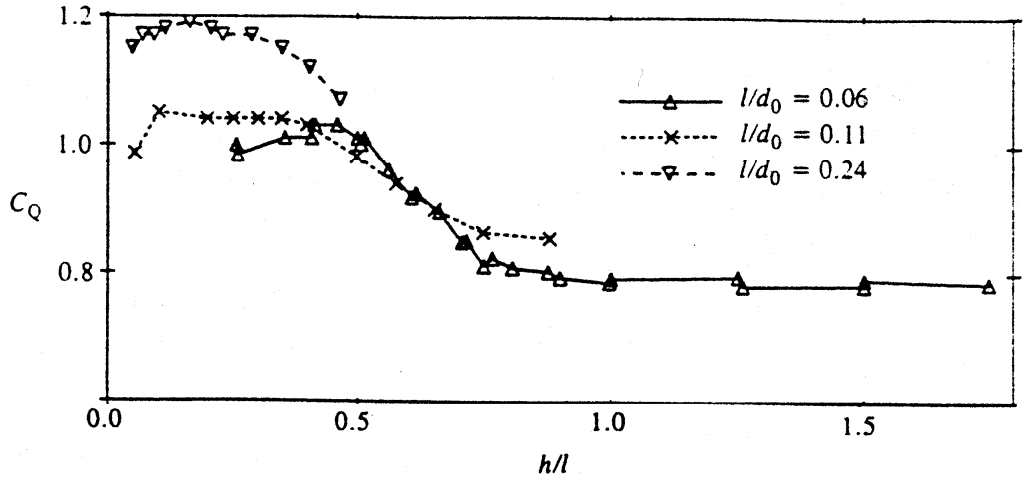

Figure 34. Flow coefficient for chamfered socket and 45°-cone poppet [6]. [Kuvaa muutettava seuraavasti: $h \rightarrow h_g$, $l \rightarrow l_g$, $d_0 \rightarrow d_1$, $C_Q \rightarrow C_q$].

3.4.3 Circular throttle

Fluid mechanics of a sharp edged short throttle is well known and therefore measurement and throttling devices can be reliably designed based on the available measurement data. However, the required diameter of the throttle is often so tiny that it impossible to manufacture a sharp-edged throttle plate. This results into the throttle being a cylindrical hole with significant length/diameter-ratio ($l_{thr}/D_{H,thr}$). In the following is presented some research findings for such throttles and empirical equations for calculating the flow number in cases of different $l_{thr}/D_{H,thr}$-ratios and Reynold's numbers. [Tässä olisi kuva paikallaan]

Many hydraulics handbooks assume that flow velocity and pressure in *vena contracta* are the same as in the adhering point of the flow. In this case the flow coefficient C_d can be determined with the momentum equation and contraction coefficient C_c. Assuming that the contraction coefficient has a value of 0.61 the flow coefficient takes the value of 0.84. This correlates well with the measurements made with high Reynold's numbers. [vai "This correlates with the measurements made with very high Reynold's numbers", kumpaa suomenkielisen tekstin virkkeessä tarkoitettiin?]. Hall [10] has presented an analytical equation for a adhered turbulent flow:

$$C_d = 1 - 0.184\left(\frac{l_{thr}}{D_{H,thr}} - 1.0 + 1.11 Re^{0.25}\right)^{0.8} Re^{-0.2} \qquad (3.38)$$

[Onko kaavassa kirjoitusvirhe ensimmäisessä kertoimessa, pitäisikö olla 0.84?]

When the discharge coefficient is examined as a function of Reynold's number it remains relatively constant (*ultimate discharge coefficient* $C_{d,u}$) for a certain value of ratio $l_{thr}/D_{H,thr}$ when *Re* is higher than 1000. Figure 35 presents $C_{d,u}$ as a function of ratio $l_{thr}/D_{H,thr}$. When the ratio takes values from zero to one the $C_{d,u}$ increases rapidly from 0.61 to 0.78. In the range $1 < l_{thr}/D_{H,thr} < 2$ the $C_{d,u}$ increases somewhat moderately and when $l_{thr}/D_{H,thr} > 2$ the $C_{d,u}$ decreases almost linearly taking the value of 0.74 at point $l_{thr}/D_{H,thr} \approx 10$.

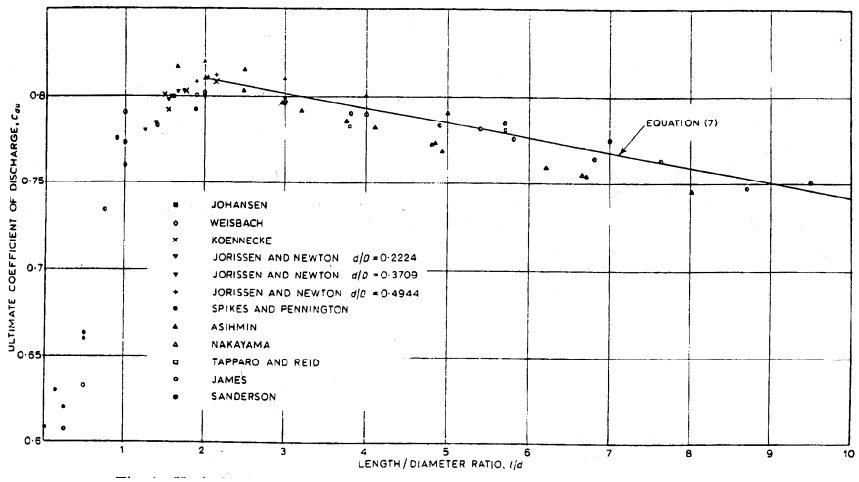

Figure 35. Ultimate discharge coefficient $C_{d,u}$ as a function of ratio $l_{thr}/D_{H,thr}$. [Kuvaa muutettava seuraavasti: $l \rightarrow l_{thr}$, $d \rightarrow D_{H,thr}$, $C_{du} \rightarrow C_{d,u}$].

With values $l_{thr}/D_{H,thr} > 2$ the diameter ratio $D/D_{H,thr}$ of the throttle becomes significant. In the following the diameter ratios of $D/D_{H,thr} > 0.25$ have been omitted since the effect of $D/D_{H,thr}$ - ratio is desired to be eliminated from the results. Taking this into account the following relation between $C_{d,u}$ and $l_{thr}/D_{H,thr}$ has been established ($2 < l_{thr}/D_{H,thr} < 10$) [10]. [Mikä on alkuperäistekstin iso D?, tarvitaan KUVA!]

$$C_{d,u} = 0.827 - 0.0085\frac{l_{thr}}{D_{H,thr}} \qquad (3.39)$$

Figure 36 presents the discharge coefficient as a function of Reynold's number for case $l_{thr}/D_{H,thr} = 2$.

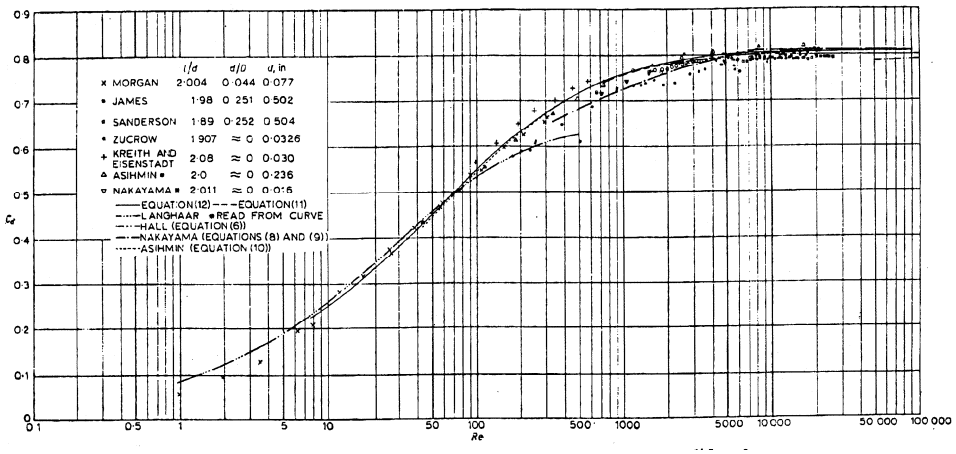

Figure 36. Discharge coefficient as a function of Reynold's number; $l_{thr}/D_{H,thr} = 2$ [10]. [Kuvaa muutettava seuraavasti: $l \rightarrow l_{thr}$, $d \rightarrow D_{H,thr}$, iso-D?, mikä on pikku-d:n alaindeksi kuvassa?, $C_d \rightarrow C_d$].

Figure 37 presents the typical distribution of pressure coefficient C_p. With $l_{thr}/D_{H,thr} = 4$ the adhering of flow manifests itself in form of clear rise of pressure. With $l_{thr}/D_{H,thr} = 1$ perfect adhering does not occur and with $l_{thr}/D_{H,thr} = 0.5$ two different behaviors can be detected. In the first case the pressure remains equal to the downstream pressure for the whole length of the throttle. In the second case $C_p = -0.16$ for the whole length of the throttle which corresponds well to the measurement results presented in the figure.

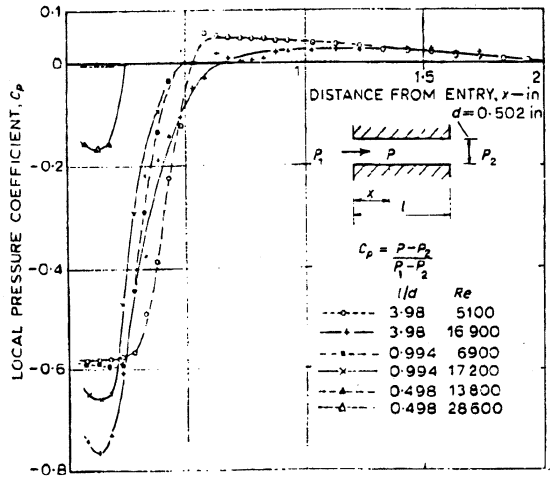

Figure 37. Pressure distribution in a throttle [9]. [Kuvaa muutettava seuraavasti: $C_p \rightarrow C_p$, $l \rightarrow l_{thr}$, $d \rightarrow D_{H,thr}$, $P_1 \rightarrow p_1$, $P_2 \rightarrow p_3$, $P \rightarrow p$].
[Kuvan havainnollisuus on surkea, millainen kuva on ollut lähdeteoksessa, x-akseli?]

The flow coefficient of a ”long” circular throttle is affected by several factors. The shape of the front end of the throttle has a significant effect to the flow coefficient. With chamfered or rounded front end edge the flow coefficient (and discharge coefficient) takes higher values than with sharp edged front end. Figure 38 presents the dependence of flow coefficient and flow rate on the pressure difference over the throttle for a sharp edged and chamfered throttle. The results also show the effect of cavitation which causes the saturation of the flow rate and the decreasing of the value of flow coefficient C_q. The value of Reynold's number in these resuls is in range 1100–5500 [10].

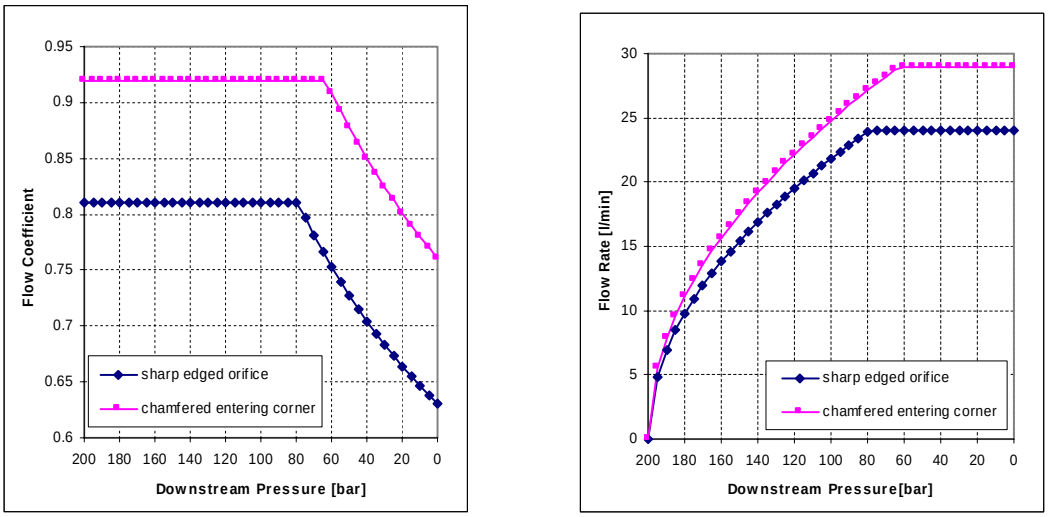

Figure 38. Flow coefficients and characteristic curves for sharp edged and chamfered throttle (p_1 = constant = 200 bar; $D_{H,thr}$ = 2.0 mm) [9]. [Kuvaa muutettava seuraavasti: downstream pressure $\rightarrow p_3$, flow coefficient $\rightarrow C_q$, flow rate $\rightarrow q_V$].

Also the fluid has been noted to have and effect to the flow rate anf flow coefficient of a throttle. Figure 39 presents experimentally measured values for flow coefficient with some typical oils used in hydraulics. Flow starts to cavitate when downstream pressure reaches value p_3 » 80–70 bar, the cavitation is indicated by the reducing flow coefficient value.

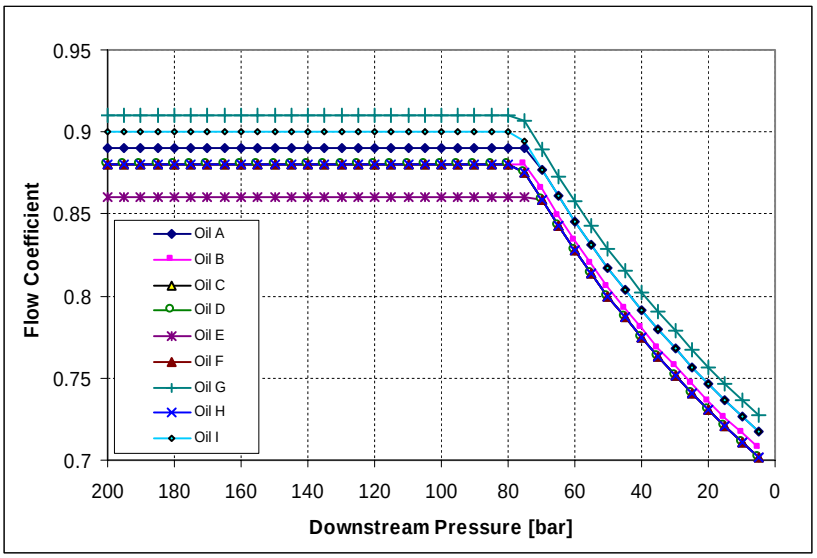

Figure 39. Flow coefficient for some different oils. (p_1 = constant = 200 bar; $D_{H,thr}$ = 2.0 mm) [9]. [Kuvaa muutettava seuraavasti: downstream pressure → p_3, flow coefficient → C_q].

In the design of a throttle the following matters should be considered [12]:

1. Values of $l_{thr}/D_{H,thr} < 1.5$ should be avoided since the value of C_d varies strongly in this type of throttles and hysteresis can occur.

2. With $2 < l_{thr}/D_{H,thr} < 10$, C_d is relatively constant when Reynold's number is higher than 2×10^4. In this case the $C_{d,u}$ can be calculated with an empirical equation:

$$C_{d,u} = 0.827 - 0.0085\frac{l_{thr}}{D_{H,thr}}$$

3. With $10 < Re < 2\times10^4$, discharge coefficient can be calculated with an empirical equation:

$$\frac{1}{C_d} = \frac{1}{C_{d,u}} + \frac{20}{Re^*}\left(1 + 2.25\frac{l_{thr}}{D_{H,thr}}\right) - \frac{0.005}{1 + 7.5\left(\log(0.00015)Re^*\right)}\frac{l_{thr}}{D_{H,thr}} \qquad (3.40)$$

where $Re^* = Re\dfrac{\sqrt{1 - \left(\dfrac{D_{H,thr}}{D}\right)^2}}{C_d}$

[Mikä on iso-D?]

3.5 Flow forces in spool and seat valves

In valves the fluid flows through throttles which results into changes in the momentum of the fluid flow. These changes in turn induce forces upon the solid bodies placed in the flow path. These forces are usually called flow forces, but also Bernoull forces or hydraulic reaction forces.

Magnitude of flow forces can be solved on the basis of the change in momentum.

Momentum is defined as product of mass and velocity:

$$\mathbf{I} = m\,\mathbf{v} \tag{3.41}$$

The support force that affects to fluid equals the magnitude of the change in momentum.

$$\mathbf{F} = \frac{\mathrm{d}\mathbf{I}}{\mathrm{d}t} = \frac{\P m}{\P t}\mathbf{v} + \frac{\P \mathbf{v}}{\P t}m \tag{3.42}$$

When examining the static flow forces the non-stationary part of the equation (*3.42*) is left out.

$$\mathbf{F} = \frac{\mathrm{d}m}{\mathrm{d}t}\mathbf{v} \tag{3.43}$$

The flow force that is induced to the flow path's wall by the flowing fluid is a reaction to the support force and is thus of equal magnitude but reverse in direction.

$$\mathbf{F}_\mathrm{f} = -\mathbf{F} \tag{3.44}$$

Consider the case in Figure 40. The cross-sectional flow area decreases in the direction of flow which causes the acceleration of fluid.

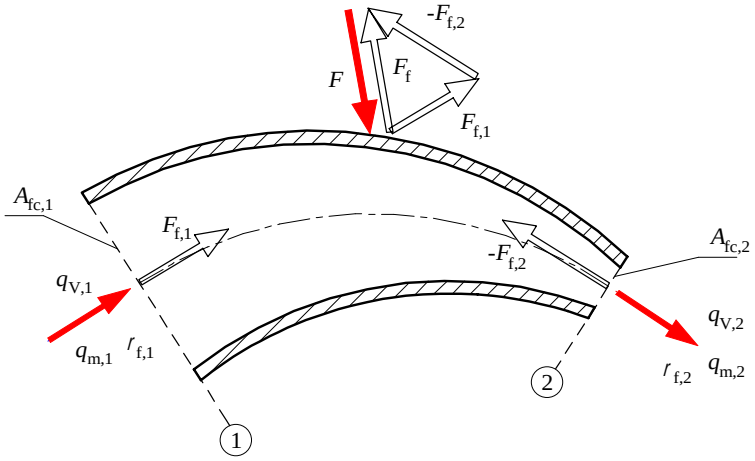

Figure 40. Flow in a pipe.

A mass flow enters the flow volume in point 1

$$\frac{\mathrm{d}m_1}{\mathrm{d}t} = \rho_{\mathrm{f},1}\, q_{\mathrm{V},1} \tag{3.45}$$

This induces a flow force whose impact has the same direction as the flow velocity

$$\mathbf{F}_{\mathrm{f},1} = \rho_{\mathrm{f},1}\, q_{\mathrm{V},1}\, \mathbf{v}_1 \tag{3.46}$$

Respectively for the point 2 (taking into account the signs)

$$\frac{\mathrm{d}m_2}{\mathrm{d}t} = -\rho_{\mathrm{f},2}\, q_{\mathrm{V},2} \tag{3.47}$$

$$\mathbf{F}_{\mathrm{f},2} = -\rho_{\mathrm{f},2}\, q_{\mathrm{V},2}\, \mathbf{v}_2 \tag{3.48}$$

Resultant forces are

$$\mathbf{F}_{\mathrm{f}} = \mathbf{F}_{\mathrm{f},1} - \mathbf{F}_{\mathrm{f},2} \tag{3.49}$$

The flow condition is assumed to be stationary, i.e., the fluid is incompressible which means that density and flow rate are constant in the considered flow volume.

$$\begin{cases} \rho_{\mathrm{f},1} = \rho_{\mathrm{f},2} = \rho_{\mathrm{f}} \\ q_{\mathrm{V},1} = q_{\mathrm{V},2} = q_{\mathrm{V}} \end{cases} \tag{3.50}$$

Thus the flow force takes form

$$\mathbf{F}_{\mathrm{f}} = \rho_{\mathrm{f}}\, q_{\mathrm{V}} (\mathbf{v}_2 - \mathbf{v}_1) \tag{3.51}$$

The magnitude of the flow force depends on the density of the fluid, flow rate and the change in the flow velocity in the considered flow volume.

The direction of flow force depends on the direction of the flow as shown in Fig. 40.

3.5.1 Spool valves

Consider the flow forces affecting to the spool valve presented in Fig. 41. The control volume is defined with dashed line.

Since the structure of the valve body limits the movement of the spool to be purely axial, only the x-axis direction has to be condidered. The flow forces affecting in the y-axis direction cause a reaction force that falls only to the bearings.

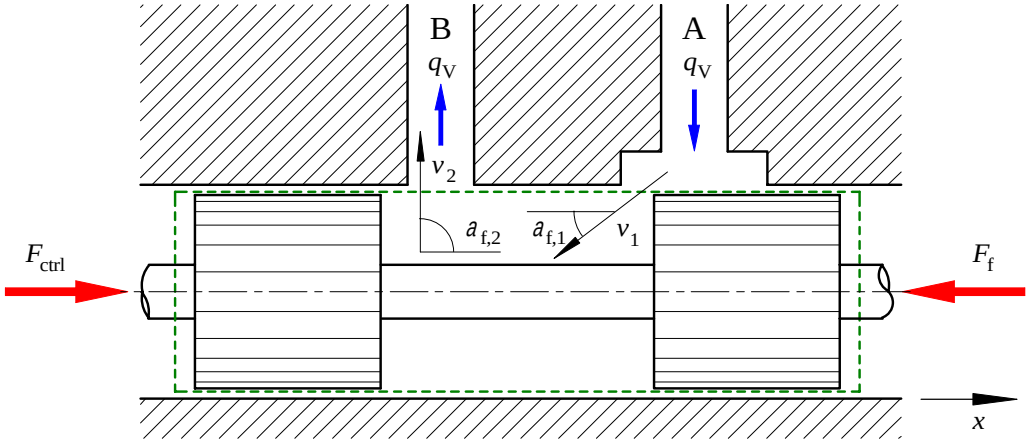

Figure 41. Flow forces in spool valve.

Taking into account the flow angle $\alpha_{f,1}$ the equation of flow force for the incoming flow can be witten as

$$F_{f,1} = \frac{dm}{dt} v_1 \cos(\alpha_{f,1}) \qquad (3.52)$$

and for the outgoing flow (when the throttle is only at the incoming edge as in Fig. 41)

$$F_{f,1} = -\frac{dm}{dt} v_2 \cos(\alpha_{f,2}) = 0, \text{ when } \alpha_{f,2} = 90^0 \qquad (3.53)$$

Resultant force is

$$F_{f,r} = -\rho_f q_V v_1 \cos(\alpha_{f,1}) \qquad (3.54)$$

In a spool valve constructed like the valve in Fig. 41 the flow force has an valve closing effect and it acts like a spring that tries to close the valve with a force whose magnitude depends on the displacement of the spool (i.e. the compression of the spring).

Generally, the flow force in spool valves has always an valve closing effect.

In the following an equation for the valve closing flow force is derived on grounds on the valve dimensions.

Flow velocity in the point of *vena contracta* of a throttle is roughly

$$v_{vc} = \sqrt{\frac{2\Delta p}{\rho_f}} \qquad (3.55)$$

Flow rate in a throttle is

$$q_{V,thr} = C_q A_{fc} \sqrt{\frac{2\Delta p}{\rho_f}} \qquad (3.56)$$

Cross-sectional flow area of the spool valve is

$$A_{\mathrm{fc}} = \pi D_{\mathrm{vs}} x_{\mathrm{vs}} \tag{3.57}$$

where D_{vs} = spool diameter
x_{vs} = length of the flow path opening

Flow force takes the form

$$\begin{aligned} F_{\mathrm{f,r}} &= -2 C_{\mathrm{q}} \pi D_{\mathrm{vs}} x_{\mathrm{vs}} \Delta p \cos(\alpha_{\mathrm{f,1}}) \\ &= -k_{\mathrm{R,h}} x_{\mathrm{vs}} \end{aligned} \tag{3.58}$$

missä k_{hyd} = hydraulinen jousivakio

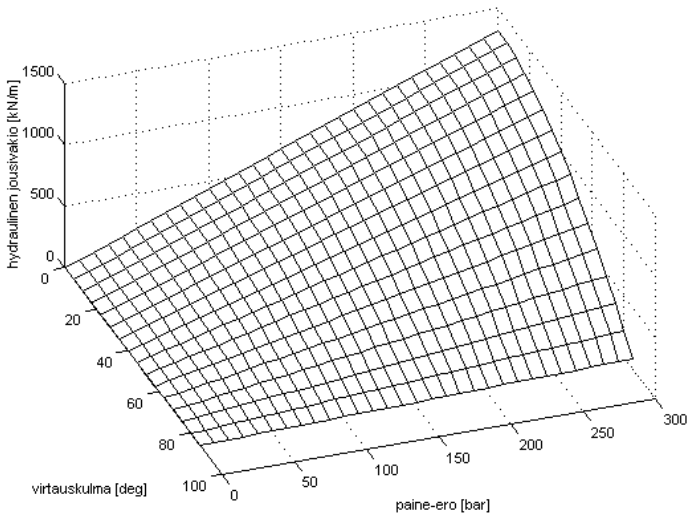

Figure 42. Hydraulic spring constant of a spool valve (C_{q} = 0.7, D_{vs} = 10 mm) as a function of flow angle α_{f} and pressure difference Δp. [Kuvan tekstit käännettävä englanniksi. Kuvaa muutettava seuraavasti: virtauskulma → α_{f}, paine-ero → Δp, hydraulinen jousivakio → $k_{\mathrm{R,h}}$].

3.5.2 Seat valves

Compared to a spool valve the seat valve is more complicated since the flow direction has different effect on the valve and also the flow geometry in the valve can be more complicated.

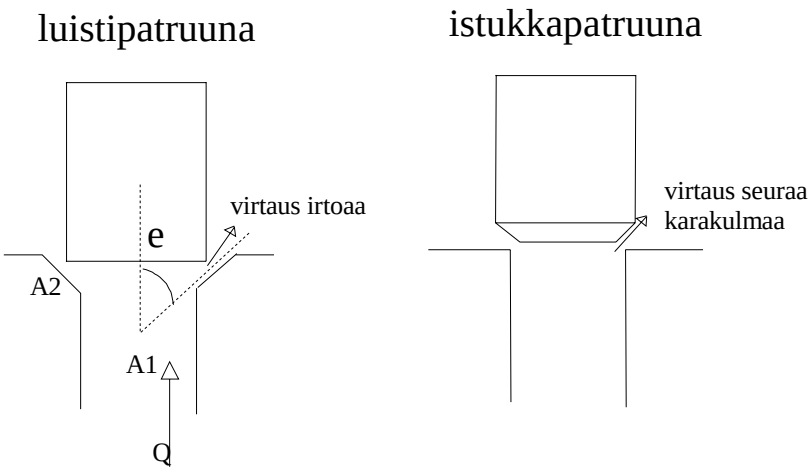

Figure 43. Cartridge type seat valves. [Kuvan tekstit käännettävä englanniksi. Kuvaa muutettava seuraavasti: $Q \rightarrow q_V$, $A_1 \rightarrow A_{fc,1}$, $A_2 \rightarrow A_{fc,2}$, e $\rightarrow \alpha_{soc}$].

The incoming flow induces an opening flow force

$$\begin{aligned} F_{f,1} &= \rho_f q_V v_1 \\ &= \rho_f \frac{q_V^2}{A_{fc,1}} \\ &= \rho_f C_q^2 \frac{A_{fc,2}^2}{A_{fc,1}} \frac{2\Delta p}{\rho_f} \\ &= 2 C_q^2 \frac{A_{fc,2}^2}{A_{fc,1}} \Delta p \end{aligned} \qquad (3.59)$$

where $A_{fc,1}$ = cross-sectional area of the cartridge
$A_{fc,2}$ = cross-sectional area of the throttle

Respectively the closing flow force caused by the outgoing flow

$$\begin{aligned} F_{f,2} &= \rho_f q_V v_1 \cos(\alpha_{soc}) \\ &= \rho_f C_q A_{fc,2} \sqrt{\frac{2\Delta p}{\rho_f}} \sqrt{\frac{2\Delta p}{\rho_f}} \cos(\alpha_{soc}) \\ &= C_q A_{fc,2} 2\Delta p \cos(\alpha_{soc}) \end{aligned} \qquad (3.60)$$

Resulting total flow force

$$F_{f,r} = F_{f,1} - F_{f,2}$$
$$= 2C_q \Delta p A_{fc,2} \left(C_q \frac{A_{fc,2}}{A_{fc,1}} - \cos(\alpha_{soc}) \right) \qquad (3.61)$$

The flow forces in a cartridge valve are
- mainly closing when the flow direction conforms to Fig. 43
- mainly closing when the flow direction is opposite to Fig. 43

An expression for a case when the flow force takes a value of zero can be derivated on grounds of equation (*3.61*)

$$F_{f,r} = 0 \Rightarrow C_q A_{fc,2} = A_{fc,1} \cos(\alpha_{soc}) \Rightarrow A_{fc,2} = \frac{A_{fc,1} \cos(\alpha_{soc})}{C_q} \approx A_{fc,2} = A_{fc,1} \qquad (3.62)$$

This takes place when the cross-sectional area of the throttle is (almost) the sama as the cross-sectional area of the cartridge.

Johnston et al. [6] studied the effect of various design parameters on the static flow forces (and flow coefficient) of cartridge valves. The medium used was water and the study was limited to flows whose Reynold's number was greater than 2500 and no cavitation was present.

The studied parameters were
- cone angle of the cartridge
- flow angle
- compensated poppet (pin)
- chamfered valve housing

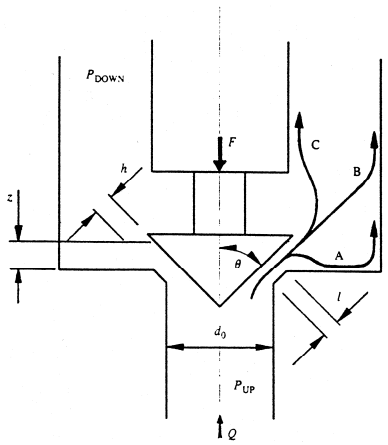

Figure 44. Geometry of cartridge valve. [sama kuin kuva 30] [Kuvaa muutettava seuraavasti: $z \rightarrow x$, $h \rightarrow h_g$, $l \rightarrow l_g$, $d_0 \rightarrow d_1$, $\theta \rightarrow \alpha_{pop}$, $Q \rightarrow q_V$, $P_{UP} \rightarrow p_1$, $P_{DOWN} \rightarrow p_3$].

Figure 44 presents the geometry of the studied valve and the possible flow types (A, B, C). Although the flow angle of the fluid flow in general follows the chamfering of the poppet this does not necessarily happen always. So called Coanda effect may cause the flow to adhere to the surface of the poppet or valve housing thus leading to curved flow. In cases of cone shaped poppets the flow can take three forms (i.e. the above mentioned flow types). According to the study it is not always possible to predict the behavior of the flow. If it conforms to case A, the

measured flow forced are larger than the theoretically calculated. This flow type is dominant with high values of cone angle and small openings. Type B is dominant in most cases and conforms to the cone angle used in theoretic equations. Type C appears mostly with small cone angles.

Figure 45 presents the measured and theoretical values of flow force for cases where the cone angle of the cartridge has values 30°, 45° and 60°. Diameter of the cartridge is 34 mm and the valve housing is sharp edged (see Fig. 43, valve on the right).

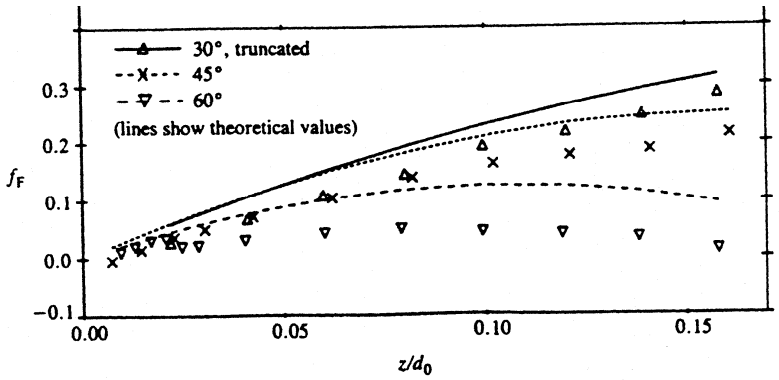

Figure 45. Effect of cone angle on flow force ($F_{f,mn}$ = 1 - measured force/nominal pressure force, x/d_1 = relative opening of the valve). [Kuvaa muutettava seuraavasti: $z \rightarrow x$, $d_0 \rightarrow d_1$, $f_F \rightarrow F_{f,mn}$].

In general, the flow forces decrease with growing cone angle. The theoretical and measured results correspond each other qualitatively, but in a quantitative sense the results include inaccuracy especially at larger openings.

Effect of flow forces can be reduced with compensation structures. This is demonstrated in Fig. 46 which presents a comparison between uncompensated and compensated poppet. The effect of compensation does not show at small valve openings, but at larger openings the flow forces are reduced considerably due to the changed flow angle. Notice that at the region of discontinuity of the flow force the valve may behave unstably.

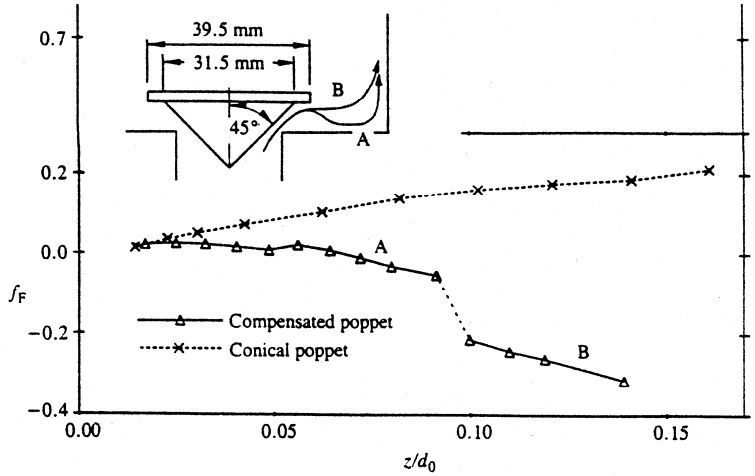

Figure 46. Effect of poppet compensation on flow forces. [Kuvaa muutettava seuraavasti: $z \rightarrow x$, $d_0 \rightarrow d_1$, $f_F \rightarrow F_{f,mn}$].

When valve housing has a chamfer conforming to the cone angle of the poppet, an annular contact area exists between the valve housing and poppet. Figure 48 presents the behavior of flow force with three different lengths of chamfer.

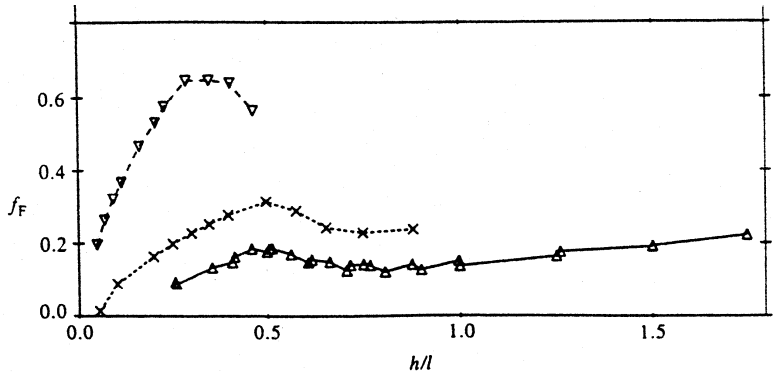

Figure 47. Effect of 45° chamfered valve housing on the flow forces (curves from up to down l_g/d_1 = 0.24, 0.11, 0.06 → Fig. 45 [vaiko sittenkin 44?]) [Kuvaa muutettava seuraavasti: $h \rightarrow h_g$, $l \rightarrow l_g$, $f_F \rightarrow F_{f,mn}$].

The effect of chamfer shows especially with small openings. With large openings the values of flow forces approach the values determined for sharp edged valve housing. If the length of the chamfer is small compared to the length of the opening the effect of chamfer is insignificant.

3.5.3 Dynamic flow forces

Until now the review has been concentraded solely on the static flow forces, i.e., the forces that exist on steady-state conditions. In transient conditions the flow is not constant and the accelerating motion of the fluid adds a dynamic component to the total flow force. These phenomena are present especially when valve is opened or closed.

Dynamic flow force is

$$F_{f,d} = \rho_f \, l_{vc} \, A_{fc} \frac{d}{dt} v = \rho_f \, l_{vc} \, A_{fc} \frac{d}{dt}\left(\frac{q_V}{A_{fc}}\right) = \rho_f \, l_{vc} \frac{dq_V}{dt} \qquad (3.63)$$

where l_{vc} = length of vena contracta
A_{fc} = cross-sectional area of the flow

In this the fluid has been assumed to be incompressible. Thus the dynamic flow force $F_{f,d}$ is due to the required change in the fluid's momentum.

In most cases the dynamic flow forces are relatively small compared to static forces [4].

Flow rate in a throttle is

$$q_V = k_A \, x \sqrt{\frac{2\Delta p}{\rho_f}} \quad \Rightarrow \quad \frac{dq_V}{dt} = k_A \frac{dx}{dt} \sqrt{\frac{2\Delta p}{\rho_f}} \qquad (3.64)$$

Equation of motion for the poppet of a cartridge valve takes form

$$m\frac{\mathrm{d}^2x}{\mathrm{d}t^2}+b_\mathrm{v}\frac{\mathrm{d}x}{\mathrm{d}t}+k_\mathrm{R,h}\,x=\Delta p\,A_\mathrm{pop,e} \qquad (3.65)$$

where m = mass of the poppet
b_v = coefficient of viscose damping
$k_\mathrm{R,h}$ = hydraulic spring constant

The transfer function of the system is

$$G(s)=\frac{x}{\Delta p}=\frac{A_\mathrm{pop,e}}{m\mathrm{s}^2+b_\mathrm{v}\,\mathrm{s}+k_\mathrm{R,h}}=\frac{\frac{A_\mathrm{pop,e}}{k_\mathrm{R,h}}}{\frac{m}{k_\mathrm{R,h}}\mathrm{s}^2+\frac{b_\mathrm{v}}{k_\mathrm{R,h}}\mathrm{s}+1} \qquad (3.66)$$

The gain of the system is

$$K_\mathrm{S}=\frac{A_\mathrm{pop,e}}{k_\mathrm{R,h}} \qquad (3.67)$$

The natural angular velocity of the system is

$$w_\mathrm{n}=\sqrt{\frac{k_\mathrm{R,h}}{m}} \qquad (3.68)$$

The damping of the system is

$$z_\mathrm{d}=\frac{Y}{k_\mathrm{R,h}}=\frac{Y_1+Y_2+Y_3}{k_\mathrm{R,h}} \qquad (3.69)$$

Term a is is comprised of following factors:
Y_1 = damping coefficient due to dynamic flow force
Y_2 = viscose friction coefficient
Y_3 = coefficient due to end cushioning of the valve

Valve can be underdamped or even unstable.

3.6 Measurements with a seat valve

In the following are presented flow force measurement results for a cartridge type NG 16 sized pressure relief valve which are compared with values obtained using the above presented theoretical equations.

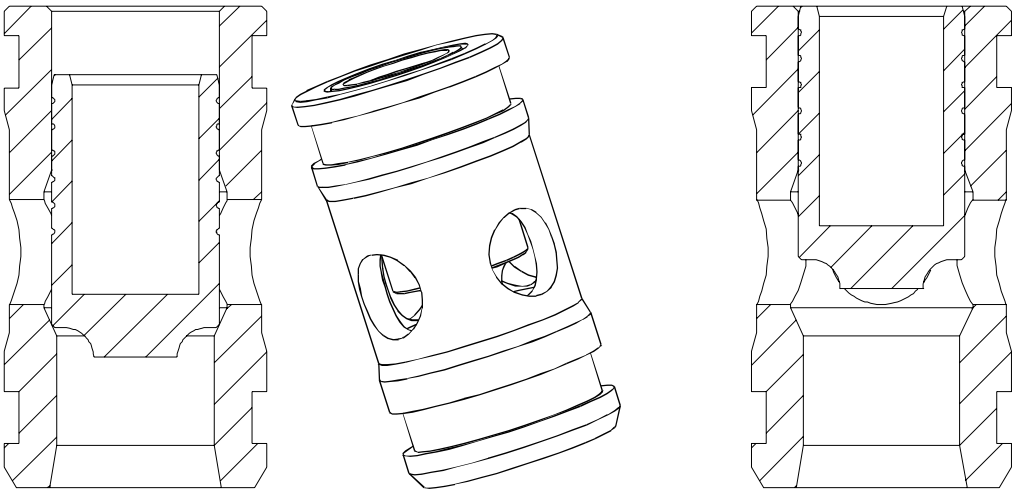

Figure 48. Cartridge type pressure relief valve (left closed and right fully open). Manufacturer Hydrolux. [Kuvaan voisi lisätä selkeyttäviä merkintöjä, Deetä ja Aata ja muita]

End surface area of the cartridge poppet

$$A_{\mathrm{pop,e}} = \frac{p}{4} D_{\mathrm{pop}}{}^{2} = \frac{p}{4}(15.99\,\mathrm{mm})^{2} = 200.81\,\mathrm{mm}^{2} \qquad (3.70)$$

The spring constant of the spring used in the valve was experimentally determined to be 7.9532 N/mm. This spring is not shown in the Fig. 48, but is placed inside the cartridge and it has an valve closing effect, i.e., it pushes the cartridge downwards to the position shown left in Fig. 48.

Measured quantities were: pressure difference over the cartridge, pressures at valve inlet and outlet, flow rate through the valve and position of the cartridge.

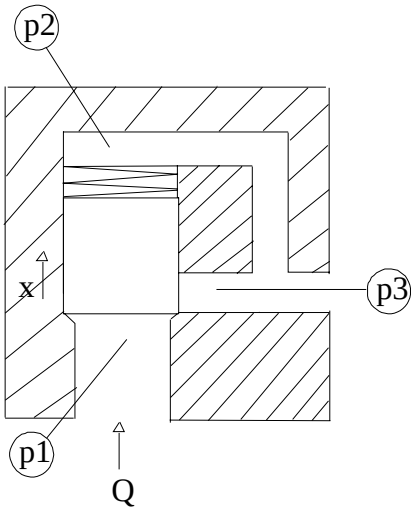

Figure 49. Location of pressure transducers in valve block. [Kuvaa muutettava seuraavasti: Q → q_V, p1 → p_1, p2 → p_2, p3 → p_3,]. Lisäksi lisätään tulokanava halkaisija d_1.

In the measurements the supply pressure (p_1) was slowly increased the purpose being to calculate the values of static flow forces from the measurement results. These and the characteristic curve of the valve is presented in Fig. 50.

Assume that the cross-sectional area of the throttle in the whole transition range of the cartridge is the area that exists between the sharp-formed poppet and the socket (i.e. chamfered valve body). Then the approximation for cross-sectional flow area as a function of cartridge's transition x is [11]:

$$A_{\mathrm{fc,pop}}(x) = \pi\, x \sin\left(\frac{\alpha_{\mathrm{soc}}}{2}\right) d_1 + \frac{x}{2}\sin(\alpha_{\mathrm{soc}}) \qquad (3.71)$$

[Pitäisikö jälkimmäisessä sulkulausekkeessa kuitenkin olla plussan sijasta miinus, vertaa kuva 53]

In reality the cross-sectional flow area does not grow linearly as a function of cartridge's transition due to the construction of the cartridge and in practice at larger values of transitions the area is somewhat larger than the formula (*3.71*) gives because of the radial openings in the valve. Nevertheless, the purpose of the study was to find out what level of accuracy is achievable in calculation of flow forces using the theoretical data found in literature and the readily measurable valve dimensions.

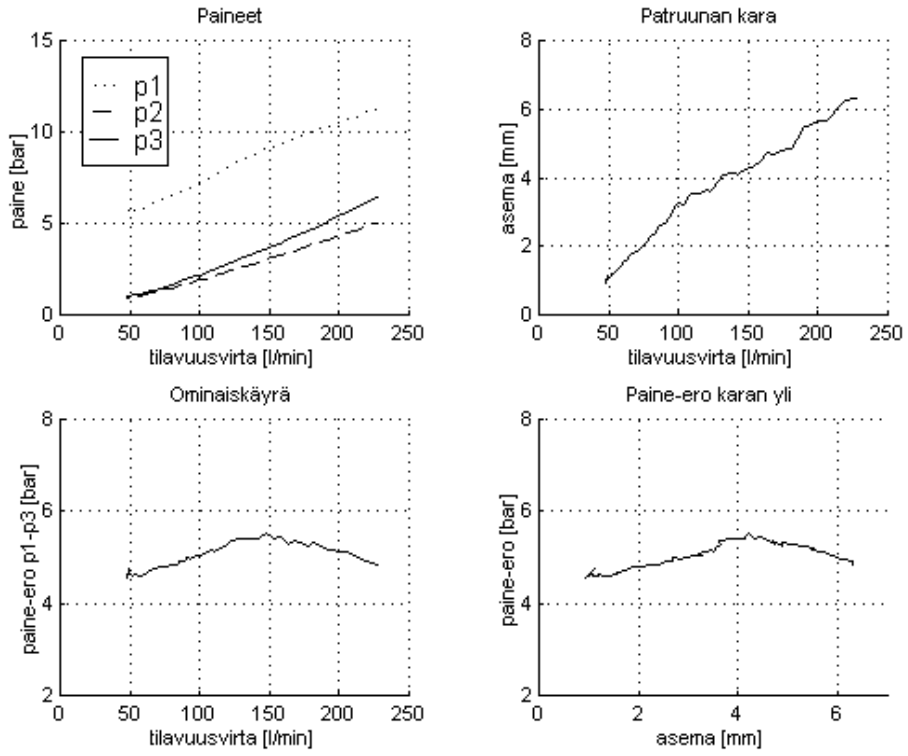

Figure 50. Measurement results. [Kuvan tekstit käännettävä englanniksi. Kuvaa muutettava seuraavasti: paine → p, tilavuusvirta → q_V, asema → x, paine-ero p1-p3 → p_1- p_3, paine-ero → Δp, p1 → p_1, p2 → p_2, p3 → p_3].

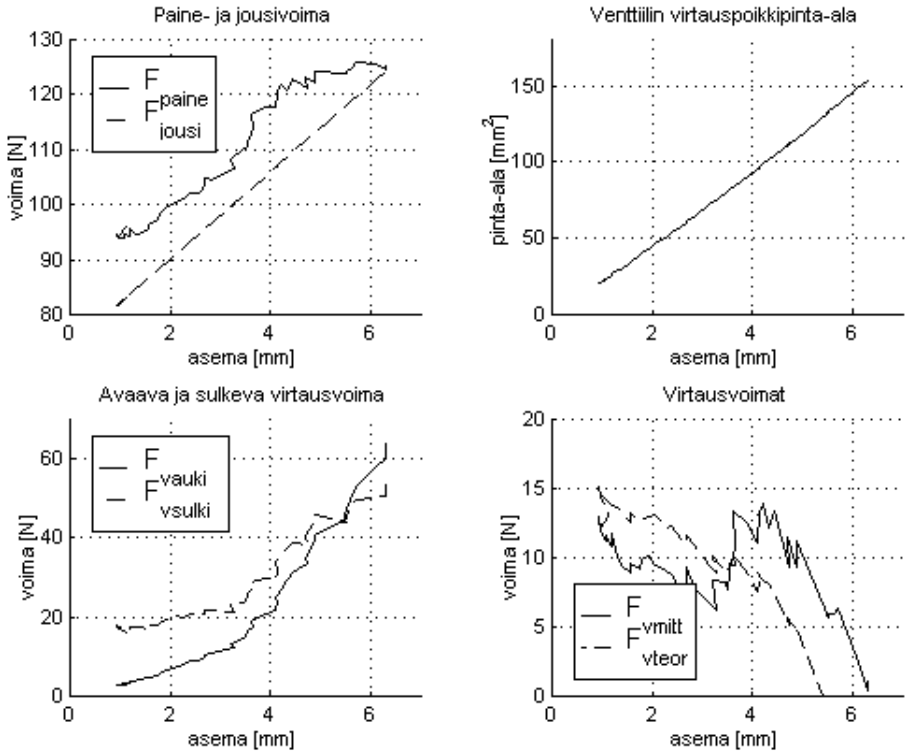

Figure 51. Measurement results. [Kuvan tekstit käännettävä englanniksi. Kuvaa muutettava seuraavasti: asema → x, voima → F, pinta-ala → $A_{fc,pop}$, F_{paine} → F_p, F_{jousi} → F_R, F_{vauki} → $F_{f,open}$, F_{vsulki} → $F_{f,closed}$, F_{vmitt} → $F_{f,meas}$, F_{vteor} → $F_{f,theor}$]

The upper left diagram of Fig. 51 presents the experimentally determined spring force and the measured pressure force over the cartridge. The difference between these originates from the flow forces in the valve. The lower left diagram presents the opening and closing flow forces calculated with the equations shown above. The lower right diagram presents the theoretical flow force (joint effect of opening and closing flow force) and the result obtained with measurements.

The measured and the calculated values of flow forces correspond relatively well to each other taking into account the simplifications made in deriving the equations and the possible sources of errors in measurements [voiko näin sanoa, kysehän voi olla vain puhtaasta sattumasta, jossa kaavan yksinkertaistukset ja mittausvirheet kallistavat tuloksia samaan suuntaan?]. With larger openings the valve opening flow force increases relatively faster compared to the valve closing flow force and the resultant force approaches zero. Through the whole cartridge transition range the magnitude of the flow forces are on average about 10 % of the valve spring force.

Table 2. Dimensions and operating point of the valve

m_{pop}	mass of cartridge	10 g
D_{pop}	diameter of cartridge	16 mm
α_{soc}	cone [vai socket] angle	45°
h_g	radial gap	1 mm
l_{thr}	length of throttle	1 mm
l_{fr}	length of frictional area	10 mm
$D_{thr,d}$	diameter of damping throttle	1 mm
C_q	discharge coefficient	0.7
r_f	fluid density	900 kg/m^3
n	fluid viscosity	30 cSt
Δp	pressure difference over valve	10 bar
x	position of poppet	5 mm
dx/dt	velocity of poppet	50 mm/s

[Mikä on damping throttle, sellaista ei ole venttiilikuvissa?]

The following calculated values represent the dynamics of this valve in the defined operating point:

- gain = -4.05×10^{-8}
- nominal angular velocity = 703 rad/s
- damping = -27.3

- static flow force = -24.7 N
- dynamic flow force = 1.5 N
- viscose friction force = 0.00075 N
- end cushioning damping force = 0.12 N

In this operation point the valve is unstable because of the effect of the dynamic flow forces.

Valve vibrates with an amplitude of 0.22 mm.

4 Valve modeling

Classified by their function or operation principle hydraulic valves can be divided to
- directional control valves
- pressure valves
- flow valves

Hydraulic valves are comprised of throttles whose cross-sectional flow area can be changed with an external control signal. The valve may have its own internal dynamics and may include following non-idealities:
- shapes of orifices
- flow forces
- spool valve lap
- leakage
- hysteresis
- time delay

Taking these characteristics into account is possible, but it complicates the model and accessing the needed parameter information may become troublesome or even impossible. The detail level of the model is determinated by the purpose of which the model is used for.

4.1 Connection ports

A hydraulic component can be externally linked to various types of connecting quantities
- hydraulic (pressure, flow rate)
- mechanical (position, velocity, acceleration, force, angular velocity, angular acceleration, torque)
- control (current, voltage, relative value)

When modeling hydraulic components, the most commonly used principle is to link the component model to the adjoining fluid volume models. In this case the input of the component models are the pressures of fluid fields and the output is the flow rate (or rates) through the component.

4.2 Model types

Based on the dependence of the model on the experimental data the models can be classified as
- analytic
- empiric
- semi-empiric

models.

An analytic model is based on the physical equations of the component. The values for model parameters are defined either according to the laws of physics or experimentally. The usability of the model in different operating conditions depends on the simplifications made when deriving the model. Identification of some parameters can be difficult.

Empiric (experimental) model is developed using so-called “black box” approach. The model repeats only the dependence that has been measured to exist between input and output quantities and the model is valid only for the system that it was identified with.

Semi-empiric, so-called ”grey box” model is a combination of the two previous. Likewise the analytical model it is based in the laws of physics, but some of its parameter values have been defined by testing the modeled system or a part of it. Validity of the model depends on the analytic part and identification of the model is easy in general, but requires measurement results.

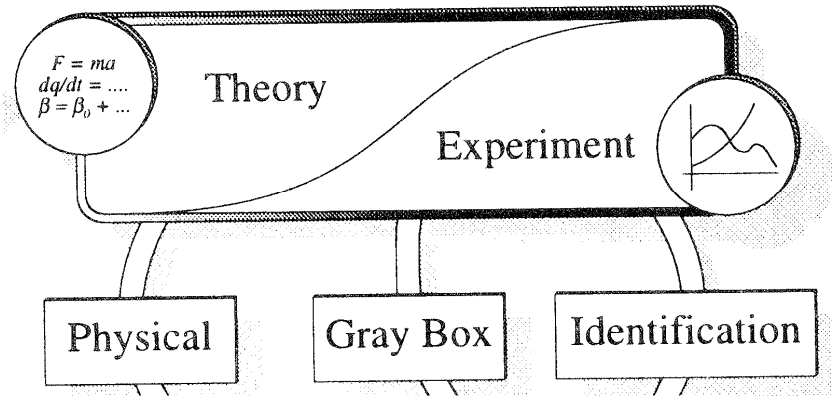

Figure 52. Modeling types.

4.3 Most common throttle geometries

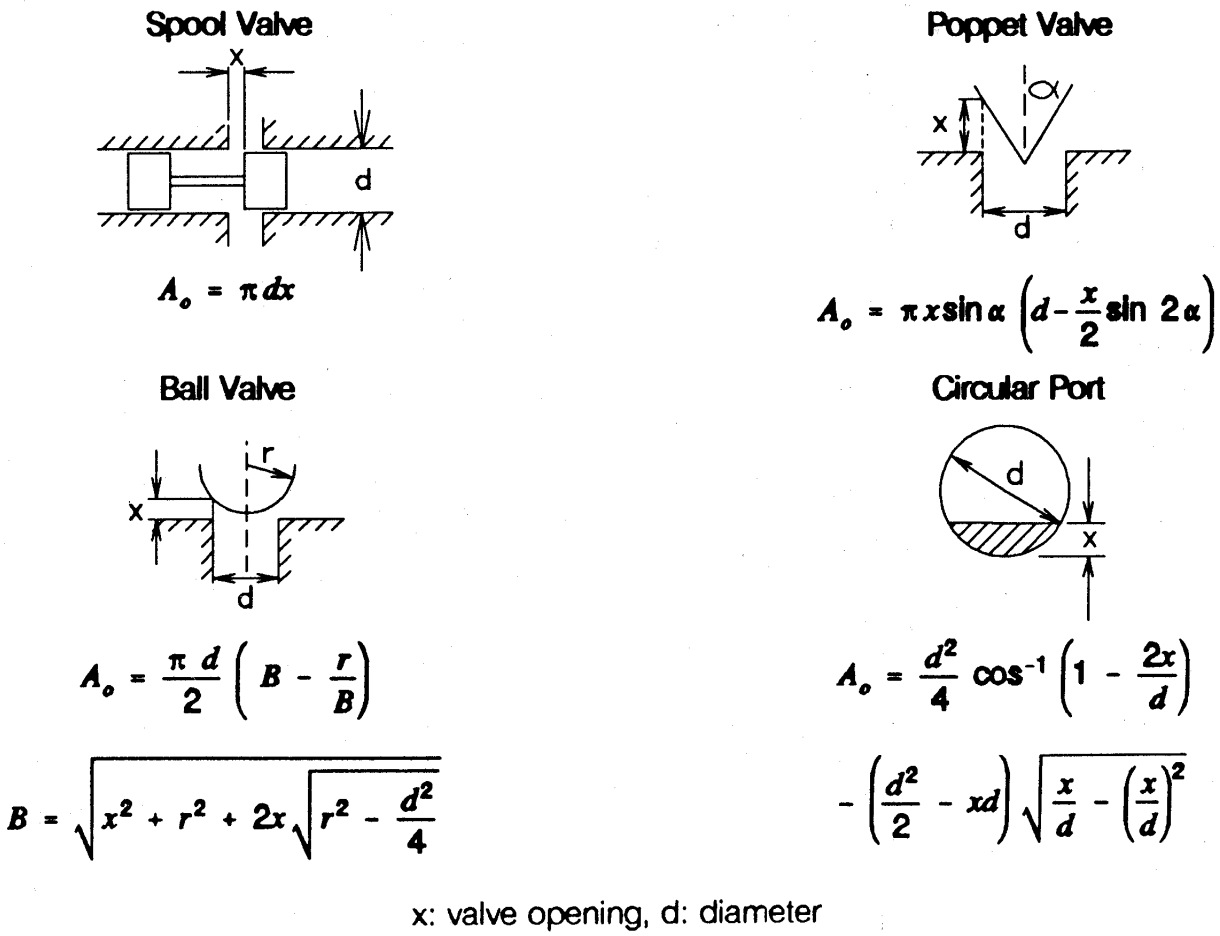

Figure 53. Throttle geometries with corresponding equations for flow areas. [Kuvaa muutettava seuraavasti: d → D_{vb} (spool valve), A_o → A_{fc}, r → r_{pop}, d → d_1 (ball valve ja poppet valve), B → Y, α → α_{pop}, d → d_{vp} (circular port)]

4.4 Submodels

A model for hydraulic valve can be divided into following submodels:

- compute the relative position (i.e. the momentary position in relation to the maximum position 0 → ±1) of spool or poppet. This position can be determined either by forced control or by integrating the equation of motion derived for valve spool/poppet.
- with this relative position compute the relative cross-sectional area of the throttle (0 → 1)
- with this relative area and the pressure across the valve use a throttle model to compute the flow rate through the valve. This throttle model is a basic primitive (or an element) that can be used to model any valve whatsoever.

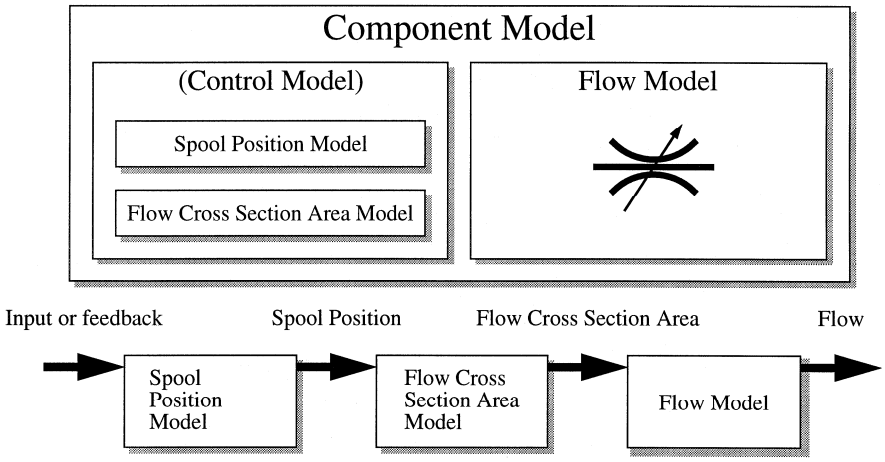

Figure 54. Component model with its submodels.

4.5 4/3 directional control valve

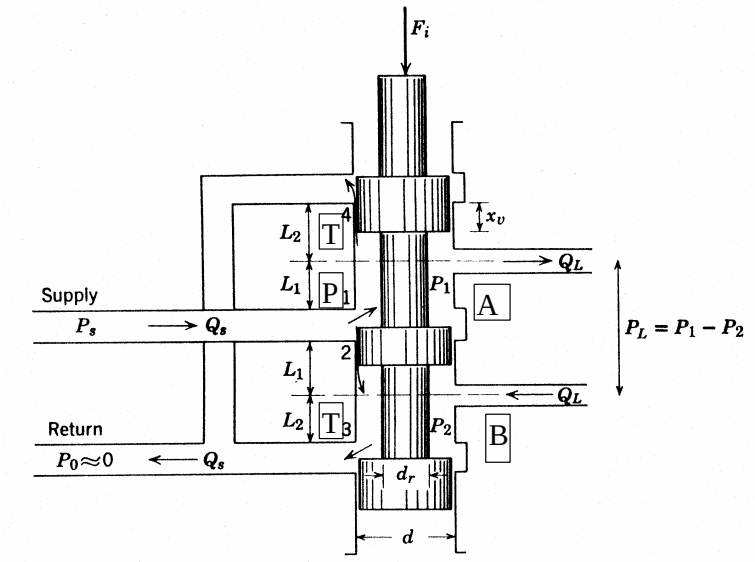

Figure 55. Schematic cross-section of 4/3 directional control valve. [Kuvaa muutettava seuraavasti: $P_s \rightarrow p_1$, $P_0 \rightarrow p_4$, $P_1 \rightarrow p_2$, $P_2 \rightarrow p_3$, $P_L \rightarrow p_L$, $Q_s \rightarrow q_{V,1}$, $Q_L \rightarrow q_{V,L}$, $d \rightarrow D_{vb}$, $d_r \rightarrow d_{vs}$, $x_v \rightarrow x_{vs}$, $L_1 \rightarrow l_{vb,1}$, $L_2 \rightarrow l_{vb,2}$, $F_i \rightarrow F_{ctrl}$].

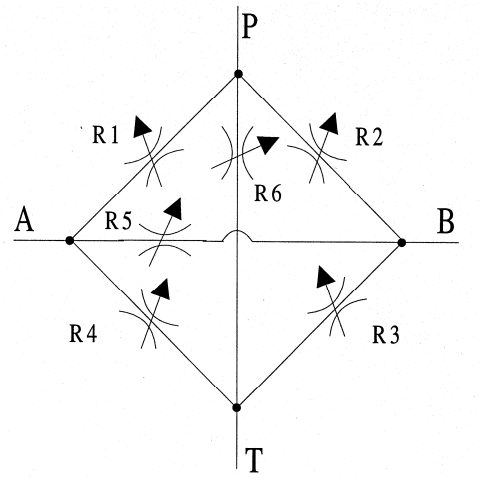

Figure 56. Flow paths of 4/3 directional control valve in Fig. 55. [Kuvaa muutettava seuraavasti: R1 → R_1, R2 → R_2, R3 → R_3, R4 → R_4, R5 → R_5, R6 → R_6]

1. Idealize the 4-way valve as six Wheatstone-bridge circuited throttles.
2. Derive the spool's equation of motion as a function of the control parameter.
3. Derive the throttle equations for each flow path as a function of spool position.
4. Identify the maximum openings of flow paths from the characteristic curves (q_V,Δp) of the valve.
5. Compute the relative opening $\left(\frac{C_q A_{fc}}{C_q A_{fc}^{max}}\right)$ for each flow path as a function of spool position .

When the inertial force, flow forces and spring force are omitted the equation of motion for spool can be written as

$$\frac{\mathrm{d}x_{vs}}{\mathrm{d}t} = F_{ctrl} = K_I I \qquad (4.1)$$

where I = control current of the solenoid and K_I = gain.

When assuming the valve to be zero-lapped and symmetric and the change in cross-sectional flow area to be linear, equations for relative openings (0 → 1) of each flow path can be written as

$$
\begin{cases}
A_{\mathrm{fc,1,rel}} = \dfrac{x_{\mathrm{vs}}(t)}{\left|x_{\mathrm{vs}}^{\max}\right|} & \text{, when } x_{\mathrm{vs}}(t) > 0 \\
A_{\mathrm{fc,1,rel}} = 0 & \text{, when } x_{\mathrm{vs}}(t) \le 0 \\
A_{\mathrm{fc,2,rel}} = \dfrac{\left|x_{\mathrm{vs}}(t)\right|}{\left|x_{\mathrm{vs}}^{\max}\right|} & \text{, when } x_{\mathrm{vs}}(t) < 0 \\
A_{\mathrm{fc,2,rel}} = 0 & \text{, when } x_{\mathrm{vs}}(t) \ge 0 \\
A_{\mathrm{fc,3,rel}} = 1 - \dfrac{x_{\mathrm{vs}}(t)}{\left|x_{\mathrm{vs}}^{\max}\right|} & \text{, when } x_{\mathrm{vs}}(t) > 0 \\
A_{\mathrm{fc,3,rel}} = 0 & \text{, when } x_{\mathrm{vs}}(t) \le 0 \\
A_{\mathrm{fc,4,rel}} = 1 - \dfrac{\left|x_{\mathrm{vs}}(t)\right|}{\left|x_{\mathrm{vs}}^{\max}\right|} & \text{, when } x_{\mathrm{vs}}(t) < 0 \\
A_{\mathrm{fc,4,rel}} = 0 & \text{, when } x_{\mathrm{vs}}(t) \ge 0 \\
A_{\mathrm{fc,5,rel}} = \mathrm{f}(x_{\mathrm{vs}}(t)) \\
A_{\mathrm{fc,6,rel}} = \mathrm{f}(x_{\mathrm{vs}}(t))
\end{cases}
\qquad (4.2)
$$

The maximum opening for each flow path can be defined with parameters (q_V,Δp). The values for these parameters are selected to conform the characteristic curve of the valve flow path in question.

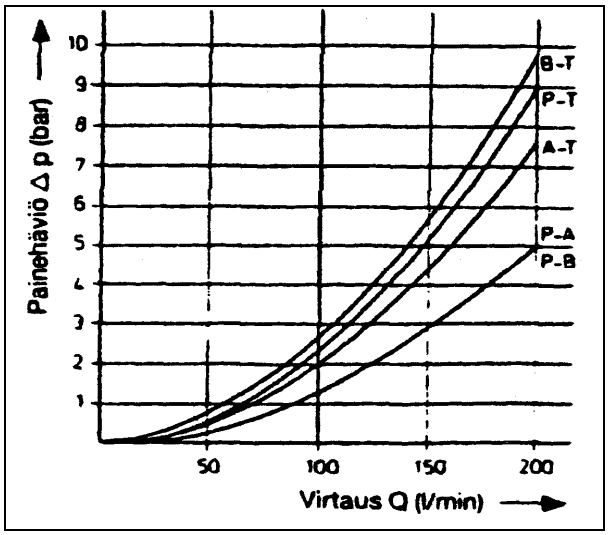

Figure 57. Characteristic curves of 4/3 directional control valve. [Kuvan tekstit käännettävä englanniksi. Kuvaa muutettava seuraavasti: painehäviö Δ p → Δ*p*, Virtaus Q → q_V].

$$
\begin{aligned}
C_{\mathrm{q}} A_{\mathrm{fc,P\to A}}^{\max} &= \frac{q_{\mathrm{V,P\to A}}}{\sqrt{\frac{2}{r_{\mathrm{f}}} \Delta p_{\mathrm{P\to A}}}} \\
C_{\mathrm{q}} A_{\mathrm{fc,P\to B}}^{\max} &= \frac{q_{\mathrm{V,P\to B}}}{\sqrt{\frac{2}{r_{\mathrm{f}}} \Delta p_{\mathrm{P\to B}}}} \\
C_{\mathrm{q}} A_{\mathrm{fc,B\to T}}^{\max} &= \frac{q_{\mathrm{V,B\to T}}}{\sqrt{\frac{2}{r_{\mathrm{f}}} \Delta p_{\mathrm{B\to T}}}} \\
C_{\mathrm{q}} A_{\mathrm{fc,A\to T}}^{\max} &= \frac{q_{\mathrm{V,A\to T}}}{\sqrt{\frac{2}{r_{\mathrm{f}}} \Delta p_{\mathrm{A\to T}}}} \\
C_{\mathrm{q}} A_{\mathrm{fc,A\to B}}^{\max} &= \frac{q_{\mathrm{V,A\to B}}}{\sqrt{\frac{2}{r_{\mathrm{f}}} \Delta p_{\mathrm{A\to B}}}} \\
C_{\mathrm{q}} A_{\mathrm{fc,P\to T}}^{\max} &= \frac{q_{\mathrm{V,P\to T}}}{\sqrt{\frac{2}{r_{\mathrm{f}}} \Delta p_{\mathrm{P\to T}}}}
\end{aligned}
\qquad (4.3)
$$

Flow rates passing through the valve flow paths are

$$
\begin{aligned}
q_{\mathrm{V,P\to A}} &= A_{\mathrm{fc,1,rel}}\, C_{\mathrm{q}}\, A_{\mathrm{fc,P\to A}}^{\max} \sqrt{\frac{2}{r_{\mathrm{f}}} \Delta p_{\mathrm{P\to A}}} \\
q_{\mathrm{V,P\to B}} &= A_{\mathrm{fc,2,rel}}\, C_{\mathrm{q}}\, A_{\mathrm{fc,P\to B}}^{\max} \sqrt{\frac{2}{r_{\mathrm{f}}} \Delta p_{\mathrm{P\to B}}} \\
q_{\mathrm{V,B\to T}} &= A_{\mathrm{fc,3,rel}}\, C_{\mathrm{q}}\, A_{\mathrm{fc,B\to T}}^{\max} \sqrt{\frac{2}{r_{\mathrm{f}}} \Delta p_{\mathrm{B\to T}}} \\
q_{\mathrm{V,A\to T}} &= A_{\mathrm{fc,4,rel}}\, C_{\mathrm{q}}\, A_{\mathrm{fc,A\to T}}^{\max} \sqrt{\frac{2}{r_{\mathrm{f}}} \Delta p_{\mathrm{A\to T}}} \\
q_{\mathrm{V,A\to B}} &= A_{\mathrm{fc,5,rel}}\, C_{\mathrm{q}}\, A_{\mathrm{fc,A\to B}}^{\max} \sqrt{\frac{2}{r_{\mathrm{f}}} \Delta p_{\mathrm{A\to B}}} \\
q_{\mathrm{V,P\to T}} &= A_{\mathrm{fc,6,rel}}\, C_{\mathrm{q}}\, A_{\mathrm{fc,P\to T}}^{\max} \sqrt{\frac{2}{r_{\mathrm{f}}} \Delta p_{\mathrm{P\to T}}}
\end{aligned}
\qquad (4.4)
$$

First-order transfer function for the valve spool is

$$
G_{\mathrm{x,I}}(\mathrm{s}) = \frac{x_{\mathrm{vs}}(\mathrm{s})}{I(\mathrm{s})} = \frac{K_{\mathrm{I}}}{t_{\mathrm{t}}\,\mathrm{s}+1} \qquad (4.5)
$$

and the transfer function from spool position to flow rate (e.g., in flow path P → A)

$$G_{\mathrm{f,x,P\text{®}A}}(\mathrm{s}) = \frac{q_{\mathrm{V,P\text{®}A}}(\mathrm{s})}{x_{\mathrm{vs}}(\mathrm{s})} = K_{\mathrm{qV,P\text{®}A}} = \frac{C_{\mathrm{q}}\, A_{\mathrm{fc,P\text{®}A}}^{\max}}{x_{\mathrm{vs}}^{\max}} \sqrt{\frac{2}{r_{\mathrm{f}}} \Delta p_{\mathrm{P\text{®}A}}} \qquad (4.6)$$

Thus the transfer function of the valve takes the form

$$G_{\mathrm{f,I,P\text{®}A}}(\mathrm{s}) = \frac{q_{\mathrm{V}}(\mathrm{s})}{I(\mathrm{s})} = G_{\mathrm{x,I}}(\mathrm{s})\, G_{\mathrm{f,x,P\text{®}A}}(\mathrm{s}) = \frac{K_{\mathrm{I}}\, K_{\mathrm{qV,P\text{®}A}}}{t_{\mathrm{t}}\,\mathrm{s}+1} = \frac{K_{\mathrm{I}} \dfrac{C_{\mathrm{q}}\, A_{\mathrm{fc,P\text{®}A}}^{\max}}{x_{\mathrm{vs}}^{\max}} \sqrt{\dfrac{2}{r_{\mathrm{f}}} \Delta p_{\mathrm{P\text{®}A}}}}{t_{\mathrm{t}}\,\mathrm{s}+1} \qquad (4.7)$$

4.6 Pressure relief valve

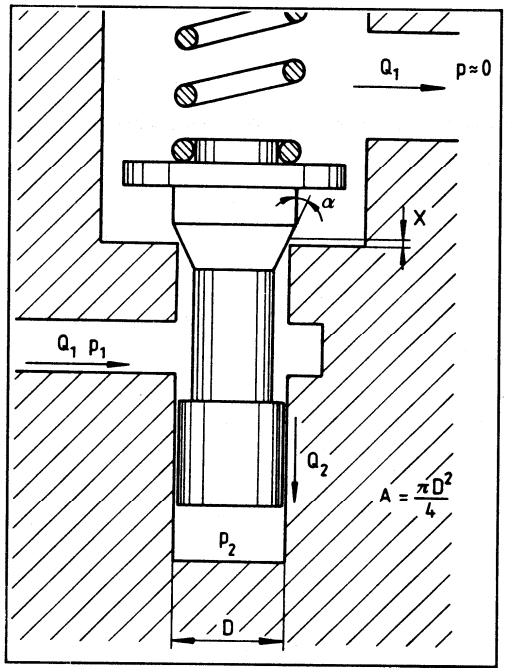

Figure 58. Principled cross-section of pressure relief valve. [Kuvaa muutettava seuraavasti: D → D_{vs}, A → $A_{\mathrm{vs,e}}$, Q_1 → $q_{\mathrm{V,1}}$, Q_2 → $q_{\mathrm{V,2}}$, ulosvirtauskanavan Q_1 → $q_{\mathrm{V,3}}$, p_1 → p_1, p_2 → p_2, ulosvirtauskanavan p → p_3, α → α_{pop}]. Lisäksi kuvan D-mitta on muutettava osoittamaan karan halkaisijaa.

1. Derive the spool's equation of motion
2. Derive the throttle equations for the flow path of the valve
3. Derive an equation linking together spool position and throttle opening
4. Identify the maximum opening of the throttle from the characteristic curve (q, Δp) of the valve
5. Identify the values for the parameters of the equation of motion from the characteristic curve (q, Δp) of the valve

Valve's equation of motion can written as

$$m\frac{\mathrm{d}^2x}{\mathrm{d}t^2} = F_\mathrm{p} + F_\mathrm{R} + F_\mathrm{B} + F_\mathrm{f} + F_\mathrm{pre}$$

$$= \Delta p\, A_\mathrm{vs,e} - k_\mathrm{R}\, x - b_\mathrm{v}\frac{\mathrm{d}x}{\mathrm{d}t} - k_\mathrm{R,h}\, x\,\Delta p - p_\mathrm{ref}\, A_\mathrm{vs,e}\text{, when } m \approx 0 \quad \Rightarrow \tag{4.8}$$

$$\frac{\mathrm{d}x}{\mathrm{d}t} = \frac{A_\mathrm{vs,e}(\Delta p - p_\mathrm{ref}) - x(k_\mathrm{R} + k_\mathrm{R,h}\,\Delta p)}{b_\mathrm{v}}$$

[Voimille laitettava selitykset!, Mikä on Δp, entä p_{ref}? Selitykset!]

In steady-state conditions the derivative is

$$\frac{dx}{\mathrm{d}t} = 0 \tag{4.9}$$

which allows the equation of motion to be written as

$$x = \frac{(\Delta p - p_\mathrm{ref})\, A_\mathrm{vs,e}}{k_\mathrm{R} + k_\mathrm{R,h}\,\Delta p} \tag{4.10}$$

In case of spool valve the following dependence can be written to spool position and cross-sectional area of the throttle

$$C_\mathrm{q} A_\mathrm{fc} = C_\mathrm{q}\,\pi\, D_\mathrm{vb}\, x \tag{4.11}$$

[Tarvitaan kuva luistiventtiilistä merkintöineen!]

Turbulent throttle equation is of form

$$q_\mathrm{V,thr} = C_\mathrm{q}\, A_\mathrm{fc}\sqrt{\frac{2\Delta p}{\rho_\mathrm{f}}} \tag{4.12}$$

By substituting this to the previously presented the equation for steady-state condition of the valve takes the form

$$q_\mathrm{V} = \frac{C_\mathrm{q}\,\pi\, D_\mathrm{vb}\,(\Delta p - p_\mathrm{ref})\, A_\mathrm{vs,e}}{k_\mathrm{R} + k_\mathrm{R,h}\,\Delta p}\sqrt{\frac{2\Delta p}{\rho_\mathrm{f}}} \tag{4.13}$$

The following set of equations can be formed on grounds of the parameters defined from the given characteristic curves.

$$\begin{cases} q_{V,1} = \dfrac{C_q \pi D_{vb} (p_1 - p_{1,ref}) A_{vs,e}}{k_R + k_{R,h} p_1} \sqrt{\dfrac{2 p_1}{r_f}} \\ q_{V,2} = \dfrac{C_q \pi D_{vb} (p_2 - p_{2,ref}) A_{vs,e}}{k_R + k_{R,h} p_2} \sqrt{\dfrac{2 p_2}{r_f}} \end{cases} \qquad (4.14)$$

[p_{ref} –muuttujille on laitettava selitykset!]

Using this set of equations it's possible to solve expressions for both mechanical and hydraulic spring constants to be used in simulation.

An expression for the parameter describing the valve dynamics can be derived using the mechanical and hydraulic spring constants and the time constant of the valve which is given as a parameter and defined at certain operation point of pressure p_{op}.

$$y_{valve,op} = t_t \left(k_R + k_{R,h} p_{op}\right) \qquad (4.15)$$

Equation of motion takes now form

$$\frac{\mathrm{d}C_q A_{fc}}{\mathrm{d}t} = \frac{\frac{p}{4} D_{vb}^{\,2} (p_1 - p_{1,ref}) - \frac{C_q A_{fc}}{C_q \pi D_{vb}} \left(k_R + k_{R,h} p_1\right)}{b_v} \quad , 0 \le C_q A_{fc} \le C_q A_{fc}^{max} \qquad (4.16)$$

[Onko ylläoleva kaava oikein, vai tulisiko sen kuulua:]

$$\frac{\mathrm{d}C_q A_{fc}}{\mathrm{d}t} = \frac{\frac{p}{4} D_{vb}^{\,2} (p_1 - p_{1,ref}) C_q \pi D_{vb} - C_q A_{fc} \left(k_R + k_{R,h} p_1\right)}{b_v} \quad , 0 \le C_q A_{fc} \le C_q A_{fc}^{max} \qquad (4.16)$$

[?]

$$\begin{cases} q_V = C_q A_{fc} \sqrt{\dfrac{2|\Delta p|}{r_f}} & , |\Delta p| \ge 0 \\ q_V = 0 & , |\Delta p| \le 0 \end{cases} \qquad (4.17)$$

$\Delta p = p_1 - p_2$ [näiden merkintöjen on täsmättävä venttiilin kuvan merkintöihin, kuva tulossa?]

$q_{V,1} = -q_V$

$q_{V,2} = q_V$

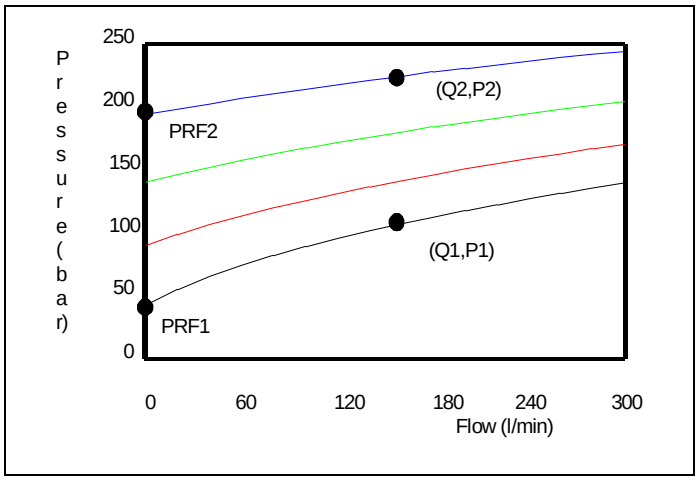

Figure 59. Identification of parameters from the characteristic curves of the valve. [Kuvaa muutettava seuraavasti: Q1 → $q_{V,1,ch}$, P1 → $p_{1,ch}$, PRF1 → $p_{1,ch,ref}$, Q2 → $q_{V,2,ch}$, P2 → $p_{2,ch}$, PRF2 → $p_{2,ch,ref}$, Flow → q_V, Pressure → p].

Parameter identification (notation according to Fig. 59):

$$k_R = \frac{(p_{1,ch} - p_{1,ch,ref}) - k_{R,h} q_{V,1,ch} \sqrt{p_{1,ch}}}{\frac{q_{V,1,ch}}{\sqrt{p_{1,ch}}}} \tag{4.18}$$

$$k_{R,h} = \frac{(p_{2,ch} - p_{2,ch,ref}) - (p_{1,ch} - p_{1,ch,ref}) \frac{q_{V,2,ch}\sqrt{p_{1,ch}}}{q_{V,1,ch}\sqrt{p_{2,ch}}}}{q_{V,2,ch}\sqrt{p_{2,ch}} - \frac{q_{V,2,ch}}{\sqrt{p_{2,ch}}} p_{1,ch}} \tag{4.19}$$

$$y_{valve,op} = t_t \left(k_R + k_{R,h} \Delta p_{op}\right) \tag{4.20}$$

$$C_q A_{fc}^{max} = \frac{q_{V,sat}}{\sqrt{\frac{2\, p_{sat}}{r_f}}} \tag{4.21}$$

where

$(p_{1,ch}, q_{V,1,ch})$, $(p_{2,ch}, q_{V,2,ch})$ = (q_V,p)-points of characteristic curves
$p_{1,ch,ref}$, $p_{2,ch,ref}$ = set pressures of characteristic curves
$(p_{sat}, q_{V,sat})$ = saturation point of the valve

[Missä kuva?]
Figure 60. Time constant as a function of pressure level.

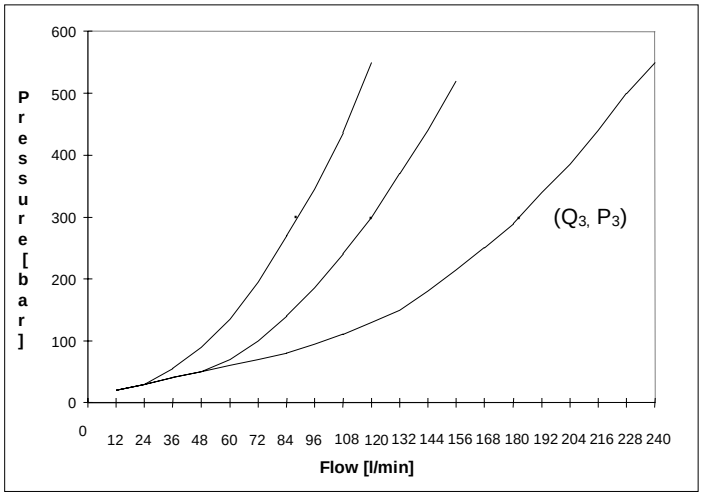

Figure 61. Saturation of different valve sizes. [Kuvaa muutettava seuraavasti: Flow → q_V, Pressure → p, Q_3 → $q_{V,sat}$, P_3 → p_{sat}]

5 System modeling

5.1 Topology

Formulation of the model can be eased by dividing it into testable modular subsystems which represent typical parts of mechanical engineering like pipes and valves. The model is divided into fluid fields and hydraulic components that transmit the bidirectional pressure-flow rate interaction.

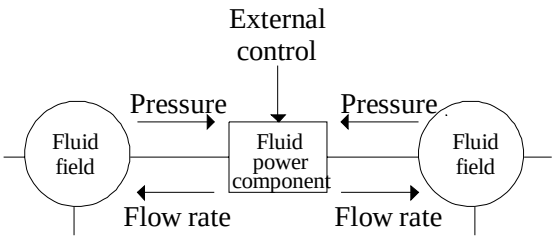

Figure 62. Topology of the model.

The model of hydraulic system is thus compiled of modular fluid field models and hydraulic component models. Fluid fields are fuid volumes that lay between components and connect to each other via hydraulic components. The actuator model is the link between hydraulic and mechanical system. Because of the model structure the hydraulic system can be divided to subsystems of various levels which eases up the testing of the model.

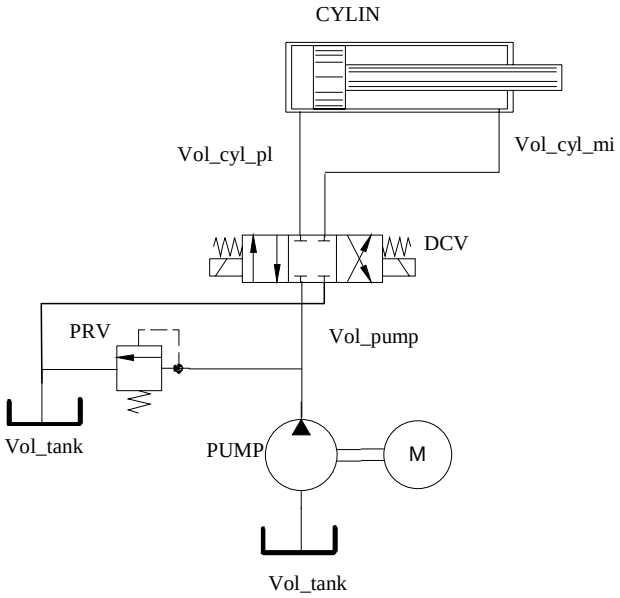

Figure 63. An example of a model for hydraulic system.

Component models of the example system (Fig. 63)

1. Pump
   - PUMP
2. Pressure relief valve
   - PRV
3. 4/3 directional control valve
   - DCV
4. Cylinder
   - CYLIN
5. Flexible fluid field models
   – Vol_pump
   – Vol_cyl_pl
   – Vol_cyl_mi
6. Constant pressure fluid field models
   – Vol_tank

In the model of hydraulically operated mechanism the mechanism is modeled with Lagrangian model equations in which the interaction between the parts of mechanism is eliminated. The process material field and the interaction between structure field and process material field is usually case-spesific.

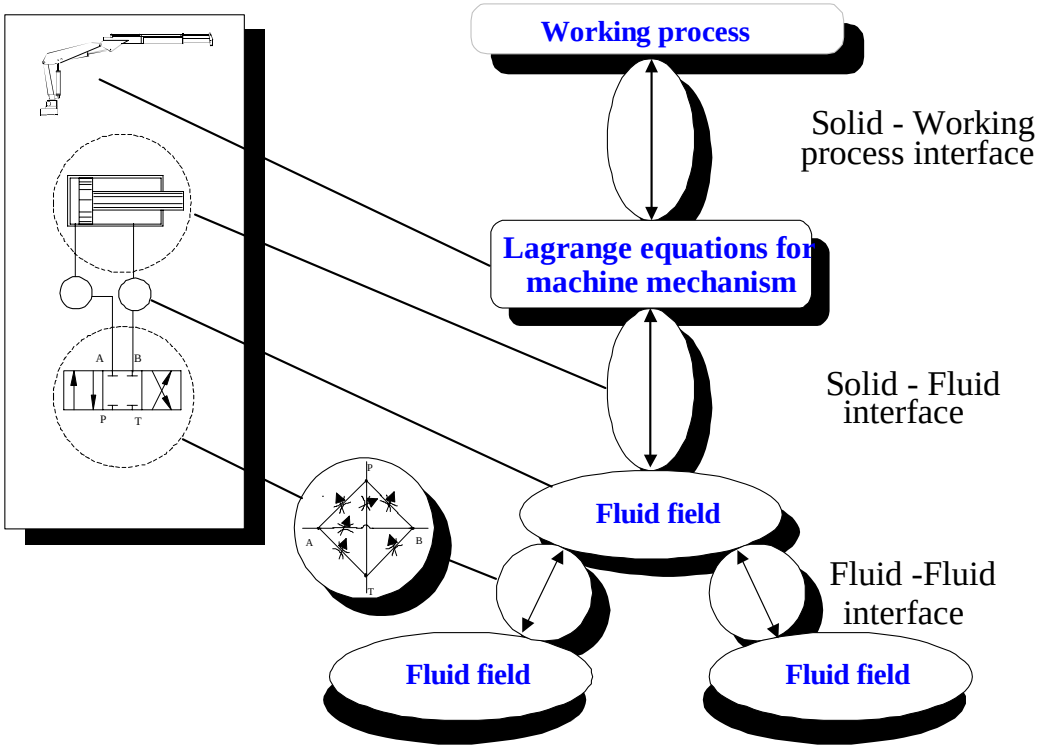

Figure 64. Transmission of bidirectional interaction in hydraulically controlled multibody system.

Because the limiting equations (i.e. component models) between fluid fields are non-linear the field equations cannot be solved simultaneously like the case is in mechanics with Lagrangien equations. In solving system the pressure dependent flow rates are computed first and after this are solved the pressure derivatives that depend on the flow rates. The throttle equations cause an algebraic loop to the model which can cause problems depending on the solve of the differential

Hydraulikomponenttimallit

Models for hydraulic components [tässä pitäisi olla periaatetasoinen laatikkokuva ilman sen suurempaa informaatioarvoa.]

...

Nestekenttämallit

Fluid field models [tässä pitäisi olla periaatetasoinen laatikkokuva ilman sen suurempaa informaatioarvoa.]

...

5.2 Parameterisation

In order to achieve as much object oriented model structure as possible also the model parameters should be grouped as follows:

1. System parameters that affect the entire system. These are, e.g., parameterisation of valve control, set pressure of pressure relief valve, external loading of cylinder, etc.
2. Component parameters that define the characteristics of the component. These are the components dimensions and points of characteristic curves. Also the fluid is a component in a system and its parameters are parameters of the fluid component.

The component parameters are stored in component-specific data bases.

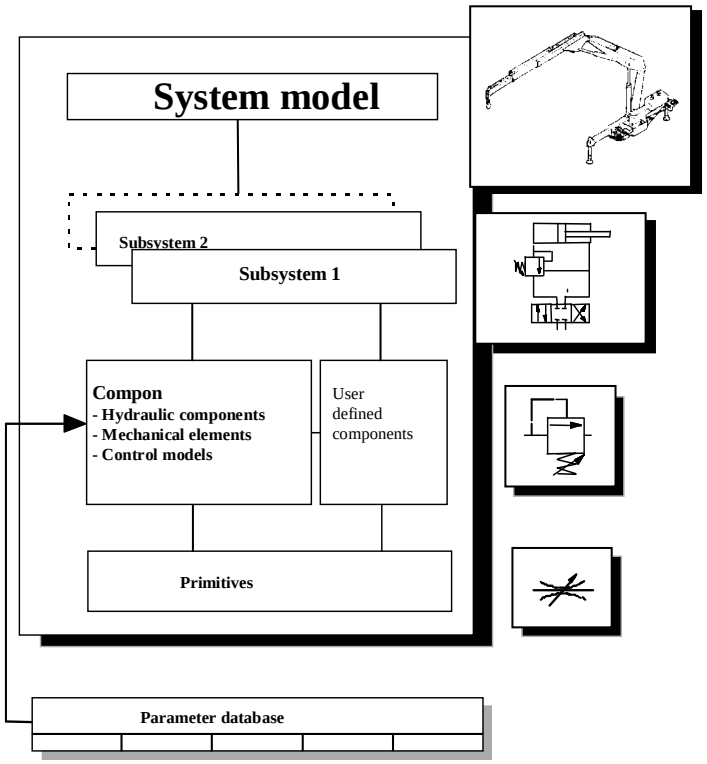

Figure 65. Parameterisation of a model and model structure.

5.3 Fluid fields

Because of the topology two type of fluid fields are needed

1. Flexible fluid field in which the derivative of pressure is solved from the equation of continuity. Depending on the approximation level the model takes into account the elasticities of the fluid, the free air in the fluid and possibly also the structure. Model parameters are volume and structural compression modulus.
2. Constant pressure fluid field in which the pressure does not depend on the flow rate. This model is needed, e.g., in reservoir lines and it can be used to represent a source of constant pressure. Model parameter is pressure.

5.4 Mathematical stiffness of the model

Consider the system in Fig. 66 and the time constants affecting to its operation.

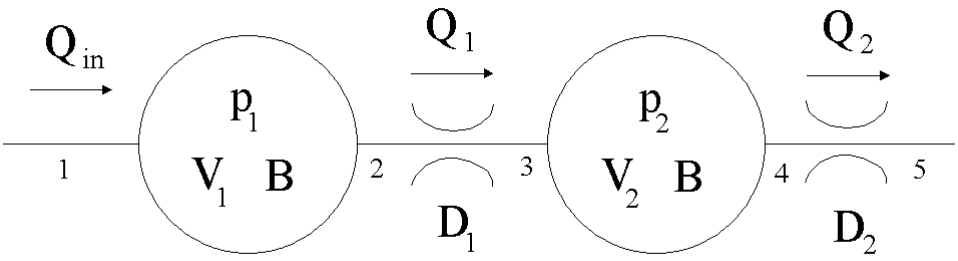

Figure 66. System example. [Kuvaa muutettava seuraavasti: $Q_{in} \rightarrow q_{V,1}$, $Q_1 \rightarrow q_{V,2}$, $Q_2 \rightarrow q_{V,3}$, $p_1 \rightarrow p_1$, $p_2 \rightarrow p_2$, $V_1 \rightarrow V_1$, $V_2 \rightarrow V_2$, $B \rightarrow K_f$, $D_1 \rightarrow D_{H,1}$, $D_2 \rightarrow D_{H,2}$].

System pressures and flow rates can be described simplified as follows:

$$\begin{cases} q_{V,1} - q_{V,2} = \dfrac{V_1}{K_f}\dfrac{\mathrm{d}p_1}{\mathrm{d}t} \\ q_{V,2} = C_q \dfrac{p}{4} D_{H,1}^{\,2} \sqrt{\dfrac{2(p_1 - p_2)}{r_f}} \\ q_{V,2} - q_{V,3} = \dfrac{V_2}{K_f}\dfrac{\mathrm{d}p_2}{\mathrm{d}t} \\ q_{V,3} = C_q \dfrac{p}{4} D_{H,2}^{\,2} \sqrt{\dfrac{2\,p_2}{r_f}} \end{cases} \qquad (5.1)$$

where

V = volumes
K_f = bulk modulus of fluid
p = pressures
D_H = hydraulic diameter of throttles
C_q = flow coefficient of the throttle

Flow rates through the throttles can be written as

$$\begin{aligned} q_{\mathrm{V},1} &= k_{\mathrm{v},1}\sqrt{p_1 - p_2} \quad ; \quad k_{\mathrm{v},1} = C_{\mathrm{q}}\frac{\pi}{4}D_{\mathrm{H},1}^{\,2}\sqrt{\frac{2}{\rho_{\mathrm{f}}}} \\ q_{\mathrm{V},2} &= k_{\mathrm{v},2}\sqrt{p_2} \qquad ; \quad k_{\mathrm{v},2} = C_{\mathrm{q}}\frac{\pi}{4}D_{\mathrm{H},2}^{\,2}\sqrt{\frac{2}{\rho_{\mathrm{f}}}} \end{aligned} \tag{5.2}$$

and thus the time derivatives for the pressures are

$$\begin{aligned} \frac{\mathrm{d}p_1}{\mathrm{d}t} &= \frac{K_{\mathrm{f},1}}{V_1}\left(q_{\mathrm{V},1} - q_{\mathrm{V},2}\right) = \frac{K_{\mathrm{f},1}}{V_1}\left(q_{\mathrm{V},1} - k_{\mathrm{v},1}\sqrt{p_1 - p_2}\right) \\ \frac{\mathrm{d}p_2}{\mathrm{d}t} &= \frac{K_{\mathrm{f},2}}{V_2}\left(q_{\mathrm{V},2} - q_{\mathrm{V},3}\right) = \frac{K_{\mathrm{f},2}}{V_2}\left(k_{\mathrm{v},1}\sqrt{p_1 - p_2} - k_{\mathrm{v},2}\sqrt{p_2}\right) \end{aligned} \tag{5.3}$$

Linearization of the equation (*5.3*) in operation point ($p_{1,\mathrm{op}}$, $p_{2,\mathrm{op}}$) results into following linear equation:

$$\begin{cases} \dfrac{\mathrm{d}p_1}{\mathrm{d}t} \approx \dfrac{K_{\mathrm{f},1}}{V_1}\left[q_{\mathrm{V},1} - k_{\mathrm{v},1,\mathrm{op}}\left(p_{1,\mathrm{op}} - p_{2,\mathrm{op}}\right)\right] \\ \dfrac{\mathrm{d}p_2}{\mathrm{d}t} \approx \dfrac{K_{\mathrm{f},2}}{V_2}\left[k_{\mathrm{v},1,\mathrm{op}}\left(p_{1,\mathrm{op}} - p_{2,\mathrm{op}}\right) - k_{\mathrm{v},2,\mathrm{op}}\,p_{2,\mathrm{op}}\right] \end{cases} \tag{5.4}$$

where:

$$\begin{aligned} k_{\mathrm{v},1,\mathrm{op}} &= \frac{C_{\mathrm{q}}\,\pi\,D_{\mathrm{H},1}^{\,2}}{2\sqrt{2\,\rho_{\mathrm{f}}\left(p_{1,\mathrm{op}} - p_{2,\mathrm{op}}\right)}} \\ k_{\mathrm{v},2,\mathrm{op}} &= \frac{C_{\mathrm{q}}\,\pi\,D_{\mathrm{H},2}^{\,2}}{2\sqrt{2\,\rho_{\mathrm{f}}\,p_{2,\mathrm{op}}}} \end{aligned} \tag{5.5}$$

Choosing the pressures to be state variables the equation (*5.4*) can be written in state form:

$$\begin{bmatrix} \dfrac{\mathrm{d}p_1}{\mathrm{d}t} \\ \dfrac{\mathrm{d}p_2}{\mathrm{d}t} \end{bmatrix} = \begin{bmatrix} -k_{\mathrm{v},1}\dfrac{K_{\mathrm{f}}}{V_1} & k_{\mathrm{v},1}\dfrac{K_{\mathrm{f}}}{V_1} \\ k_{\mathrm{v},1}\dfrac{K_{\mathrm{f}}}{V_2} & -\left(k_{\mathrm{v},1}+k_{\mathrm{v},2}\right)\dfrac{K_{\mathrm{f}}}{V_2} \end{bmatrix} \begin{bmatrix} p_1 \\ p_2 \end{bmatrix} + \begin{bmatrix} \dfrac{K_{\mathrm{f}}}{V_1} \\ 0 \end{bmatrix} q_{\mathrm{V},1} \tag{5.6}$$

Time constants of the system can be found out by solving the eigenvalues of this state equation which in turn are the solutions of the characteristic equation:

$$\Gamma_{1,2} = -\frac{1}{2}\frac{K_f\, k_{v,1} V_2 + K_f\left(k_{v,1} + k_{v,2}\right)V_1}{V_1\, V_2} \pm \frac{1}{2}\sqrt{\left(\frac{K_f\, k_{v,1} V_2 + K_f\left(k_{v,1} + k_{v,2}\right)V_1}{V_1\, V_2}\right)^2 - 4\frac{K_f^{\,2}\, k_{v,1}\, k_{v,2}}{V_1\, V_2}} \tag{5.7}$$

From this equation the time constants are derived as

$$\begin{cases} t_{t,1} = -\dfrac{1}{\Gamma_1} \\ t_{t,2} = -\dfrac{1}{\Gamma_2} \end{cases} \tag{5.8}$$

Consider the following case of numerical example where the values of volume V_2 and diameter $D_{H,1}$ vary

p_1	= 247 bar	V_1	= 1 l
p_2	= 245 bar	K_f	= 1500 MPa
C_q	= 0.7	$D_{H,2}$	= 1.5 mm
ρ_f	= 900 kg/m^3	V_2	= 0.01–1.0 l
		$D_{H,1}$	= 1.5–10 mm

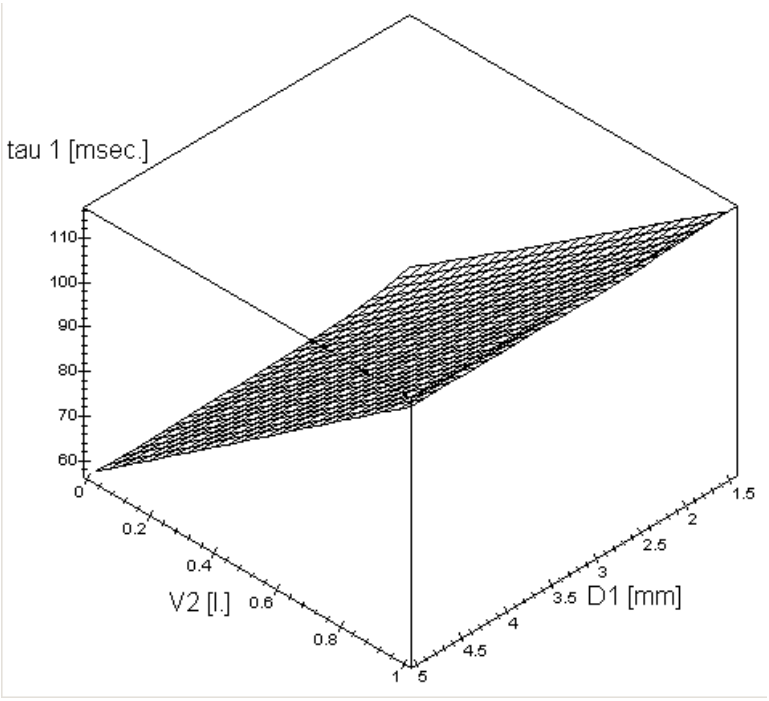

Figure 67. [Kuvaa muutettava seuraavasti: D1 → $D_{H,1}$, V2 → V_2, tau 1 → $\tau_{t,1}$].

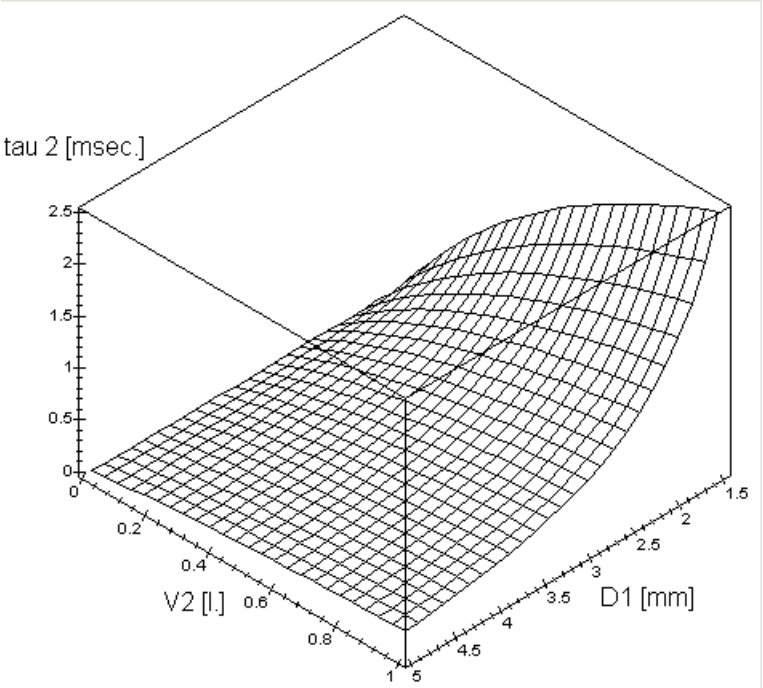

Figure 68. [Kuvaa muutettava seuraavasti: D1 → $D_{H,1}$, V2 → V_2, tau 2 → $\tau_{t,2}$].

First mode of the system is associated with the changes in pressures of both volumes. Second mode is associated with the leveling of the pressures between the volumes. Since the magnitudes of the modes differ somewhat from each other (first mode 100 ms, second mode 2 ms) the system has some numerical stiffness. The situation gets much worse if the value of throttle diameter $D_{H,1}$ is increased since this leads to a situation where the pressures p_1 and p_2 are strongly connected to each other and the numerical solving of the system is difficult. Likewise the decreasing of the volume V_2 complicates the numerics.

In summary:

- avoid large throttles between volumes. Always try to reduce a number of large throttles into one smaller throttle.
- avoid small fluid volumes if possible

6 Modeling actuators and friction

6.1 General

This chapter discusses the dynamic modeling of hydraulic cylinders and motors. The weight is on the cylinder modeling since this is the hardest task, and the motors are covered only where their modeling differs from modeling of cylinders. Both cylinders and motors are subjected to significant friction forces or torques. Modeling of friction under dynamic conditions is discussed separately at the end of this chapter. The principle used here is to derive for each component a model that is concurrently as simple as possible but which also represents the dynamics of the component well enough in general. Some simplifications that can be made to the equations in most cases are done without mentioning them separately. When needed, the reader has to be able to apply the more accurate theory discussed in previous chapters.

6.2 Cylinder modeling

6.2.1 Nomenclature and assumptions

Here only the modeling of an asymmetric cylinder is discussed since the symmetric cylinder is a special case of the asymmetric cylinder. Likewise only the double acting cylinder is discussed since a model for single acting cylinder is easily created by dropping out half of the equations. Figure 69 presents schematic structure of an asymmetric cylinder and the nomenclature used in modeling.

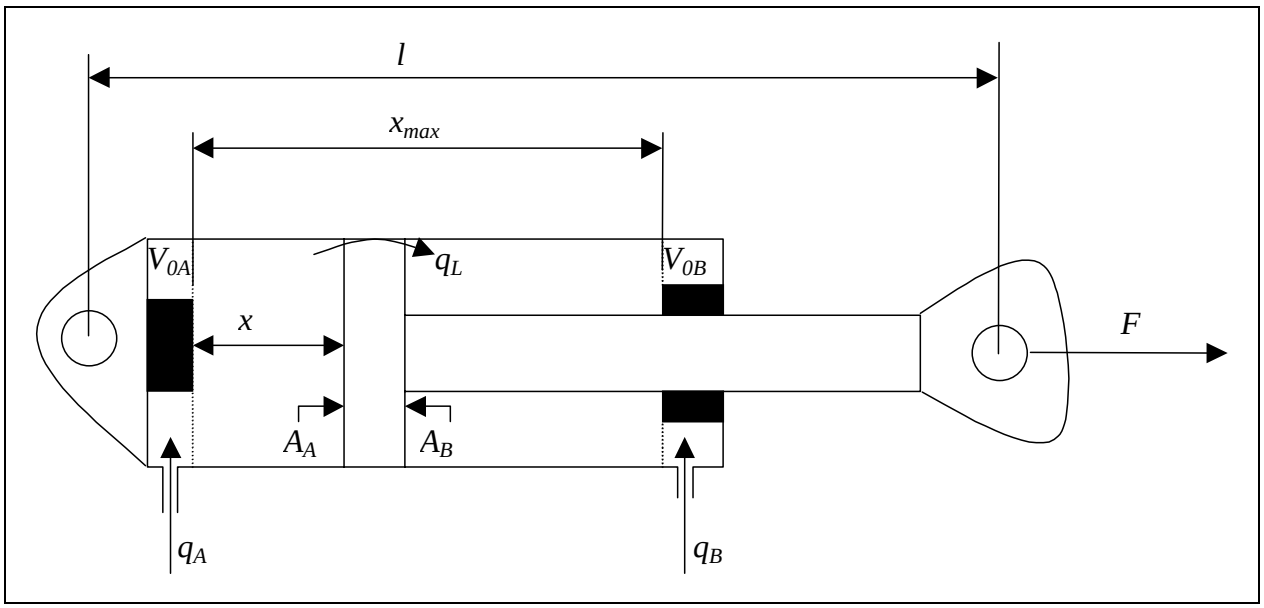

Figure 69. Asymmetric cylinder and the related nomenclature. [Kuvaa muutettava seuraavasti: $q_A \rightarrow q_{V,cyl,1}$, $q_B \rightarrow q_{V,cyl,3}$, $q_L \rightarrow q_{V,cyl,d}$, $A_A \rightarrow A_{cyl,1}$, $A_B \rightarrow A_{cyl,3}$, $V_{0A} \rightarrow V_{cyl,1,e}$, $V_{0B} \rightarrow V_{cyl,3,e}$, $l \rightarrow l_{cyl,fp}$, $x \rightarrow x_{cyl}$, $x_{max} \rightarrow x_{cyl}^{max}$, $F \rightarrow F_{cyl}$]. [Täydennetään kuvaan tiedot: $p_{cyl,1}$, $p_{cyl,3}$, $A_{cyl,3}$ (männänvarren poikkipinta-ala)].

Symbols used in Fig. 69:

$q_{V,cyl,1}$ Flow rate into piston side volume of the cylinder [m^3/s]
$q_{V,cyl,3}$ Flow rate into piston rod side volume of the cylinder [m^3/s]
$q_{V,cyl,d}$ Leakage flow from piston side to piston rod side volume [m^3/s]
$p_{cyl,1}$ Pressure in piston side volume [Pa]
$p_{cyl,3}$ Pressure in piston rod side volume [Pa]
x_{cyl} Distance of the piston from the cylinder end at piston side [m]
x_{cyl}^{max} Maximum distance of the piston from the cylinder end at piston side [m]
$\dot{x}_{cyl}$ Piston velocity [m/s]
$l_{cyl,fap}$ Distance between the cylinder fastening points [m]
$A_{cyl,1}$ Cross-sectional piston area [m^2]
$A_{cyl,2}$ Cross-sectional piston rod area [m^2]
$A_{cyl,3}$ Cross-sectional piston area minus cross-sectional piston rod area [m^2]
F_{cyl} *Net* force of the cylinder [N]
$F_{\mu,cyl}$ Friction force of the cylinder [N]
$V_{cyl,1,e}$ Wasted volume at the piston side of the cylinder [m^3]
$V_{cyl,3,e}$ Wasted volume at the piston rod side of the cylinder [m^3]

The direction of movement and piston and piston rod sides are defined so that increasing x_{cyl} increases the volume at piston side and reduces it at piston rod side. Following assumptions are made in deriving the cylinder model:

- No external leakage flow exists
- Internal leakage flow is assumed to be laminar
- Pressure is divided evenly in the cylinder volumes

6.2.2 Basic equations

Basically a cylinder is nothing but two changing volumes and a force equation. The state equation of volume is of form:

$$\dot{p} = \frac{K_e}{V}\left(\Sigma q_V - \dot{V}\right) \qquad (6.1)$$

where K_e is the effective bulk modulus of volume V. The piston and piston rod side volumes are

$$V_{cyl,1} = V_{cyl,1,e} + A_{cyl,1}\, x_{cyl} \quad , \quad V_{cyl,3} = V_{cyl,3,e} + A_{cyl,3}\left(x_{cyl}^{max} - x_{cyl}\right) \qquad (6.2)$$

Differentiating these gives the changes in volumes

$$\dot{V}_{cyl,1} = A_{cyl,1}\,\dot{x}_{cyl} \quad , \quad \dot{V}_{cyl,3} = -A_{cyl,3}\,\dot{x}_{cyl} \qquad (6.3)$$

Leakage flow is assumed to be laminar and is thus of form

$$q_{V,cyl,d} = k_{v,cyl,d}\left(p_{cyl,1} - p_{cyl,3}\right) \qquad (6.4)$$

Usually the leakage flow can be assumed to be zero ($q_{V,cyl,d} = 0$). Substituting the equations (*6.2*)–(*6.4*) in to the state equation of volume results into following equations for the pressures in piston and piston rod side volumes:

$$\begin{aligned} \dot{p}_{cyl,1} &= \frac{K_{e,1}}{V_{cyl,1,e} + A_{cyl,1}\, x_{cyl}} \left(q_{V,cyl,1} - k_{v,cyl,d} \left(p_{cyl,1} - p_{cyl,3} \right) - A_{cyl,1}\, \dot{x}_{cyl} \right) \\ \dot{p}_{cyl,3} &= \frac{K_{e,1}}{V_{cyl,3,e} + A_{cyl,3} \left(x_{cyl}^{max} - x_{cyl} \right)} \left(q_{V,cyl,3} + k_{v,cyl,d} \left(p_{cyl,1} - p_{cyl,3} \right) + A_{cyl,3}\, \dot{x}_{cyl} \right) \end{aligned} \qquad (6.5)$$

The effective bulk moduluses for piston and piston rod side volumes can be computed by applying the equations presented in Chapter 2. These equations manifest that the effective bulk modulus depends on the pressure and on the content of free air in the fluid, but not on the size of the volume and therefore also not on the position of the piston. Usually the values for bulk moduluses are impossible to compute and experimentally defined values are used instead. A typical value is 1000–1400 MPa, while the theoretical value is approximately 1500 MPa.

Net force of the cylinder is

$$F_{cyl} = p_{cyl,1}\, A_{cyl,1} - p_{cyl,3}\, A_{cyl,3} - F_{\mu,cyl} \qquad (6.6)$$

Modeling of the friction force F_m is discussed in Chapter 6.4.

6.2.3 Inputs and outputs of cylinder model

Pressures $p_{cyl,1}$ and $p_{cyl,3}$, and also the force of the cylinder F_{cyl} can be solved with the equations (*6.2*)–(*6.6*) when the position x_{cyl} and the velocity $\dot{x}_{cyl}$ of the piston, and the flow rates $q_{V,cyl,1}$ and $q_{V,cyl,3}$ are known. Hereby the input-output relation is in accordance with Fig. 70.

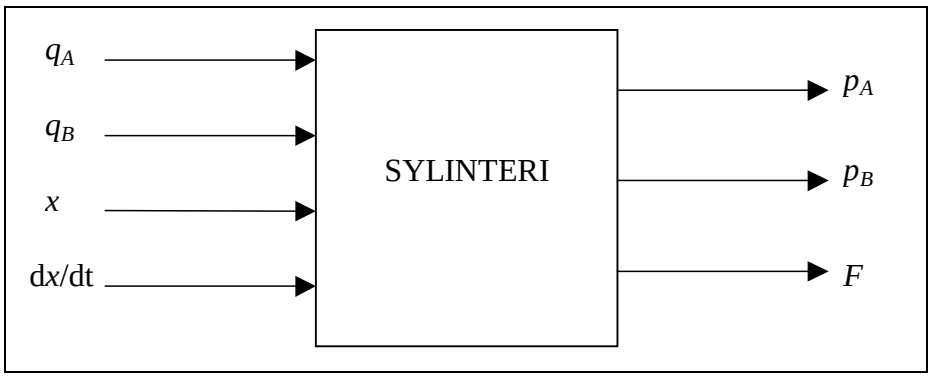

Figure 70. Inputs and outputs of cylinder model. [Kuvan tekstit käännettävä englanniksi. Kuvaa muutettava seuraavasti: SYLINTERI → Cylinder, $q_A \rightarrow q_{V,cyl,1}$, $q_B \rightarrow q_{V,cyl,3}$, $x \rightarrow x_{cyl}$, dx/dt → dx_{cyl}/dt, $p_A \rightarrow p_{cyl,1}$, $p_B \rightarrow p_{cyl,3}$, $F \rightarrow F_{cyl}$].

6.2.4 Connecting cylinder model to other components

Connecting cylinder to mechanism model

The output of the cylinder model is force as shown in Fig. 70. Thus the cylinder does not generate movement as is often erroneously thought. Cylinder generates force that induces the movement of the mechanism connected to it. From this mechanism it is possible to compute the values for the position and velocity of the cylinder piston which are then returned to the cylinder model. At its simplest the mechanism is a mass connected to the end of the cylinder having the same velocity as the piston. However, the condition is generally more complex than this as it is in the hydraulic crane presented in Fig. 71.

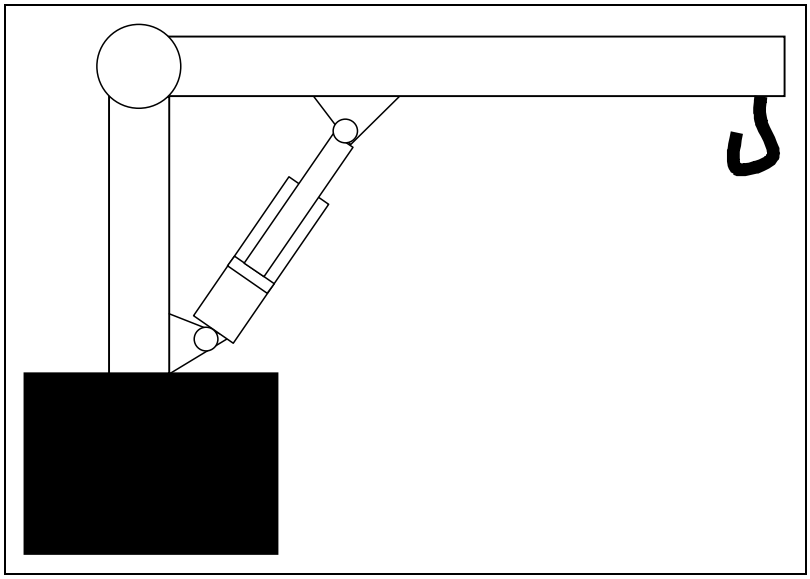

Figure 71. Hydraulic crane. [Kuvaan on lisättävä selittäviä tekstejä].

When modeling the system in Fig. 71, the cylinder generated force has to be converted to torque that affects in the system in relation to the joint connecting together the column and the boom of the crane. This torque induces a rotating motion of the boom in relation to the joint. Thus it is possible to compute the position of the piston from the rotation angle of the boom and the velocity of the piston from the rotational (angular) velocity of the boom. It should be noted that position and velocity of the cylinder piston are generally not the state variables of the system. In literature there are several cases where connection between cylinder and mechanism is done erroneously using artificial springs or other tricks of this kind.

In general, the equation of motion for any mechanism can be written as

$$\mathbf{M}\ddot{\mathbf{z}} + \mathbf{H}(\mathbf{z}, \dot{\mathbf{z}}) = \mathbf{Q} \qquad (6.7)$$

where **M** is the inertia matrix of the mechanism, **z** is the vector of mechanical states, **H** is the vector function that encompasses i.a. the Coriolis, centrifugal, frictional and gravitational forces/torques and **Q** is the vector of generalized forces (may encompass both forces and torques). The generalized forces depend on the force of the cylinder and mechanical states **z**. The position of cylinder piston in turn depends on the states z and the velocity of the piston depends

both on the states $\mathbf{z}$ and their derivatives $\dot{\mathbf{z}}$. In this general form the interaction between cylinder and mechanism is in accordance of the block diagram presented in Fig. 72.

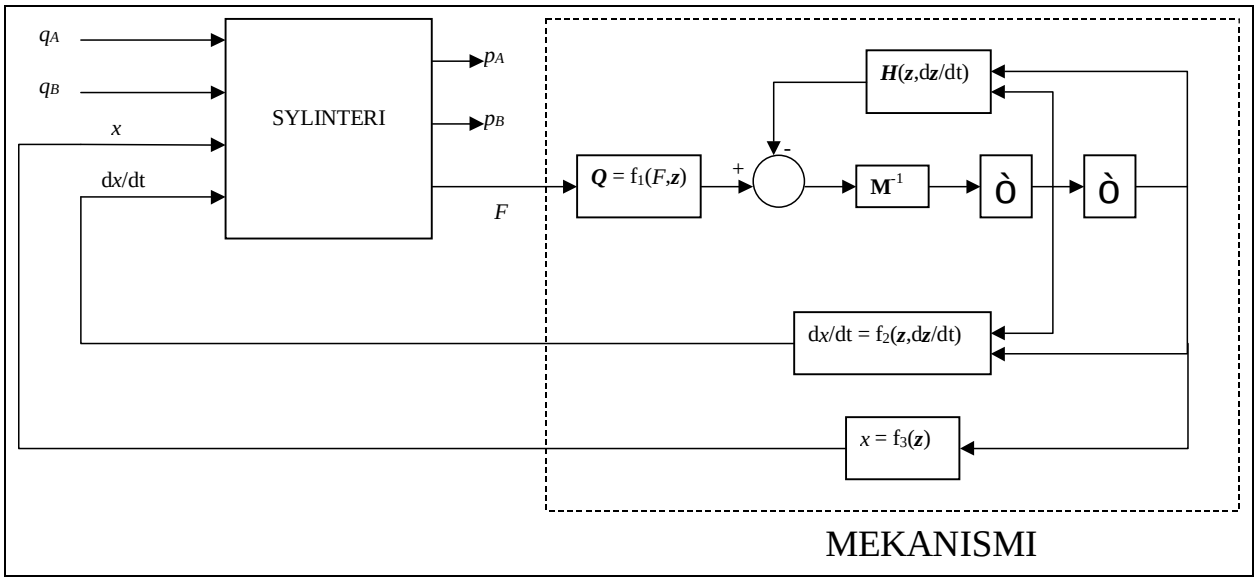

Figure 72. Connecting cylinder model to general mechanism model. [Kuvan tekstit käännettävä englanniksi. Kuvaa muutettava seuraavasti: SYLINTERI → Cylinder, MEKANISMI → Mechanism, $q_A \rightarrow q_{V,cyl,1}$, $q_B \rightarrow q_{V,cyl,3}$, $x \rightarrow x_{cyl}$, $dx/dt \rightarrow dx_{cyl}/dt$, $p_A \rightarrow p_{cyl,1}$, $p_B \rightarrow p_{cyl,3}$, $F \rightarrow F_{cyl}$]. Muutokset myös Mekanismi-osuuteen ja sinne lisäksi kursivoinnit.

Connecting cylinder with throttle

Connecting cylinder model with a throttle goes easily since the cylinder model uses flow rates as inputs and the throttle in turn is a component whose output is the flow rate that passes through the component at a certain pressure difference over it. In several cases the flow ports (of piston and piston rod side) of a cylinder create significant throttles. Adding these throttles to the cylinder model of Fig. 70 results to a model (see Fig. 73) whose inputs are the pressures just outside flow ports ($p_{cyl,fp,1}$ and $p_{cyl,fp,3}$) and outputs are the flow rates to these ports. The pressures in cylinder piston and piston rod side volumes are now the internal states of the cylinder model.

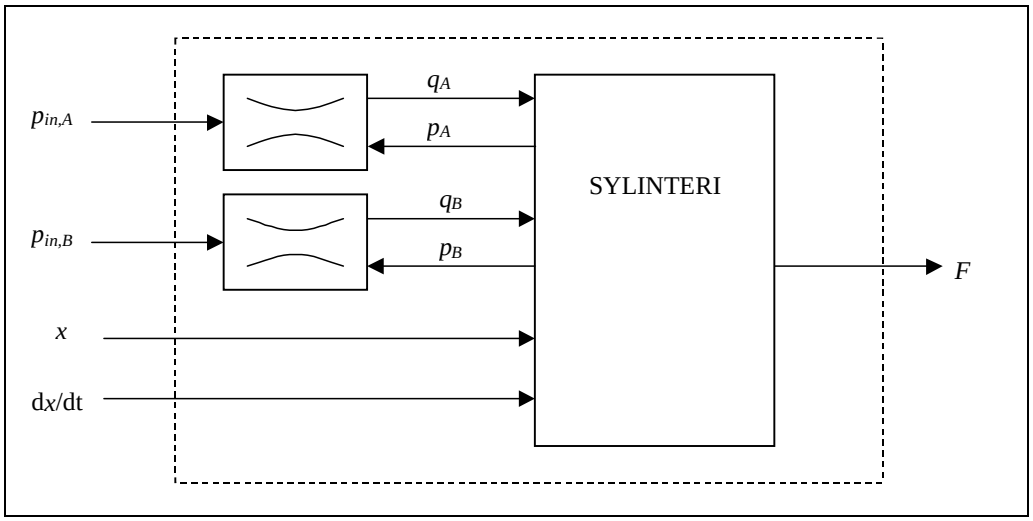

Figure 73. Cylinder model where the flow gates are included as throttles. [Kuvan tekstit käännettävä englanniksi. Kuvaa muutettava seuraavasti: SYLINTERI → Cylinder, $q_A \rightarrow q_{V,cyl,1}$, $q_B \rightarrow q_{V,cyl,3}$, $x \rightarrow x_{cyl}$, dx/dt → dx_{cyl}/dt, $p_A \rightarrow p_{cyl,1}$, $p_B \rightarrow p_{cyl,3}$, $F \rightarrow F_{cyl}$, $p_{in,A} \rightarrow p_{cyl,fp,1}$, $p_{in,B} \rightarrow p_{cyl,fp,3}$].

Many simulation softwares for hydraulics use this type of cylinder model, i.e., they expect that the cylinder flow ports always encompass throttles. Therefore they require port dimensions as parameters.

Connecting cylinder with valve

In most cases the cylinder is connected to the directional control valve with short pipes or hoses. Also in most cases the flow velocities are so low that the pressure losses in pipes/hoses and cylinder flow ports are insignificant. This allows connecting the valve model directly to cylinder model as presented in Fig. 74.

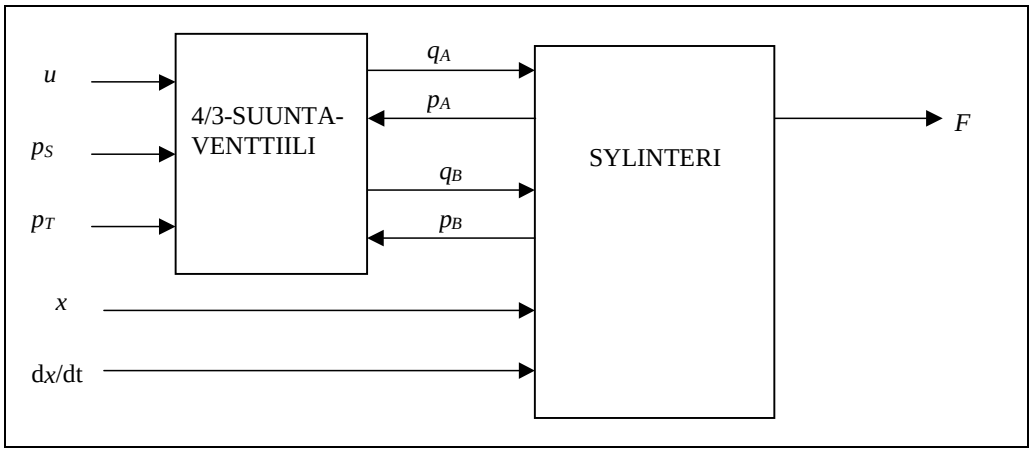

Figure 74. Direct connection between cylinder and directional control valve model. [Kuvan tekstit käännettävä englanniksi. Kuvaa muutettava seuraavasti: SYLINTERI → Cylinder, 4/3-SUUNTAVENTTIILI → 4/3 Directional Control Valve, $q_A \rightarrow q_{V,cyl,1}$, $q_B \rightarrow q_{V,cyl,3}$, $x \rightarrow x_{cyl}$, dx/dt → dx_{cyl}/dt, $p_A \rightarrow p_{cyl,1}$, $p_B \rightarrow p_{cyl,3}$, $F \rightarrow F_{cyl}$, $u \rightarrow u_{valve}$, $p_S \rightarrow p_{valve,1}$, $p_T \rightarrow p_{valve,2}$].

When using the direct connection of Fig. 74 the volume of the pipe or hose has to be added to the corresponding cylinder volume (piston or piston rod side volume) in equation (*3.32*). In general the bulk modulus of a pipe is so large that it can be ignored, but since the bulk modulus of a hose is much smaller (100–800 MPa) it has to be taken into account in computing the effective bulk modulus. Assuming that fluid is free of air bubbles and the elasticity of the cylinder tube can be ignored the equation for the effective bulk modulus for the piston side volume is

$$\frac{1}{K_{\mathrm{e},1}} = \frac{1}{K_{\mathrm{f}}} + \frac{V_{\mathrm{hose},1}}{V_{\mathrm{cyl},1,\mathrm{e}} + V_{\mathrm{hose},1} + A_{\mathrm{cyl},1}\, x_{\mathrm{cyl}}} \frac{1}{K_{\mathrm{hose},1}} \tag{6.8}$$

where $V_{\mathrm{hose},1}$ is the hose volume at the piston side of the cylinder and $K_{\mathrm{hose},1}$ is the bulk modulus of the same hose. The effective bulk modulus is a function of piston position. The effective bulk modulus for the piston rod side of the cylinder can be defined respectively.

If the pressure losses in cylinder flow ports are significant the pipes and hoses can be modeled as separate volumes and use the model presented in Fig. 73. The intercations are presented in Fig. 75.

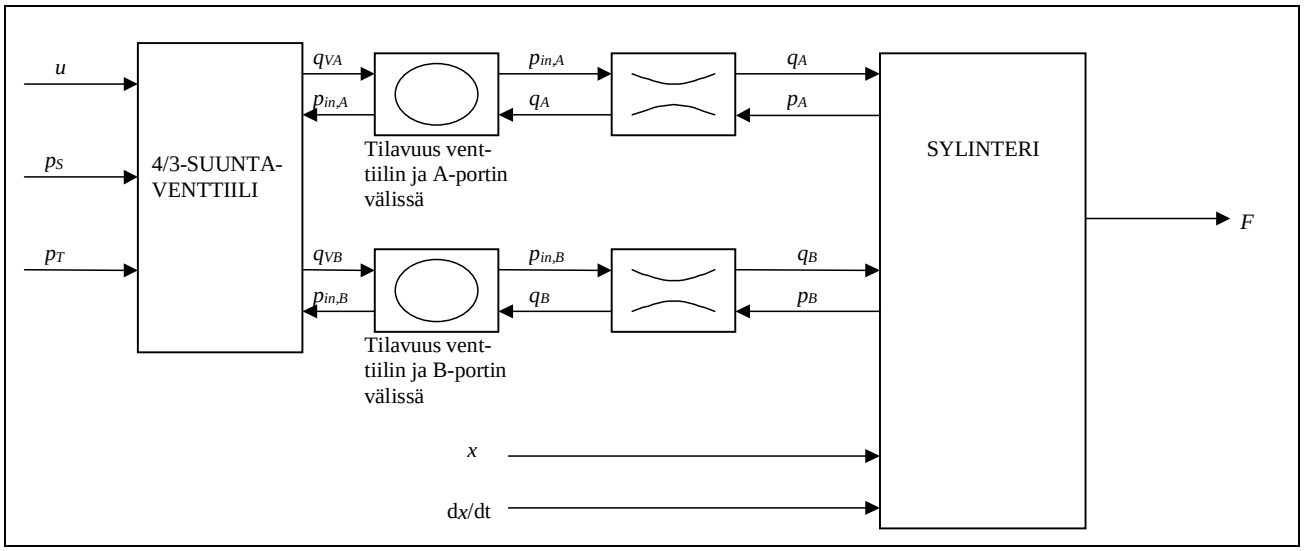

Figure 75. Connecting the cylinder model in Fig 73 to a directional control valve. [Kuvan tekstit käännettävä englanniksi. Kuvaa muutettava seuraavasti: SYLINTERI → Cylinder, 4/3-SUUNTAVENTTIILI → 4/3 Directional Control Valve, Tilavuus venttiilin ja A-portin välissä → Volume between valve and piston side flow port of cylinder, Tilavuus venttiilin ja B-portin välissä → Volume between valve and piston rod side flow port of cylinder, $q_A \rightarrow q_{\mathrm{V,cyl,1}}$, $q_B \rightarrow q_{\mathrm{V,cyl,3}}$, $x \rightarrow x_{\mathrm{cyl}}$, $\mathrm{d}x/\mathrm{d}t \rightarrow \mathrm{d}x_{\mathrm{cyl}}/\mathrm{d}t$, $p_A \rightarrow p_{\mathrm{cyl,1}}$, $p_B \rightarrow p_{\mathrm{cyl,3}}$, $F \rightarrow F_{\mathrm{cyl}}$, $p_{in,A} \rightarrow p_{\mathrm{cyl,fp,1}}$, $p_{in,B} \rightarrow p_{\mathrm{cyl,fp,3}}$, $q_{VA} \rightarrow q_{\mathrm{V,cyl,1,vol}}$, $q_{VB} \rightarrow q_{\mathrm{V,cyl,3,vol}}$, $u \rightarrow u_{\mathrm{valve}}$, $p_S \rightarrow p_{\mathrm{valve,1}}$, $p_T \rightarrow p_{\mathrm{valve,2}}$].

A negative side of this approach is that the model becomes more complex. Computing pressures in small volumes also requires special solvers (sc. stiff solver) which are not included in every simulation software. Nevertheless this approach has also a positive side since there is no need to compute the effective compression (bulk) modulus separately as it is done automatically.

So there are two alternative methods to connect cylinder and directional control valve, but which one is worth using? In real-time simulations direct connection of Fig. 74 is almost the only option since stiff solvers are usually not available for real time simulations (stiff solvers are iterative of

nature and thus the time used to compute a single integration step cannot be defined beforehand). This is especially the case if the pipes/hoses are short and the cylinder flow ports are spacious. In normal off-line simulation one can use whichever method. With a good stiff solver the simulation does not slow down even when using the method of Fig. 75. This method is also better in the sense that it can be applied in all cases.

6.2.5 Modeling cylinder ends

One often encountered problem in cylinder modeling is that the piston does not remain in its operating region, i.e., between cylinder ends. In reality the movement of piston is stopped by the cylinder ends, but the simulation model is not aware of these restrictions unless they are included in the model. In simulations running "through" the end of cylinder usually leads to a state where the fluid volume decreases to zero and the simulation halts (in this case every properly operating integration algorithm sends an error message). There is at least one practical method to model the cylinder ends; they are modeled as stiff springs. One should neither consider restrictions for integrators nor integrator resetings since they aren't universal methods (the position of piston is not necessarily a state that could be restricted). If the ends are modeled as stiff springs the collision of piston to the cylinder end may cause strong vibrations that slow down the simulation. Therefore it is advisable to use artificial dampers that are active only at the cylinder ends. The force induced by the ends can be calculated as

$$F_{\mathrm{cyl,e}} = \begin{cases} -k_{\mathrm{R,cyl,e}}\, x_{\mathrm{cyl}} - b_{\mathrm{v,cyl,e}}\, \dot{x}_{\mathrm{cyl}} & , \quad x_{\mathrm{cyl}} < 0 \\ 0 & , \quad 0 \le x_{\mathrm{cyl}} \le x_{\mathrm{cyl}}^{\max} \\ -k_{\mathrm{R,cyl,e}}\left(x_{\mathrm{cyl}} - x_{\mathrm{cyl}}^{\max}\right) - b_{\mathrm{v,cyl,e}}\, \dot{x}_{\mathrm{cyl}} & , \quad x_{\mathrm{cyl}} > x_{\mathrm{cyl}}^{\max} \end{cases} \qquad (6.9)$$

Since the cylinder end is modeled as spring, the piston penetrates slightly inside the end. The larger the spring constant the smaller the penetration. On the other hand a large spring constant complicates the simulation. The spring constant of the cylinder end should be selected so, that the maximum force of the cylinder induces a small penetration of magnitude, e.g., 0.2 mm. A suitable value for the extra damping coefficient is of magnitude $0.5\times(k_{\mathrm{R,cyl,e}}\times m_{\mathrm{L,e}})^{0.5}$ where $m_{\mathrm{L,e}}$ is the effective inertial load reduced [onko tämä oikea termi englanniksi?] to the cylinder. It should be noted that in general, running the cylinder to the end should never happen in practice. Therefore the end model does not need to be fully detailed. Most important is to prevent the piston from passing the cylinder end so much that the fluid volume reaches a value of zero.

6.3 Modeling hydraulic motor

6.3.1 Modeling of torque motor

Figure 76 presents a typical torque motor. Since its working principle resembles cylinder the modeling of this component does not differ much from the modeling of a cylinder. The position of the piston x_{cyl} is replaced with rotation angle φ_{tm} [rad], that indicates how much the axle of the motor has turned from the end numbered with 1. The velocity of the piston is replaced with the derivative of rotation angle and the piston areas $A_{\mathrm{cyl,1}}$ and $A_{\mathrm{cyl,3}}$ are replaced with the swept volume in radians $V_{\mathrm{tm,rad}}$ [m^3/rad]. The output of torque motor is torque [Nm] instead of force. In contrary to cylinders, when modeling torque motors the leakage flow has usually be taken into account.

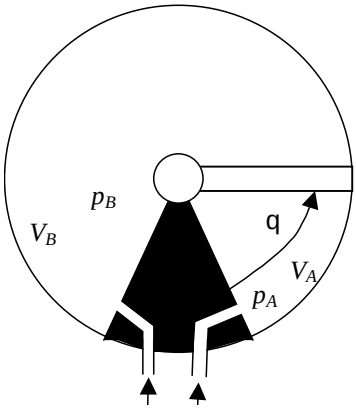

Figure 76. Principle of a torque motor. [Kuvaa muutettava seuraavasti: $p_A \rightarrow p_{tm,1}$, $p_B \rightarrow p_{tm,2}$, $V_A \rightarrow V_{tm,1}$, $V_B \rightarrow V_{tm,2}$, $q \rightarrow j_{tm}$].

6.3.2 Modeling of motors with unrestricted rotation angle

Most common types of hydraulic motors with unrestricted rotation angle are gear, piston and vane motors. Exact modeling of these components is difficult and only a simplified model is presented here. One notable difficulty in modeling these motors is that the swept volume is not constant but a function of rotation angle. Therefore the input flow of a, e.g., piston motor pulsates if the rotational velocity of the motor is constant. Detailed modeling of this phenomena requires detailed knowledge of the motor geometry and thus one usually contents to use a constant value for the swept volume. Likewise the changing swept volume also the sizes of the pressurized fluid volumes on the inflow and outflow sides of the motor depend on the prevailing rotation angle of the motor axle. Usually also with these one contents with constant volumes. With these assumptions the pressure equation of the motor takes form:

$$\begin{aligned} \dot{p}_{m,1} &= \frac{K_{e,1}}{V_{m,1,e}}\left(q_{V,m,1} - k_{v,m,d,1}\left(p_{m,1} - p_{m,2}\right) - k_{v,m,d,2}\, p_{m,1} - V_{m,rad}\,\dot{j}_m\right) \\ \dot{p}_{m,2} &= \frac{K_{e,2}}{V_{m,2,e}}\left(q_{V,m,2} + k_{v,m,d,1}\left(p_{m,1} - p_{m,2}\right) - k_{v,m,d,2}\, p_{m,2} + V_{m,rad}\,\dot{j}_m\right) \end{aligned} \qquad (6.10)$$

where $V_{m,rad}$ is the swept volume of the motor in radians [m^3/rad]. Coefficient $k_{v,m,d,1}$ represents the internal laminar leakage from the high pressure side of the motor to the low pressure side and coefficient $k_{v,m,d,2}$ represents the external laminar leakage from the motor to a separate leakage line (in birectional motors). The leakage model used here is quite simplified since in reality the leakage depends also on, e.g., rotational velocity. For more complex leakage models see, e.g. [1]. Volumes $V_{m,1,e}$ and $V_{m,2,e}$ contain both the small volumes that are embodied in motor structure, but which still are not part of the swept volume, and the volumes of pipes/hoses between motor and its control valve. In contrary to cylinders, the flow ports of a motor are not usually modeled as throttles since the internal volumes of a motor are small. The torque equation yields to

$$T_m = V_{m,rad}\left(p_{m,1} - p_{m,2}\right) - T_{\mu,m} \qquad (6.11)$$

Modeling of the friction torque T_m is discussed in following chapter.

6.4 Friction modeling

6.4.1 Introduction

Friction is a very complex phenomena that contains i.a. contingency and physical phenomena that are largely unknown. Therefore the best model for friction is always the rough estimate of the real case. Some of the difficult phenomena related to friction are i.a. static friction, stick-slip phenomenon (a jerky motion that manifests itself at certain velocities) and the time and frequency dependence of the friction force. In addition, with hydraulic components the friction force or torque depends also on the pressures in cylinder or motor volumes

6.4.2 Friction force in cylinder

It is generally known that the dependence of friction force on velocity in a cylinder complies approximately with the curve presented in Fig. 77. With zero speed the friction force equals the static friction force F_S. If the forces affecting to the piston exceed the magnitude of the static friction, the piston starts to move. With increasing velocity the friction decreases until it reaches minimum value at speed $v_\mu^{\min}$. This minimum value of friction is usually called the Coulomb friction F_C. After this point, when the velocity again increases, the friction force starts to increase with a slope b_v which is usually called the viscose friction coefficient. With negative velocities of piston the condition is generally a mirror image of the positive velocity shown in Fig. 77.

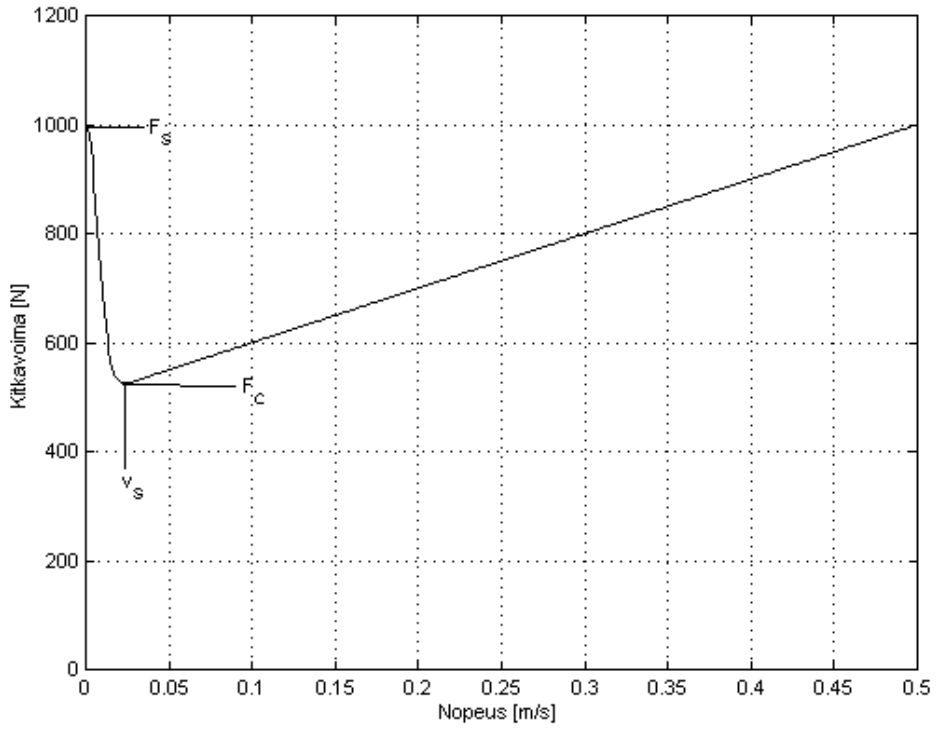

Figure 77. Friction force as a function of velocity. [Kuvan tekstit käännettävä englanniksi. Kuvaa muutettava seuraavasti: Kitkavoima → F_μ, Nopeus → v_{cyl}, F_S → F_S, F_C → F_C, v_s → $v_\mu^{\min}$].

One much used equation for describing the dependence of friction on velocity is:

$$F_{\mu,\mathrm{cyl}}\left(\dot{x}_{\mathrm{cyl}}\right)=\mathrm{sgn}\left(\dot{x}_{\mathrm{cyl}}\right)\left(F_{\mathrm{C}}+\left(F_{\mathrm{S}}-F_{\mathrm{C}}\right)e^{-\left(\frac{\dot{x}_{\mathrm{cyl}}}{v_{\mu}^{\min}}\right)^{2}}\right)+b_{\mathrm{v}}\,\dot{x}_{\mathrm{cyl}} \tag{6.12}$$

where

$$\mathrm{sgn}\left(\dot{x}_{\mathrm{cyl}}\right)=\begin{cases}1, & \dot{x}_{\mathrm{cyl}}\geq 0\\ -1, & \dot{x}_{\mathrm{cyl}}<0\end{cases} \tag{6.13}$$

In order not to make the case too easy, the friction force depends also heavily on the pressures in the cylinder volumes. This is because the friction force results from the piston and piston rod seals dragging against their counter surfaces (cylinder tube wall and piston rod) and with increasing pressure the seals are pressed harder against these surfaces. Since on the piston rod side there are two seals under pressure (piston seal and piston rod seal) the pressure in this side has greater effect on the cylinder friction force than the pressure at the piston side. Taking into account this pressure dependence of friction force the equation for friction force takes form:

$$F_{\mu,\mathrm{cyl}}\left(\dot{x}_{\mathrm{cyl}},p_{\mathrm{cyl},1},p_{\mathrm{cyl},3}\right)=\Upsilon\left(p_{\mathrm{cyl},1},p_{\mathrm{cyl},3}\right)\mathrm{sgn}\left(\dot{x}_{\mathrm{cyl}}\right)\left(F_{\mathrm{C}}+\left(F_{\mathrm{S}}-F_{\mathrm{C}}\right)e^{-\left(\frac{\dot{x}_{\mathrm{cyl}}}{v_{\mu}^{\min}}\right)^{2}}\right)+b_{\mathrm{v}}\,\dot{x}_{\mathrm{cyl}} \tag{6.14}$$

Defining the exact value of function $\Upsilon(p_{\mathrm{cyl},1},\ p_{\mathrm{cyl},3})$ is very difficult and requires plenty of measurements. The easiest way to avoid this is to make an assumption that $\Upsilon(p_{\mathrm{cyl},1},\ p_{\mathrm{cyl},3}) = 1$ and choose the other friction parameters so that the modeling accuracy is good in typical operating condition. A little bit more accurate model for this function could be, e.g.:

$$\Upsilon\left(p_{\mathrm{cyl},1},p_{\mathrm{cyl},2}\right)=1+\frac{1}{p_{\mathrm{cyl,ref}}}\left(\frac{p_{\mathrm{cyl},1}}{3}+\frac{2p_{\mathrm{cyl},2}}{3}\right) \tag{6.15}$$

This equation assumes that 1/3 of the increase of the friction force is due of the pressure $p_{\mathrm{cyl},1}$ and 2/3 of the pressure $p_{\mathrm{cyl},3}$ (assuming that the piston rod is on this side). Parameter $p_{\mathrm{cyl,ref}}$ dictates the growth rate of the friction force when the pressures increase. This model has no physical background whatsoever, it has just prooved to be a *pretty good* model for *a certain* cylinder.

With these equations there are lot of parameters whose correct values should be “quessed”. The best modeling accuracy is achieved by running measurements with the cylinder in several operating conditions. However, measuring the static friction F_{S} and the descending section of the friction curve is difficult to do in practice. A rule of thumb is: the magnitude of static friction is usually 5–15 % of the maximum force F_{cyl} of the cylinder at maximum pressures and the magnitude of Coulumb friction F_{C} is 20–50 % smaller. With low pressures the friction force is about 1/2–1/3 of these values. The lowest value of friction force appears usually at velocities 3–15 mm/s. The value of viscose friction coefficient b_{v} can be selected to be the same as the value of, e.g., static friction. Anyhow, these values must be taken with caution and the parameters must be tuned to their final values using at least one measured response.

6.4.3 Friction torque of hydraulic motor

As with the cylinders, the friction torque of a hydraulic motor is a function of velocity and the pressures prevailing in the volumes of the component. However, in case of motors the modeling is easier in the respect that the component manufacturers report much more loss information for the component than they do with cylinders. In the best case the manufacturer reports both the hydromechanical efficiency η_{hm} as a function of rotational velocity at few pressure differences and also the starting torque of the motor. This information can be used in deducing the loss torques. If the hydromechanical efficiency is known, the loss torque is:

$$T_{\mu,m} = V_{m,rad}\,\Delta p\,(1-\eta_{hm}) \qquad (6.16)$$

The loss torque curve can be extrapolated to zero velocity when bearing in mind that the loss torque at zero speed equals the starting torque of the motor. However, the efficiency curves announced by the manufacturer enable judging the magnitude of the loss torque only at certain pressure differencies and some of the manufacturers do not inform any efficiency curves at all. A more accurate model is obtained by measuring the characteristics of the motor and by fitting a suitable loss torque curve to the measurement data.

6.4.4 Modeling friction for simulation

Assume that the friction force of a cylinder (or friction force of a hydraulic motor) is known as a function of velocity and the pressures prevailing in the component volumes. Despite of this, adding the friction to the component model is not an easy task. The simplest way is to subtract the friction force directly from the cylinder force, however, this does not work at zero velocity. At this speed the friction force is by no means equal with friction force as the equations (?) and (?) assume, but exactly equal with the sum of the other forces affecting to the cylinder. At zero speed the friction force automatically adjusts itself so that the total force of the cylinder is zero and the cylinder stays put. If this is not taken into account in the model, the friction force pushes the cylinder on both sides of the zero speed and the system becomes almost impossible to simulate. If the system includes only one actuator which has only inertial load it is in principle possible to integrate some logic and integrator resetings in the model in a way that eneble the model to operate correctly also at zero speed. However, this is surprisingly difficult and it is not an universal solution (it does not work, e.g., in booms or if the load is a flexible structure). Because of this, the reseting of integrators in neither discussed here nor recommended at all. In the following are presented two possible solutions that work and can be simulated.

Use of modified signum function

In this approach the sgn function is approximated with a function that is not discontinuous [vaiko irregular?] at zero velocity. One good approximation to use is the hyperbolic tangent which lets the sgn function to be approximated as

$$\mathrm{sgn}(\dot{x}_{cyl}) \approx \tanh(K_{sgn}\,\dot{x}_{cyl}) \quad , \quad K_{sgn} = 1000 - 20000 \qquad (6.17)$$

Figure 78 presents the shape of this approximative function for some values of parameter K_{sgn}.

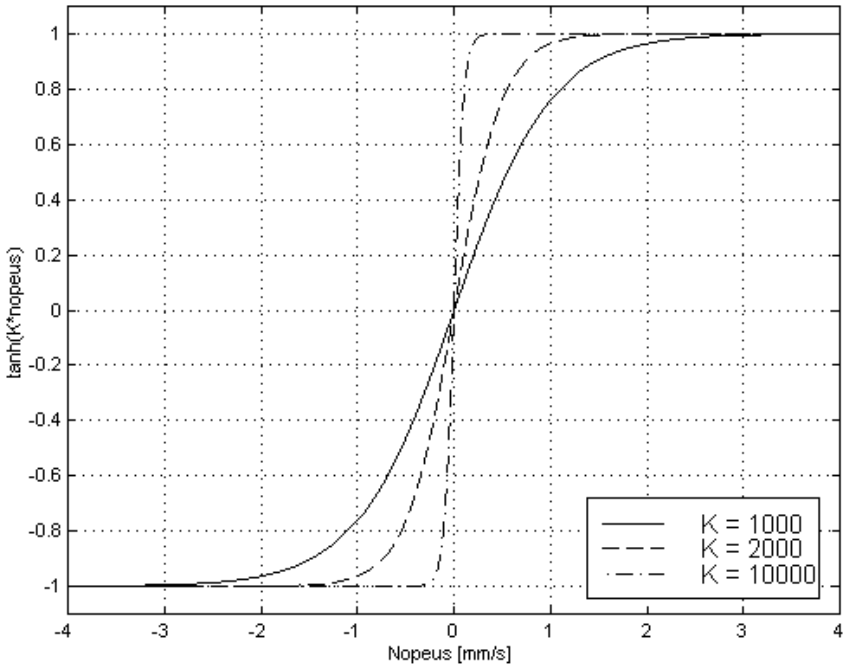

Figure 78. Approximating signum function with hyperbolic tangent function. [Kuvan tekstit käännettävä englanniksi. Kuvaa muutettava seuraavasti: tanh(K*nopeus) → tanh(K_{sgn} v_{cyl}), Nopeus → v_{cyl}, K → K_{sgn}].

This modeling method is simple and numerically effective. In practice this model operates so that in the vicinity of zero speed the velocity settles to a value that deviates slightly from zero so that the forces are in equilibrium. Thus the actuator drifts slowly although the friction should hold it still. In hydraulic motors this does not cause problems because drifting occurs anyway due to the leakage. In cylinders this behavior of the model deviates from the real case and leads to errors in longer simulations. This error is the smaller the larger value for parameter K_{sgn} is used. On the other hand the simulation becomes numerically more difficult if the value of K_{sgn} is increased and the solvers that require constant step size are not necessarily able to integrate correctly in the vicinity of zero velocity.

Dynamic friction model

Consider the cylinder in Fig. 79. In the upper picture the cylinder is not subjected to any force and the piston rests on seals (for simplicity the piston rod seals are omitted from the picture). Assume that the cylinder is now subjected to a load force $F_{cyl,L}$ that is lower in magnitude than the static friction force. The lower picture shows how the seal yields and piston moves somewhat dependent on the seal. However, the seal does not start to slide since the applied force does not overcome the static friction force F_S. If the force $F_{cyl,L}$ is increased the seal starts to slide while maintaining the bent shape. When the load force is removed the piston stops from moving in the direction of the force and retracts slightly because of the straightening of the seal. Thus the seal clearly behaves like a spring. It also has a damping effect because of the losses that arise in the transformations of the seal shape.

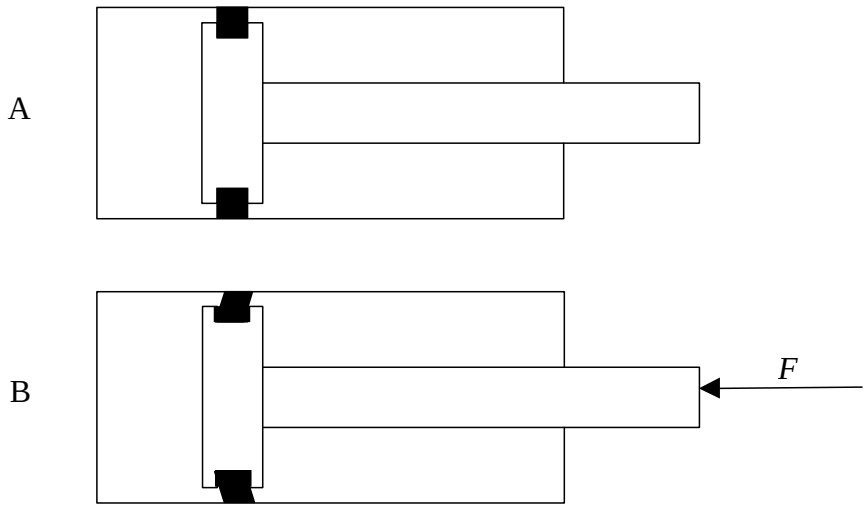

Figure 79. Bending of the piston seal when piston is subjected to a force. [Kuvaa muutettava seuraavasti: $F \rightarrow F_{\mathrm{cyl,L}}$]. [Kuvaan voisi lisätä muitakin selittäviä tekstejä ja muuttujia, ainakin muodonmuutosmitta z_{cs}].

An interesting friction model is obtained if the bend of the seal is taken as state variable and the friction force is computed on grounds of this variable. This kind of friction model is presented in [1]. Originally this model was intended to be used in modeling the friction between two solid bodies since at microscopic level, the above described bending occurs with all bearing couples before they start to slide in relation to each other. However, this model is particularly suitable for modeling hydraulic cylinders because the bends of the seal are macroscopic in magnitude and easy to simulate. In this model the friction force is defined with following equations:

$$\dot{z}_{\mathrm{cs}} = \dot{x}_{\mathrm{cyl}} - \frac{k_{\mathrm{R,cs}} \left| \dot{x}_{\mathrm{cyl}} \right|}{F_{\mu}^{*}\left(\dot{x}_{\mathrm{cyl}}, p_{\mathrm{cyl,1}}, p_{\mathrm{cyl,3}}\right)} z_{\mathrm{cs}} \qquad (6.18)$$

$$F_{\mu,\mathrm{cs}} = k_{\mathrm{R,cs}}\, z_{\mathrm{cs}} + z_{\mathrm{d,cs}}\, \dot{z}_{\mathrm{cs}} + b_{\mathrm{v}}\, \dot{x}_{\mathrm{cyl}}$$

where

z_{cs} bend of the cylinder seal [m]
$k_{\mathrm{R,cs}}$ spring constant of the cylinder seal [N/m]
$\zeta_{\mathrm{d,cs}}$ damping constant of the cylinder seal [Ns/m]
b_{v} viscose friction coefficient [Ns/m]

and function F_{m}^{*} is obtained from the equation (*6.18*) by removing the viscose friction and $\mathrm{sgn}\left(\dot{x}_{\mathrm{cyl}}\right)$ thus resulting into

$$F_{\mu}^{*}\left(\dot{x}_{\mathrm{cyl}}, p_{\mathrm{cyl,1}}, p_{\mathrm{cyl,3}}\right) = \Upsilon\left(p_{\mathrm{cyl,1}}, p_{\mathrm{cyl,3}}\right)\left(F_{\mathrm{C}} + (F_{\mathrm{S}} - F_{\mathrm{C}})\, e^{-\left(\frac{\dot{x}_{\mathrm{cyl}}}{v_{\mu}^{\min}}\right)^{2}}\right) \qquad (6.19)$$

Note that the value of function F_{m}^{*} is always positive.

This simple model represents correctly meny of the friction related complex phenomena, like staying in put, stick-slip, hysteresis, etc. If you're interested to know more, see reference [1]. The friction model is also fully universal; the friction of any system can be modeled with equation (*6.18*).

The friction model of equation (*6.18*) has two new parameters, $k_{\mathrm{R,cs}}$ and $\zeta_{\mathrm{d,cs}}$. Parameter $k_{\mathrm{R,cs}}$ represents the stiffness of the cylinder seal and a value for it can be defined by estimating the magnitude of the greatest possible bend of the seal.

If the greatest possible bend is $z_{\mathrm{cs}}^{\mathrm{max}}$ then

$$k_{\mathrm{R,cs}} = \frac{F_{\mathrm{S}}}{z_{\mathrm{cs}}^{\mathrm{max}}}$$

Maximum bend can be imagined to be of magnitude 0.1–1 mm.

The value of parameter $\zeta_{\mathrm{d,cs}}$ instead is largely unknown since it depends on, i.a., the material properties of the seal. It is recommended to select a value as low as possible, however so that the friction model does not induce disturbing vibrations. If the effective inertial load of the cylinder is known, then the appropriate value for $\zeta_{\mathrm{d,cs}}$ is of the order of $0.5–2.0\times(k_{\mathrm{R,cs}}\, m_{\mathrm{L,e}})^{0.5}$.

The friction model of equation (*6.18*) is not so suitable for modeling hydraulic motors since these components do not have flexible seals. In order to obtain a realistic model, the value for $k_{\mathrm{R,cs}}$ has to be very large which in turn makes the simulation more difficult.

7 References

1. Canudas de Wit, C., Olsson, H., Åström, K.J. & Lischinsky, P. A New Model for Control of Systems with Friction. IEEE Transactions on Automatic Control, Vol. 40, No 3, 1995, pp. 419-425.
2. Ellman, A., Piché, R. 1996. A Modified Orifice Flow Formula for Numerical Simulation of Fluid Power Systems. FPST-Vol. 3, Fluid Power Systems and Technology: Collected Papers. ASME. pp. 59-63.
3. Funk, J. E., Wood, D. J., Chao, S. P. 1972. The Transient Response of Orifices and Very Short Lines. Trans. ASME, J. Basic Engng. pp. 483-491.
4. Geibler, G. 1998. Flow force coefficient - a basis for valve analysis. 11th Bath International Fluid Power Workshop.
5. Husu, M., Niemelä, I., Pyötsiä, J., Simula, M., Hauhia, M., Riihilahti, J. 1997. Flow Control Manual. Neles-Jamesbury. Helsinki. 171 p.
6. Johnston, D.N., Edge, K.A., Vaughan, N.D. 1991. Experimental investigation of flow and force characteristics of hydraulic poppet and disc valves. Proc Inst Mech Engrs Vol 205. pp.161-171.
7. Kauranne, H., Kajaste, J. Vilenius, M. 1996. Hydrauliikan perusteet. WSOY, Porvoo. 340 p.
8. Koivula, T., Ellman, A., Cavitation Behaviour of Hydraulic Orifices and Valves. SAE Paper 982038, International off-highway and powerplant congress and exposition, September 14-16, 1998, Milwaukee, USA. To be published in SAE 1998 Transactions.
9. Koivula, T., Ellman, A., Vilenius, M. The Effect of Oil Type on Flow and Cavitation Properties in Orifices and Annular Clearances. Bath Workshop on Power Transmission & Motion Control PTMC '99, 8 - 10 September 1999, University of Bath, UK. 15 p.
10. Lichtarowicz, A., Diggins, R.K., Markland, E. 1965. Discharge Coefficients for Incompressible Non-Cavitating Flow through Long Orifices. J. Mech. Eng. Sci., vol. 7, no. 2.pp. 210-219.
11. Lu Y. 1982. Durchflubkoeffizienten und Strömungskräfte an 2-Wege-Einbauventilen. O+P ”Ölhydraulik und Pneumatik” 26 Nr.1. pp. 33-36.
12. McCloy, D., Martin, M.R. 1973. The Control of Fluid Power. London, Longman Group Limited.
13. Merritt, H. E. 1967. Hydraulic Control Systems. John Wiley & Sons, Inc. New York. 358 p.
14. Schmidt, D.P., Corradini, M.L. 1997. Analytic Prediction of the Exit Flow of Cavitating Orifices. Atomization and Sprays, vol 7 pp. 603-616.
15. Stone, J.A. 1960. Discharge Coefficients and Steady State Flow Forces for Hydraulic Poppet Valves. Trans. ASME, J. Basic Engng. pp. 144-154.